Institute of Applied Problems of Physics National Academy of Sciences

Mehdi Ghannad Dezfooli

Dynamical Diffraction of X-rays in weak deformed KDP and ADP crystals

Specialty 01.010.09-Condensed Matter Physics

Thesis for the degree of

candidate of physical and mathematical sciences

Supervisor -Doctor of Physical and Mathematical Sciences,
Professor Trouni K.G.

Yerevan 2019

Contents

INTRODUCTION

Currently, X-ray diffraction is one of the most important subjects in the study of solid state physics. Gaining information about the actual structure of materials is an important task of condensed matter physics. X-rays help to solve the structural problems and also identify the physical properties of the solids. The use of electromagnetic radiation with angstrom wavelength represents a number of new high-precision methods for studying the properties and structure of crystalline and non-crystalline materials and biology.

X-ray diffraction experiments can be performed with both synchrotron and standard lab x-ray sources. The resolution of lab sources is higher but the intensity is much lower than synchrotrons. The synchrotron is an extremely powerful source of X-rays which are produced by highly energetic electrons moving in a large circle in the synchrotron. The radiation produced in this way has properties of polarization, high brilliance, high intensity and wide spectrum.

However, the study of fast processes requires monochromatic and collimated radiation with high intensive in wavelength of angstrom range. For monitoring single crystals in the technology of microelectronics and also testing non-destructive martial, first of all, there are the X-ray diffraction methods. For example, using x-rays for studying the effect of external influences on the structure of crystals, which are great interest in the technology in the field of microelectronics, instrument Engineering and nanotechnology. Relatively accessible and simple change of defects under the influence of external factors can make these effects controllable. Such studies are required to adjust composition, structure and defects of crystalline order to obtain single crystals with the desired physical properties.

Studying the structure and properties of different single crystals by X-ray diffraction methods is basic and informative. At the present time for research in this area, it is essential to have a strongly monochromatic and highly collimated and also sometimes polarized X-ray beam with a large luminosity, which is also controllable.

Relevance of the topic

Obtaining electromagnetic radiation with angstrom wavelength range and controllable parameters is one of main subjects in studying the structure of condensed matter and new materials.

Understanding the physics of diffraction of the radiation with wavelength of angstrom in the crystals under external influences is very important, because it leads to more simple and reliable methods for the study of fine structural changes in crystals with high degree of perfection, dislocation-free single crystals, and also identifying new useful properties of single crystals under external influences.

Dislocation-free single crystals are increasingly applied in various fields of modern science and technology. For example, single crystals of semiconductors (silicon, germanium, gallium arsenide, lithium niobate, quartz, etc.) are grown on industrial scale and are widely used in microelectronics as the electronic components to create large-scale integrated circuits for computers and automated systems. Monochromatic and collimated beams of high-intensity are also necessary for checking the perfect grown single crystals. X-ray diffraction methods are used in the first place as anon-destructive testing. Another area of research that has rapidly developed in recent years associates to the topographic methods in order to study the perfect crystals and some defects in the crystals.

Optics of X-ray diffraction is a new branch of physics. Since the refractive index of X-rays in solids is not very different from one, unlike optics, the creation of X-ray focusing systems seems impossible. However, in conditions of diffraction, energy flux changes at around the Bragg angle with a very small change in the direction of the incident beam near the Bragg angle. This fact is an excellent property to create X-ray focusing systems under the conditions of diffraction.

Since the coefficient of linear absorption in wavelength of angstrom range is very large, and the passage of the waves through the thin and flat samples are strongly absorbed, creating the elements of optics will require a strong incident beam ,which of course can have a negative effect on single crystals. Therefore, the subject is to study the interaction of radiation with condensed matter under various external influences in order to maximize the intensity of the reflected beam. Research on this problem presented in the thesis, which is useful and necessary.

The purpose of work

Obtaining effective control parameters x-rays and thermal neutrons; research and identification of new models of interaction and distribution of radiation in perfect single crystals in the presence of external factors (acoustic fields, temperature gradient)and obtaining the beams of intense coherent and monochrome .

The scientific novelty of work

The values of imaginary and real parts of coefficient of Fourier expansion of polarizability (χ_{hi} andχ_{hr}) for ADP and KDP crystals have been extracted by usage formula of integrated intensity of reflection in crystals with weak deformation [113].

reflectivity single crystal of ADP is measured at the position of the Laue reflection under the influence of temperature gradient perpendicular and parallel to the reflecting atomic planes with μt≈1 (where - μ the linear absorption coefficient, t -thickness of the crystal).A theoretical interpretation has been given for the reduction of the reflection coefficient and appearance of a minimum in curve of integrated intensity with temperature gradient [108,111,115].

The practical value

On the basis of the results of researches of new phenomena in the propagation of X-rays(XR), synchrotron radiation (SR)and thermal neutrons(N) in perfect single crystals under external influences, several elements of gamma-optics are developed and implemented.

X-ray monochromator (without harmonics) is created under the scheme Laue, has almost maximum luminosity and greatly improves monochromatic beam compared with Bragg monochromator.

With the help of effect of the full transfer, the continuous beams in the angstrom range can be filtered with a small energy range.

Based on the phenomenon of the full transfer and complete transparency, most of the elements of gamma optics are designed and created. Collimating monochromators, selective filters, modulators, lenses, etc., which can be widely used in science and technology, as well as in biology and medicine. Based on these studies and obtained results, the problem of space-time control of radiation in angstrom range solved by acoustic fields and temperature gradient. The results obtained in the thesis help develop the theory of the interaction between radiations in angstrom range with matter under external influences.

The main points, to be defended

1-The behavior of the integrated intensity of diffracted beams of X-ray from a single crystal of ammonium dihydrogen phosphate (ADP) in the Laue geometry under the influence of the temperature gradient applied perpendicular to the reflecting atomic planes.

2-The behavior of the integrated intensity of diffracted beams of X-ray from single crystals of ammonium dihydrogen phosphate (ADP) and quartz in the Laue geometry under the influence of the temperature gradient applied parallel to the reflecting atomic planes.

3- The method of extraction of values the imaginary and real parts of Fourier expansion coefficient of polarizability (χ_{hi} and χ_{hr})of ADP and KDP crystals.

4-The comparison between experimental and theoretical rocking curves of reflectivity for ADP crystal under influence of temperature gradient in Laue-case geometry.

CHAPTER 1. Study of the intensity of reflected and transmitted beams of X-ray passing from the crystal

1.1 Introduction and overview of the literature

1.1.1 X-ray scattering from perfect and near-perfect crystals

After the discovery of X-ray diffraction by crystals, different theories proposed for to describe the interaction of radiation with matter. The x-ray diffraction on crystals helps us to study the properties of the X-rays, the structure, physical and chemical properties of crystals. Because of this, the x-ray diffraction method is considered as a unique and powerful method for studying materials and different phenomena. The task of researchers is that the based on the diffraction pattern a substance get right conclusions about its structure.

We can inversely solve the problem with help of theoretical prediction of the exact diffraction pattern and obtain configuration (location) of atoms in the unit cell of the substance. One of these theories is the kinematic scattering theory that can describe different behavior of diffracted X-ray beam with associate to the parameters of the crystal lattice. We present main results that have been obtained by the kinematic theory of X-ray scattering[1-2].

Kinematic theory

The kinematic theory is basis on the general assumptions of the scattering of electromagnetic waves by scattering centers (atoms in the lattice).Solving the problem of the resulting secondary wave at the point located in distance greater than the size of the crystal, some assumptions are made. First, the interaction between the incident and secondary waves neglected and assumed speed of the X-ray wave in the crystal is equal to the speed of light in vacuum. This assumption leads to small errors in the locations of the diffraction maximum.

Second, supposed the incident wave only once scattered in the crystal. This assumption is valid for crystals of small size.

Third, the interaction of the wave with matter neglected due to the small size of crystal. For this reason, the kinematic theory assumes that the amplitude of the wave received by every diffracting center in the crystal is same. Law Bragg can be easily obtained by this theory

$$2d_{(hkl)}.sin\theta = n\lambda, \qquad (1.1)$$

Where $d_{(hkl)}$- distance between atomic planes (hkl), θ-Bragg angle for a reflection, n-a number of integer,λ-wavelength of beam.

In the kinematic theory, the intensity of the diffracted radiation at a point to distance R from the crystal, is given the following [1, 3]

$$I = \frac{{F_0}^2}{R^2}\frac{(sin\,\pi\vec{S}.N_1\vec{a})^2}{(sin\,\pi\vec{S}.\vec{a})^2}\frac{(sin\,\pi\vec{S}.N_2\vec{b})^2}{(sin\,\pi\vec{S}.\vec{b})^2}\frac{(sin\,\pi\vec{S}.N_3\vec{c})^2}{(sin\,\pi\vec{S}.\vec{c})^2}, \quad (1.2)$$

Where

$$S = \vec{K} - \overrightarrow{K_0}\,, \quad (1.3)$$

$\overrightarrow{K_0}$ - Incident vector,$\vec{K}$- scatter vector, $\vec{a},\vec{b},\vec{c}$ - vectors of lattices, F_0- amplitude of the scattered wave from an unit sell, which depends on the nature of the atoms in the sell and on the relative positions of atoms, R - the distance between the observed point and the crystal, N_1, N_2, N_3- the number of unit cells are in the directions $\vec{a},\vec{b},\vec{c}$ respectively.

Fig.1.1shows dependence the intensity distribution respect with number of cells in the crystal. As it is seen, when number *N* decreases the intensity distribution become wider, i.e. the width of intensity distribution is directly related to the size of diffracting crystals.

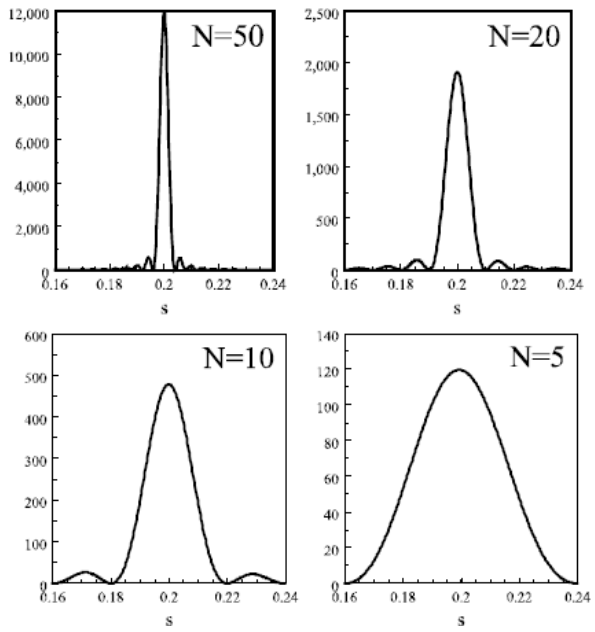

Fig.1.1 Effect of the number of cells on the intensity distribution

The expression $\frac{(\sin\pi\vec{S}.N_1\vec{a})^2}{(\sin\pi\vec{S}.\vec{a})^2}$ has a value of maximum, equal N_1^2, when value of $\overrightarrow{S}.\vec{a}$ is equal an integer number . Therefore diffracted intensity reach their maximum when

$\vec{S}.\vec{a}$=h, $\vec{S}.\vec{b}$=k, $\vec{S}.\vec{c}$=l (1.4)

These three equations are called the Laue conditions. Then maximum (1.2) obtained the following

$$I_{max} = \frac{{F_0}^2}{R^2} N^2, \qquad (1.5)$$

Where N = $N_1.N_2.N_3$. The intensity of maximum I_{max} observed in a certain small angular region in the direction of selective reflection.

Dynamic theory

Simultaneously with development of the kinematic theory, other theory so-called dynamic theory of X-ray diffraction in perfect crystals was developed by Darwin. In Darwin's dynamic theory, X-rays reflected from the crystal was considered as a steady flow of multiple reflections from parallel planes.

At each lattice plane, the incident wave generates a reflected and a transmitted wave. Each one of these in turn generates reflected and transmitted wave each time when it crosses from an atomic plane. Darwin compared his theoretical results with the experimental measurements and found them disagreement both with respect to the value of the reflected intensity and with respect to the width of the reflection domain which was very much larger than predicted. For explanation of this difference, Darwin concluded that this disagreement is due to the imperfection of the crystal, for that reason he suggested model of diffraction by a conglomerate of crystalline blocks (mosaic) and phenomena of extinction. Bragg and Ewald further refined this model. They considered that real crystals are made of mosaic of small blocks more or less missoriented with respect to one another, where each block is a perfect structure. In addition, they applied correction of primary extinction in dynamical theory. Darwin's theory leads to the same expressions of the reflectivity as the Ewald-Laue theory, but is not easily adaptable for calculation of energy paths and, for that reason, has been seldom used in the later developments of the dynamical theory. However, that is useful in the case of layered media or in the case of surface diffraction.

Laue introduced the concept of a continuous distribution of electron density in the crystal instead of concept of localization of electrons around the nucleus. This theory was confirmed by number of fundamental studies [1-5]. These theories were further developed in [6,7].

Kato [8] classified the dynamical theory of X-ray scattering into three types: a) the theory of Darwin, b) the theory of Ewald, c) the theory Laue.

In Darwin's theory, scattering elementary units are atomic plane and taken into account the interaction of waves propagating in the crystal from the first layer to the subsequent layer. Ewald developed this theory, but his theory has a much wider scope than Darwin's theory. One of the important results this theory was the introduction of the notion of wavefields. Ewald proposed point dipoles are scattering units, which localized in the crystal lattice. Dipoles within matter under external electromagnetic field have to oscillate. As a result, dipoles emit secondary electromagnetic waves with a frequency equal to the frequency of the exciting field. This process supports the propagation of the incident beam in media. In this theory, Ewald predicted interference effects with scattering x-rays.

In contrast to Ewald's dynamical theory which discusses the interaction of an electromagnetic wave with a distribution of discrete dipoles, Laue's basic assumption is the consideration to the electric negative and positive charges which are continuously distribution throughout volume of the crystal. Therefore the dielectric susceptibility, or polarizability, of the medium for x-rays can be considered asthe distribution of continuous in throughout volume of the crystal which is proportional to the electron density, i.e.the whole crystal was considered as scattering element.

The Maxwell's equations were used for propagated waves inside the crystal by Ewald and Laue's dynamical theories of x-ray diffraction. Later, Zachariasen developed this theory [7] and obtained a formula which it predicted existence of the anomalous transmission of x-rays in crystals which $\mu t \geq 10$.

In 1959, Kato and Lang experimentally discovered the interference effect by the investigation ofx-ray scattering at the wedge-shaped sections of the crystals [9]. Kato with analyze the experimental data, showed that a certain type of the interference pattern created by the spherical waves in crystals, he developed a version of the dynamical theory in the incident of spherical waves [10].

The calculation of the scattering intensity as the kinematic and dynamic theories eventually leads to the determination of the ability of radiation scattering by atomic lattice structure. Moreover, it is known that the share of nuclei in the scattering process is very small and can be neglected. Therefore, we can assume that the amplitude of wave diffracted by a crystal is the sum of the scattering waves from the appropriate electron in n atoms of a cell. This amount is determined by the expression

$$A = N.a_e.F_{hkl} \tag{1.6}$$

where N is number of unit cells in the crystal, a_e is the amplitude of the wave scattered by a free electron, F_{hkl} is called structure factor of the reflection from the planes *(h, k, l)* (in general,F_{hkl} is a complex number).

Reflectivity in Kinematic theory

The integrated reflectivity *P* is the ratio of the total energy received by detector, while the crystal is rotated, divided by the intensity of the incident beam and by the cross-section of beam Fig.1.2

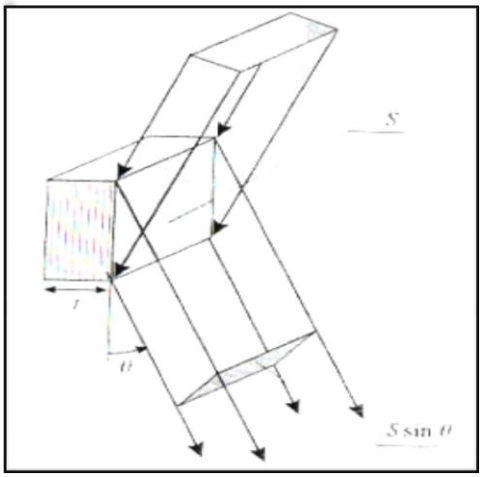

Fig.1.2cross-section of the beam diffracted by a small crystal

According to kinematic theory, the integrated reflectivity R_k from atomic planes*(hkl)* of a thick absorbing crystal in the case of transmission geometry is given by [2]:

$$R_k = \frac{e^4}{m^2c^4} \cdot \frac{1+(Cos\ 2\theta_B)^2}{2\ Sin\ 2\theta_B} \cdot \frac{\lambda^3}{V^2} \cdot |F_{hkl}|^2 \cdot \frac{t}{Cos\theta_B} \times exp\ \left(\frac{-\mu t}{Cos\theta_B}\right) \qquad (1.9)$$

Whereμ- absorption coefficient, *V* - volume of the unit cell,F_{hkl}- structure factor,λ - wavelength of incident beam, t - crystal thickness. This expression is also used for neutrons diffraction, but not quite well for high-energy electrons and certainly not so for low-energy electrons [2].

Reflectivity in Dynamic theory

According to the dynamic theory, the integrated reflectivity R_d in the case of reflected geometryfor thick and non-absorption crystal is obtained following

$$R_d=\frac{8}{3\pi}\frac{e^2}{mc^2}\cdot\frac{|C|}{sin\,2\theta_B}\cdot\frac{\lambda^2}{V}\cdot|F_{hkl}|\,, \tag{1.10}$$

Where *C* is polarization factor and in case of transmission geometry is following

$$R_d=\frac{e^2}{mc^2}\cdot\frac{|C|}{2Sin\,2\theta_B}\cdot\frac{\lambda^2}{V}\cdot|F_{hkl}|\int_0^{2\pi t/\wedge_l}J_0\,(z)dz\,, \tag{1.11}$$

Where J_0(z) is the zeroth-order Bessel function and l so-called Pendellosung distance and its value in case of the symmetric is

$$\wedge_l=\frac{mc^2\pi VCos\theta_B}{e^2\lambda C|F_{hkl}|}=\frac{\pi VCos\theta_B}{R\lambda C|F_{hkl}|}, \tag{1.12}$$

R is called the classical radius of the electron. The integrated reflectivity in the dynamic theory is proportional to $|F_{hkl}|$ and λ^2.When crystal thickness increases to large values, term of integration tends toward 1. Therefore, integrated reflectivity in the dynamic theory is proportional to $|F_{hkl}|$ and λ^2, in contrast to the value of integrated reflectivity given by kinematic theory, which is proportional to $|F_{hkl}|^2$ and λ^3.When ratio $t/\wedge_l$ tends toward zero, (1.11) is converted to

$$R_d=\frac{e^4}{m^2c^4}\cdot\frac{|C|^2}{Sin\,2\theta_B}\cdot\frac{\lambda^3}{V^2}\cdot|F_{hkl}|^2\cdot\frac{t}{Cos\theta_B} \tag{1.13}$$

That is equivalent to the expression (1.9) obtained in kinematic theory. Therefore, kinematic theory is a good approximation when crystal thickness is much smaller than l.We know which to perfect or not perfect, a crystal depends on conditions of diffraction. Freund showed this fact by experience [11]. He studied the integrate reflectivity of the (222) reflection with different wavelengths for several copper crystals with different degrees of perfection. In fig1.3Samples B_1 to B_4 are with dislocation densities 2×10^4, 4×10^4, 7×10^4, 2×10^7 dislocations/cm^2, respectively and sample C_1 is a dislocation-free.the wavelength vary from 0.03 to 1.66 A˚(the short wavelength areγ-rays).As can be seen sample C_1 behaves like a perfect crystal for wave lengths greater than 0.1 A˚ but seems quite imperfect for wavelength smaller than about 0.07 A˚. Samples B_1, B_2 and B_3 behave nearly like a perfect crystal for wavelengths above the K absorption edge of copper while for a wavelength of about 0.01 A˚ they behave like an ideal mosaic crystal. Sample B_4 behaves essentially like a mosaic crystal. these results can be interpreted by Pendellosung distance which increases with the decrease of wavelength and coherent domains in the sample appear smaller as wavelength becomes shorter, as the result sample behave like a imperfect crystal(Fig.1.3)

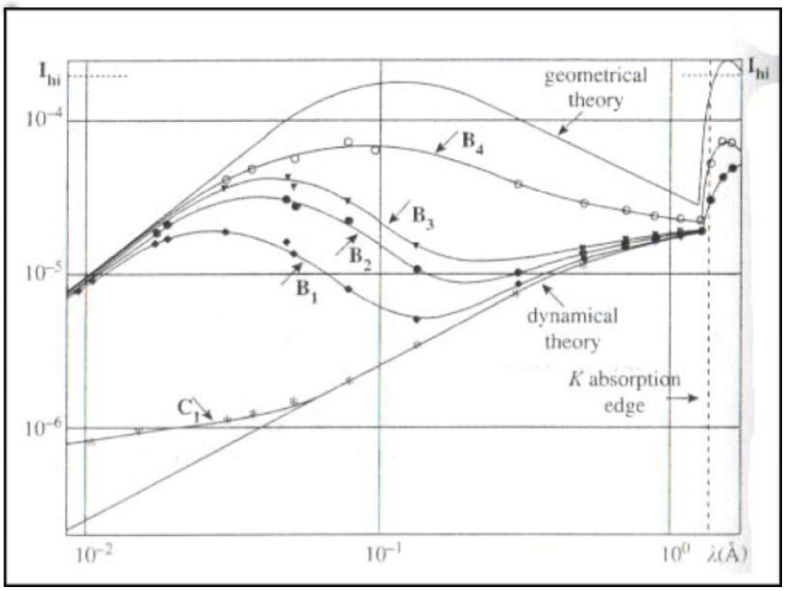

Fig.1.3 Variation integrated reflectivity with wavelength for (222)reflection of several copper crystals with different degrees of perfection.

When a crystal deform in a controlled way, it is possible, to determine between the perfect and the ideally imperfect crystal cases. These investigations began under the influences of external forces on the X-ray diffraction. The first works in this field were carried out in 1931 [12-14]. However, the first theoretical works, which tried to explain the results, were in 1961 [15-16]. One of these theories is the theory of Penning-Polder, which was modeled from propagation of light beams through inhomogeneous media. The paths of wave fields in deformed materials are bent, as light rays in a region with varying index of refraction, these paths and the variations of the reflected intensity are calculated using ray theory based on modification of dynamical theory and Fermat's principle. This theory is valid when the deformation of crystal be small enough. Condition of validity this theory (sometimes called ray theory) is following

$$\frac{\partial^2(h.u)}{\partial s_o \partial s_h} \ll \frac{1}{\Lambda^2} \tag{1.14}$$

Where h–reciprocal lattice vector, u – deformation vector, Λ - Pendellosung distance (or extinction distance) and s_o, s_h - coordinates in long of incident and reflected directions.

More description about it, can find in [15]. The case of arbitrary deformations was considered in [16], it give a set of equations for solving the problem of propagation of x-ray in any kind of the deformed crystal.

1.1.2. The effect of the external influence on the parameters of the reflected and transmitted x-ray beams

As it is known the intensity of the diffracted X-ray beams changes under the influence of external forces, such as the temperature gradient, the acoustic vibrations, mechanical stress, elastic deformation, pulse pounding, dc voltage, etc.

Studies were carried out both in the anomalous transmission ($\mu t \sim 10$) [17,18] and in non-normal transmission ($\mu t \sim 1$) [12-14, 19] of X-rays through a crystal.
The study of behavior of the intensity of the transmitted beam anomalously under external influences showed that these effects lead to the decrease in the intensity of transmitted and diffracted beams until vanish [18,20].
In addition to these studies, many studies carried out on the effect of acoustoelectric oscillation and bent crystals on the intensity of the diffracted X-rays [21, 22, 46, 69, 70,82-97]. The main results

Briefly obtained in some of these studies, are given following:

In [21] was shown that the Debye-Waller factor describes correctly the Borman effect acoustic suppression only within the short-wave range ($\lambda_s \ll \tau$, λ_s ultrasonic wavelength, τ extinction length). In [22] the rocking curves of Silicon-crystal were measured with a high angular resolution under conditions of the Borman effect resonant suppression by transverse ultrasonic vibration. It was shown that on the curves deep minima appear whose positions depend on the vibration frequency.

The many interesting theoretical and experimental results obtained in the field of dynamic X-ray scattering in distorted and bent crystals [20-22, 97-104]. We only mention them the following: as anomalous transmission of X-rays is obtained only from perfect single crystals, any effects that lead to the distortion of a perfect crystal violate conditions of the anomalous transmission. Consequently, the decrease of the intensity of the transmitted and diffracted beams is as a function of the degree of distortion, and in the case of strong distortions, they disappear. This is in good agreement with the theory of dynamic scattering of X-rays in thick crystals ($\mu t \geq 10$). With respect to the fact, this dissertation is devoted to the study of external influences on the intensity of the transmitted, absorbed and diffracted X-ray in non-anomalous mode ($\mu t \sim 1$). Therefore the following is more detailed about the results of studies of external influences on the intensity of X-rays for this case. In this area, many studies have been performed such as [12, 13,19,23-37,66,67] which related to the X-ray scattering from crystals of piezoelectric. For the first time in [12] observed changes in the intensity of the diffracted X-rays by applying an alternating voltage with the resonance frequency

on the quartz piezoelectric crystal. As result of researches determined that the intensity of the Laue reflections with the white radiation in the presence of vibration in the piezoelectric quartz is more than the intensity of the reflections of the crystal without vibration.

In [23] the crystal was set in the position of Bragg reflecting and exposed vibration. The results of this work showed that intensity and line broadening change.

In [24-26], the intensity of the reflected beam was almost no change in the excitation of the crystal with the second harmonic frequency of the crystal.

In [27]was investigated which different cuts of the crystals may change intensity of the Laue reflections. In [28] considered the dependence of the intensity of the diffracted X-ray beam on the applied voltage. This dependence is shown in Fig 1.4. As is seen from the figure, the intensity of the reflection increases up to a certain value of electric field. Further increase in voltage leads to a decrease in the intensity of the reflected X-ray beam.

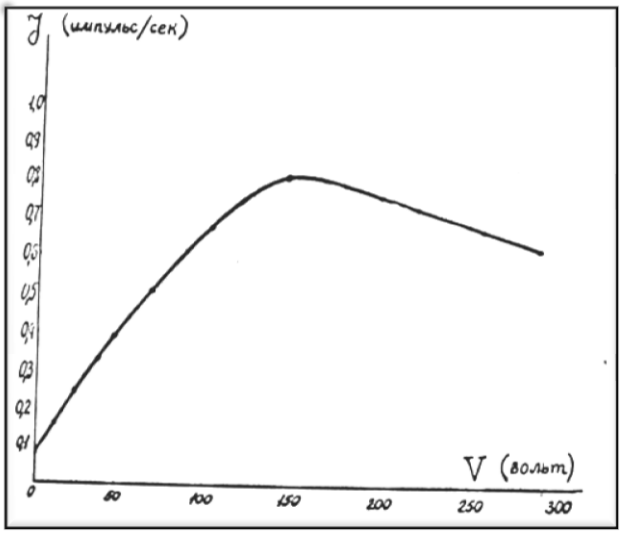

Fig.1.4. The intensity of the reflected beam versus the voltage of electric field of resonant frequency.

After a long pause of research (about 30 years) under the influence of piezoelectric effect in reflection of Laue geometry, the new phase of similar studies began. As will be seen follows, this was due to the appearance of new advanced features of X-ray radiation. Ref. [19] shows the dependence of the intensity of the diffracted X-rays on the value of the current due to the applied electric field (Fig.1.5). It shows that the intensity of the diffracted beam increases with the increase of the current up to a certain value and then it will close to saturation position. In this work used from MoK_{α} radiation and the thickness of the quartz plate was chosen such that $\mu t=1$. The

experimental results confirm the prediction of the dynamic theory of weak deformation of the non-absorbing crystal.

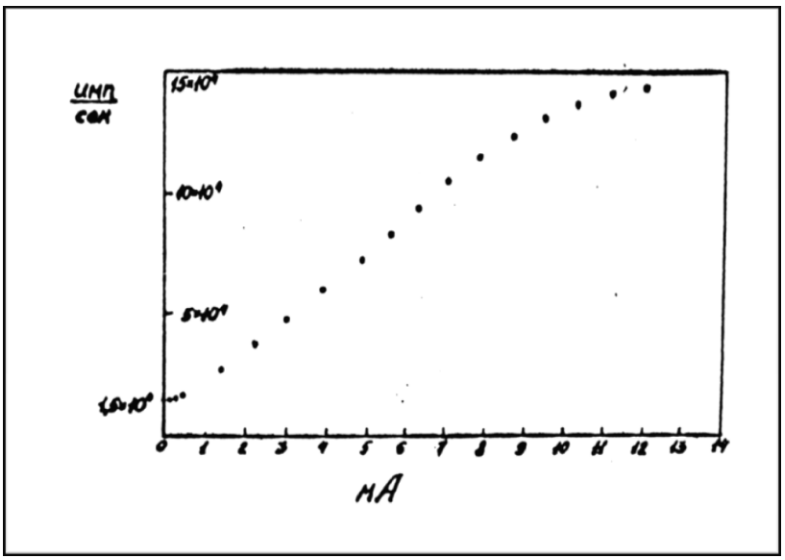

Fig.1.5. The intensity of the diffracted beam with the current (in mill amperes) applied to quartz crystal[19].

Later in [29] considered to dynamical theory of X-ray diffraction in crystals with one-dimensional modulated electron density. It obtained approximate expressions for the diffraction amplitude in the case of Laue and Bragg with modulation harmonically and the assumption that modulation does not affect in frequency of the crystal.

The effect of vibrations on the intensity of scattering of X-rays from the piezoelectric crystal has been studied in [30-37]. In [30-34] have shown that when vibration is applied the perpendicular to the primary beam and the crystal is thick enough, doublet Laue spots disappears and increases the intensity of the reflections. In [35] has studied the diffraction of X-rays from the oscillating quartz plate and pictures taken topographs in the vibration of the crystal.

In [69, 70], X-ray diffraction was experimentally studied in the Laue geometry in a germanium crystal carrying a ultrasonic wave that creates an alternating lattice deformation along the sample surface.

Authors [78] proposed and implemented a method for measuring rocking curves via the ultrasonic modulation of the lattice parameter. This method was based on the interaction of long- wavelength with X-rays in crystals.

After the discovery of the effect of complete transfer of X-rays from the direction of the transmission to the direction of the reflection [36], in work [37] with use of Takagi's equation presented an estimation of quantitative from changes in the intensity of the transmitted and reflected beams.

Thus, the summary of the results above, we can say that the excitation of the crystal by the acoustic waves is increased intensity of the diffracted X-ray intensity and the amount of increase depends on the amplitude of the applied voltage.
Similar results were obtained in the thermal neutron diffraction [38-46], under external influences on the sample.

In the continue of this section, we review the works which relate to effects of the temperature gradient and other types of external influences on distribution and intensity of the diffracted X-ray beam from a single crystal. In [36, 47-49], the studies are devoted to effect of the temperature gradient on the Laue spots. The pattern obtained under the influence of the temperature gradient compared with pattern without the temperature gradient and was found that the splitting of the Laue reflections disappears and their intensity increases.

The study of the effect of the temperature gradient on the intensity of X-ray reflections showed that the intensity of X-ray reflections strongly depends on both the magnitude and direction of the temperature gradient (the angle between the gradient vector and the normal to the reflecting atomic planes), and the arrangement of the gradient and diffraction vectors (parallel or antiparallel [51]).

The authors[47] showed that the weak temperature gradient(~15 ° C /cm) change the intensity of the Laue reflections corresponding to those planes, which are vertical (or close to vertical) to the temperature gradient vector. It was also shown that the beam exited from the part of the perfect crystal undergoes a greater change in intensity than the beam which exit from part of imperfect the crystal. The effect of gradient also depends on the value of the distance between atomic planes (see[47, 48,51]).

In [52], which is mainly experimental, the different theories about the propagation of X-rays in a slightly deformed crystals was compared and Temperature gradient was elected for deformation of the crystal by the author .Because, the mathematical expressions for such deformation are rather simple, and on the other hand, strain is easily controlled experimentally.

The study of the influence of temperature gradients (~100 c˚/cm) on the x-ray scattering in crystals found a new wave field [49]. Experimental evaluation of the intensities of the primary and the new wave fields are in good agreement with theoretical predictions.

Dynamical diffraction in a crystal with distortions is the sum of dynamic scattering in perfect regions of crystal and scattering on the distortions. This allowed Takagi [53] to create a separate theory that describes the process of dynamical diffraction inside the crystal distorted.

The authors [17,68] solved the thermal conductivity equation for two and three dimensional cases in respect to experimental conditions. They obtained expression for the displacement function which satisfies Takagi equation.

Ref. [83] Studied the dynamics of changes in the intensity Laue reflected beam while the value of the temperature gradient continuously changes. It established high sensitivity of intensity X-ray beam with a parallel arrangement of diffraction vector and the gradient vector at μt ~2.

In [106], experimentally and theoretically was investigated the behavior of the interference coefficient of absorption of X-ray in the quartz crystal under the influence of temperature gradient in Laue geometry and was shown that with the increase in temperature gradient, the coefficient of absorption of X-ray suddenly decreases until it reaches its minimum value at a certain value of temperature gradient.

[107] investigated the cross section of transmitted X-ray beam diffracted by reflecting atomic planes of quartz single crystal in Laue geometry for different values of temperature gradient applied to the crystal and was shown that the angular width of a fully pumped X-ray beam depends on the distance between the source and the studied sample and decreases with the increase in this distance.

Now, we consider several types o fexternal effects created on a crystal and lead to changes in the intensity of the diffracted beam. From this viewpoint the work of [14] is interest, it showed a significant increase in the intensity of the reflected X-ray emission from single-crystal quartz when it is placed between the plates of a capacitor, with a constant voltage (50-100 kV /cm). In [54]confirmed the main experimental results observed in[14].At the same time present a model to explain this effect and this effect was named by the authors piezoelectric effect of quasi-mosaicity.

In [54] demonstrated a significant increase in the luminosity of the diffraction of X-ray beamsat work with two-crystal spectrometer, when the two crystals was applied dc voltage, the total increase in the intensity of the reflected beamwas20-30 times while width of the lines was not changed. The

intensity of the diffracted beam begins to increase with switching voltage and the process continues much long time (several hours).

The amplification of the Bragg reflection from a quartz crystalline a strong electric field(U / t>10^5kV/ cm) was observed in [55].When turning off the electric field, intensity of the reflection took the original value.

In [56] studied the reflectivity of the quartz and ADP crystals in two forms: the ordinarily and chemically polished crystals. It demonstrated that in the shortwave region, reflective qualities of ordinary crystals higher than chemically polished crystals. With increasing wavelength, chemically polished crystals have stronger reflectivity.

In [57] studied the character of the diffracted beam from a crystal under influence of the compression of strike. It is shown that the moment of strike at the maximum intensity of the line is almost unchanged, and the line width greatly increases.

In addition to he above, there are a large number of papers devoted to dynamical X-ray scattering in bent crystals elastically.

Note that we have listed in the review of the mentioned works, which are most similar to the topics of this dissertation. As can be seen from the analysis of these studies ,in references there are not often data concerning structure and changes in the intensity of the transmitted and reflected beams and absorption in the presence of a temperature gradient and the acoustic field when $\mu t \leq 1$.

1.2 Basic equations of dynamic X-ray diffraction rays and thermal neutrons [81-83]

X-rays as the short wavelength electromagnetic waves and thermal neutrons reveal the dual nature of the interaction with matter, namely reveal the properties of both particles and waves. X-ray is electromagnetic radiation, and in dynamic scattering on the crystal lattice is considered from the point of view optical wave. So, naturally, the phenomenon of diffraction by a crystal lattice is based on classical Maxwell's theory, even though the medium is described by quantum-mechanical quantities, namely the Schrödinger electron charge density and current density. For an electron interact with an electromagnetic field, Schrodinger current density is defined

$$j = \frac{e\rho}{mc}\vec{A},$$

and accordingly

$$D = \left(1 + \frac{e\rho}{\pi m \nu^2}\right)\vec{E},$$

Where v is frequency and $\vec{E}$ is electric field intensity of X-ray waves. So the medium have a dielectric constant and polarizability following:

$$\varepsilon = 1 + \frac{e\rho}{\pi m v^2} \quad \text{and} \quad \chi = \varepsilon - 1 = \frac{e\rho}{\pi m v^2}, \tag{1.21}$$

Note that the relations (1.18) and (1.19) are considered as microscopic quantities, i.e. taking place at each point in space, because polarization vector $\vec{P}$, the field intensity $\vec{E}$, the displacement vector $\vec{D}$ and the charge distribution density ρ are functions of the coordinates.

The wave equation for the vector of the electric induction $\vec{D}$, according to Maxwell's equations would be:

$$\nabla^2\vec{\mathrm{D}} + 4\pi^2\mathrm{k}^2\vec{\mathrm{D}} + \mathrm{rotrot}\left(\chi\vec{\mathrm{D}}\right) = 0 \ , \tag{1-22}$$

Where $k = v / c = 1 / \lambda$ is the wave number in vacuum and λ is wavelength of radiation.
Let N be the average number of electrons per unit volume, so that the average charge density is equal to

$$\overline{\rho} = -eN, \tag{1-23}$$

therefore

$$-\frac{e\overline{\rho}}{\pi m v^2} = \frac{e^2 N}{mc^2\pi k^2}, \tag{1-24}$$

Inserting values of $\frac{e^2}{mc^2} = 2{,}8 \cdot 10^{-15}$м, $k^{-2} = \lambda^2 \sim 10^{-20} m^2$ and $N \sim 6 \cdot 10^{29} m^{-3}$, we find that

$$\frac{e\overline{\rho}}{\pi m v^2} < 10^{-4}. \tag{1.25}$$

Hence (1.35) have

$$\chi \simeq \frac{e\overline{\rho}}{\pi m v^2} < 0. \tag{1.26}$$

As a result, the polarizability of the medium is a periodic function of the coordinates, which is the Schrödinger charge density $\rho(\vec{r})$ space lattice of the crystal.

Now we consider the basic principles of neutron diffraction waves [83], in particular thermal neutrons waves. Neutrons are considered as neutral particles. Recently the most accurate measurements show that the electric charge of the neutron $< 10^{-21} e$. The neutron lifetime, τ = 886 s [5], is much longer than the time of a neutron within a scattering experiment. The neutron is electrically neutral but has a magnetic moment

$$\mu = -\gamma \mu_N, \tag{1.27}$$

Where $\gamma = 1.913$ and the nuclear magneton is given by $\mu_N = e\hbar/m_P$ where m_p is mass of proton. The neutron magnetic moment is coupled antiparallel to its spin, which has the value s = 1/2.

The neutron interacts with nuclei via the strong nuclear force and with magnetic moments via the electromagnetic force.

In neutrons scattering experiments, neutrons behave as particles when they are created, as waves when they scatter, and again as particles when they are detected.

The neutrons source is nuclear reactions. Bombarding a target by accelerated particles such as electrons, protons or deuterons is one way creation of the neutron. In these reactions, the output neutron is defined as one neutron for one incident particle. For large number of neutrons are used nuclear fission or nuclear fusion.

For the coherent interaction of neutron waves with condensed matter, it is necessary kinetic energy of thermal neutrons be ~ 25meV, because it is the range of energy, which is necessary for the excitation of many condensed matter. Based on de Broglie wavelength

$$\lambda = \frac{h}{P} \tag{1.28}$$

Where P is neutron momentum, for such neutrons, λ is same order of interatomic distances, which is necessary for phenomena of coherent neutron scattering and observing interference phenomena and the neutron diffraction in crystal lattice. Meanwhile, for many reactions of fission and fusion neutron energy distribution is concentrated around the energy several mev. For the selection of thermal neutrons (~ 25meV) from this distribution and reduce the number of cold (<10meV) and hot neutrons (> 100meV) are used moderator, which due to inelastic scattering are removed cold and hot neutrons. The characteristic pattern of distribution of the number of neutrons with respective energy after the moderator which is quite well described by the Maxwell distribution (see. Fig 1.6)

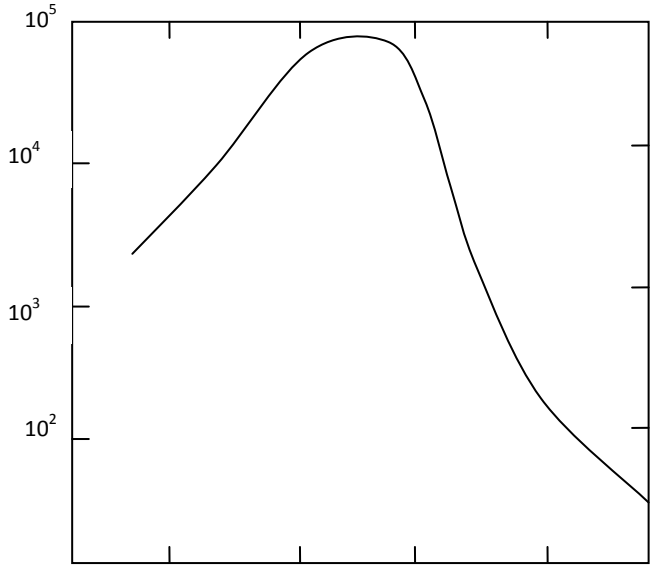

Fig. 1.6 The energy distribution of neutrons after moderator [83].

The distribution pattern of Figure 3 shows one of the characteristics of neutron beams, namely, fairly large width of energy distribution of beams.

In the many problems in dynamic neutron scattering on the crystal lattice, in particular in study the interference phenomena (pendulum effect, primary extinction, interference contrast arises in different multi-chip systems, etc.) it is necessary to neutron beams with a high degree of monoenergetic. In addition, neutron beams are emitted in a fairly wide angular range. Consequently, collimation of these beams are especially need in works that are based on the plane-wave approximation of dynamical scattering of neutron, such as registration of the rocking curves and plane wave topography, etc. The spatial concentration (focus) of neutron beams is very important, besides the above-mentioned features, neutron beams are wide enough in the spatial distribution. The latter feature becomes very important with consideration energy power of neutron sources which are much lower than the X-ray sources.

In contrast distribution of X-rays, which are described by Maxwell's equations and lead to the wave equation (1.22), the distribution of neutron waves, in particular, the thermal neutrons is described by the Schrödinger equation

$$\nabla^2\psi + \frac{8\pi^2 m_n}{h^2}\left(E - V(\vec{r})\right)\psi = 0, \quad (1.29)$$

Where $m_n$is neutron mass, E is the total energy of the neutron and $V(\vec{r})$ is the scalar potential of the medium. According to the relation of de Broglie have

$$\frac{8\pi^2 m_n}{h^2} E = k^2 = \left(\frac{2\pi}{\lambda}\right)^2, \quad (1.30)$$

Where λ is de Broglie wavelength of neutron in vacuum, we can say that $\frac{8\pi^2 m_n}{h^2} V(\vec{r})\psi$ corresponds to the term $rotrot\left(\chi\vec{D}\right)$in (1.22).

The characteristic of the medium in this case is exactly the scalar potential $V(\vec{r})$, which describes the interaction of neutrons with nuclei of the atoms of the medium. Based on the theory of neutron diffraction pseudo potential Dirac is

$$\mathrm{V}(\vec{\mathrm{r}}) = \frac{\mathrm{h}^2}{2\pi \mathrm{m_n}} \sum_{\mathrm{j}} \mathrm{b_j} \delta\left(\vec{\mathrm{r}} - \vec{\mathrm{r}}_{\mathrm{j}}\right), \quad (1.31)$$

Where $b_j$is neutron scattering length, $\delta(\vec{r}-\vec{r}_j)$ is Dirac delta function, $\vec{r}_j$is radius-vector and the summation is over all $\vec{r}_j$, i.e. over all the nuclei of the medium.

Naturally in Dirac pseudo potential (1.31) the scattering centers are considered as point, unlike X-rays, which the scattering centers distribute as continuous density $\rho(\vec{r})$. This, one of the characteristic when consider in the neutron diffraction waves. The potential (1.31) is a periodic function of the coordinates of the crystal lattice which can be represented as a Fourier series:

$$V(\vec{r}) = \sum_h V_h e^{2\pi i \vec{h}.\vec{r}}, \tag{1.32}$$

Where the summation is over all vectors $\vec{h}$ reciprocal lattice, and the Fourier coefficients of $V_h$defined as

$$V_h = \frac{1}{V_c}\int_{V_c} V(\vec{r}) e^{-2\pi i \vec{h}.\vec{r}} dV \tag{1.33}$$

Where$V_c$is the unit cell volume, and the integration is performed over the entire volume V_c. with consideration of (1.31) we obtain

$$V_h = \frac{2\pi h^2}{m_n V_c}\int_{V_c} \sum_j b_j \delta\left(\vec{r}-\vec{r}_j\right) e^{-2\pi \vec{h}.\vec{r}} dV = \frac{2\pi h^2}{m_n V_c}\sum_{V_c} b_j\, e^{-2\pi i \vec{h}.\vec{r}_j}\ , \tag{1.34}$$

The coefficient of Fourier – Dirac's pseudo potential can be represented as

$$V_h = \frac{2\pi h^2}{m_n V_c}\int_{V_c} \sum_j b_j e^{-2\pi i \vec{h}.\vec{r}_j} = \frac{2\pi h^2}{m_n V_c} F_h\ , \tag{1.35}$$

Where F_h is the structure factor for the vector $\vec{h}$ reciprocal lattice or reflecting atomic planes with Miller indices (hkl). Note that so defined the structure factor for neutrons is long.

X-rays interact with the medium by the Thomson scattering and susceptible to the electron density distribution in the medium, which is a periodical function of the coordinates of the crystalline medium. Therefore, the characteristic value of the interaction of X-rays with the crystal determine with structure factor which is $F_h = \rho_h V_c$ where $\rho_h$is Fourier components of the density $\rho(\vec{r})$of elementary charge.

The structure factor for x-rays is defined as:

$$F_h = \sum_{V_c} f_{aj}\left(\vec{h}\right) e^{-2\pi \vec{h}.\vec{r}_j}\ , \tag{1.36}$$

Where$f_{aj}(\vec{h})$is atomic factor or form factor of atom j at position $\vec{r_j}$. For X-ray diffraction structure factor F_h is ratio of the amplitudes of the diffracted beam for one unit cell to the scattering amplitude for a free electron.

As a result, comparison of the two cases, the scattering of X- rays and neutrons, can be changed to the replacement of F^n (for neutrons) to r_0F^x for x-rays, ($r_0 = 2{,}8 \cdot 10^{-15}m$ is the classical radius electron).

Both equations (1.22) and (1.29) describe the propagation of X-ray and neutron waves, respectively, which are in the form of an inhomogeneous wave equation and a special solution that vanishes at infinity and has a similar form for both equations. For x-rays, this solution has the form

$$\vec{D} = \frac{1}{4\pi}\int \frac{rotrot\left[\chi(\vec{r})\vec{D}(\vec{r},\acute{t})\right]}{R} d\acute{V}, \tag{1.37}$$

Where R = $[\vec{r} - \vec{r}']$is the distance between the points with the radius vectors $\vec{r}$and$\vec{r}'$, and$t' = t - \frac{R}{c}$ is time delay of the scattered wave at the point $\vec{r}$and$\vec{r}'$. For neutron waves similar solution can be written as:

$$\psi(\vec{r},t) = -\frac{2\pi m_n}{h^2}\int \frac{V(\vec{r})\psi(\acute{r},\acute{t})}{R} d\acute{V}. \tag{1.38}$$

The general solution of the inhomogeneous wave equations, according to well- known theorem of differential equations with partial derivatives can be represented as the sum of the general solution of the homogeneous wave equations and partial solutions (1.39) and (1.40), respectively:

$$\vec{D}(\vec{r},t) = \overrightarrow{D_0}(\vec{r},t) + \frac{1}{4\pi}\int \frac{rotrot\left[\chi(\vec{r})\vec{D}(\vec{r},t)\right]}{R} dV, \tag{1.39}$$

$$\psi(\vec{r},t) = \psi_0(\vec{r},t) - \frac{2\pi m_n}{h^2}\int \frac{V(\vec{r})\psi(r,t)}{R} dV, \tag{1.40}$$

Where$\overrightarrow{D_0}(\vec{r},t)$and $\psi_0(\vec{r},t)$ the general solution of the homogeneous wave equations corresponding to (1.36) and (1.37) with $\chi(\vec{r}) = V(\vec{r}) = 0$.

In the special case which the time dependence of the wave fields $\overrightarrow{D_0}(\vec{r},t)$ and $\psi_0(\vec{r},t)$ are represented in the form of $e^{i\omega t}$, i.e. wave fields are considered as monochromatic (1.39) and (1.40) are converted to the form:

$$\vec{D}(\vec{r}) = \overrightarrow{D_0}(\vec{r}) + \frac{1}{4\pi}\int \frac{rotrot\left[\chi(\vec{r})\vec{D}(\vec{r})\right]}{R} e^{2\pi ikR} dV\ , \tag{1.41}$$

$$\psi(\vec{r}) = \psi_0(\vec{r}) - \frac{2\pi m_n}{h^2}\int \frac{V(\vec{r})\psi(\vec{r})}{R} e^{2\pi ikR}\ dV, \tag{1.42}$$

where $k = \frac{\omega}{2\pi c}$ and $k = \frac{1}{h}\left(\frac{2m}{E}\right)^{1/2}$ are wave numbers in vacuum X-ray and neutron waves, respectively.

Equation (1.41) is an integro-differential, and (1.42) integral equation. Integral terms representto scattered among the area, considering to the multiple scattering inside the medium, in particular, the crystalline medium. The main differences between the processes of scattering of X-ray and neutron waves are in both equations characteristic functions $\chi(\vec{r})$ and $V(\vec{r})$. For X-ray, this function is proportional to the electron charge density $\rho(\vec{r})$ and the basic process of the scattering is Thomson scattering of electromagnetic waves by electrons and thus is characterized by the Thomson scattering length $\frac{e^2}{mc^2} = 2{,}82 \cdot 10^{-15} m$. For neutron scattering waves due to the interaction of neutrons with the nuclear of area

and under the assumption of a point scattering center due to the smallness of the effective distances ($\sim 10^{-15} m$) of nuclear interactions, the characteristic function of this interaction is the pseudo potential of the Dirac i.e.

$$V_F = \frac{(2\pi h)^2}{m_n}\delta(\vec{r}). \tag{1.43}$$

The second major difference is that, the wave of the photons are described by vector wave functions, while the wave function $\psi(\vec{r})$ of neutrons is scalar that shown in (1.39, 1.40). Other characteristics of the two fields are very similar. For example, the refractive index can be represented for both wave fields in a similar form

$$n = 1-\delta. \tag{1.44}$$

Nuclear scattering length in the same order as the Thomson length, but each atom has Z electrons and only one nuclear. On the other hand $k = \frac{1}{\lambda} \sim Å^{-1}$ is of the same order for x-rays and thermal neutrons, as a result δ is of the same order for both radiation $\delta \sim 10^{-5}$.

Now the features of the neutron absorption at the medium in comparison with the absorption of x-rays are described briefly. The absorption of waves as x-ray and neutron waves are described by the refractive index of the imaginary part

$$n = n_r + in_i. \tag{1.45}$$

The real part n_r for both radiations can be

$$n_r = 1 - \delta\ , \tag{1.46}$$

and the imaginary part describes actual loss of wave energy due to photo absorption, incoherent scattering and inelastic scattering:

$$n_i = \sum_j N_j\left(\sigma_j^p + \sigma_j^{inc} + \sigma_j^{ine}\right)/2k \tag{1.47}$$

WhereN_j is the number of atoms of various substances make the substance: $\sigma_j^p, \sigma_j^{inc} and\ \sigma_j^{ine}$ are interactions cross section of photo absorption, incoherent and inelastic, respectively. The average density of scattering can be written as

$$\overline{\rho} = \sum_j \rho_j b_j. \tag{1.48}$$

Relation between n_i and absorption coefficient μ is for

$$\mu = 2kn_i\ , \tag{1.49}$$

Finally we have

$$n = 1 - \delta + in_i\ ,\ \ \delta = \frac{2\pi}{k^2}\overline{\rho}b, n_i = \frac{\mu}{2k}\ . \tag{1.50}$$

We estimate the ratio $^{n_i}/_{\delta}$. For neutron cross-section of absorption $\sigma^\rho$is inversely proportional to k, so both the parameter δ and n_i, vary as k^{-2} and their ratio is independent of k

$$\frac{\mathrm{n_i}}{\delta} = \frac{\sigma_0^\rho}{\sigma^s}\mathrm{k_0 b}, \tag{1.51}$$

where $\sigma^s = 4\pi b^2$ is elastic scattering cross section and $\sigma_0^p = \sigma^p\frac{k}{k_0}$ is cross section for a certain selected as the initial value of k_0 (usually $k_0 = \frac{1}{\lambda_0}$ corresponds to the wave number for neutrons with a velocity $V_0 = 2000\frac{m}{s}$accordingly the length of de Broglie wave $\lambda_0 = \frac{h}{m_n V_0} \simeq 3{,}5\dot{A}$). Since$\frac{\sigma_0^\rho}{\sigma^s}\sim 1$, and $k_0 b\sim 10^{-5}$, it is obvious that $n_i \ll \delta$ and the contribution of the conventional absorption is negligible in the interaction of neutrons with matter[98].

For X-ray have

$$n_i = \frac{\overline{\rho}\sigma^{\rho}}{2k}, \tag{1.52}$$

$$\delta = \frac{2\pi}{k^2}\rho(zr_0). \tag{1.53}$$

So that the ratio

$$\frac{n_i}{\delta} = \frac{\sigma^{\rho}k}{4\pi z r_0}. \tag{1.54}$$

In turn, the photo absorption cross section of X-rays is

$$\sigma^{\rho} = \sigma_0^{\rho}\left(\frac{k_0}{k}\right)^3 z^4. \tag{1.55}$$

So have

$$\frac{n_i}{\delta} = \frac{\sigma_0^{\rho}k_0}{4\pi r_0}\left(\frac{k_0}{k}\right)^2 z^3 \quad . \tag{1.56}.$$

And since σ_0^{ρ} is ranges 0.1- 0.01and $\frac{k_0}{\text{к}} \leq 1$, the absorption becomes important for relatively heavy elements.

As a result of the above description, we can conclude:

1. The equations describing the propagation of x-rays and neutron beams in the medium, including the crystals, are similar.

2. The main difference between these two cases is negligible absorption of the neutrons while X-ray absorption is significant in crystals.

3. Point the nature of the spatial distribution of the scattering centers for neutrons and unclear distribution of these centers for the X-ray beam. The latter considered the characteristic parameters, namely, the Fourier coefficients of the electronic charge distribution for X-ray waves and the pseudopotential of Dirac for interaction of neutrons with the nuclei of the lattice atoms.

Reasons using neutrons diffraction

Neutron scattering is one of the most powerful experimental methods, to study the structure and dynamics of materials on the nanometer scale. Neutrons determine where the atoms are and what the atoms do [3].

40 years ago, neutron scattering was a strange tool for solid state physicists and crystallographers, but today it is used as wide as Biology, Earth Sciences, Planetary Science, Engineering and

nanoscience. In brief, neutrons are used in all scientific fields that deal with condensed matter. Although the neutron scattering is expensive technique.

The X-ray scattering is selected for the study of atomic and nanometer-scale structure in materials. X-ray sources are by more access and are, especially synchrotron X-ray sources, much stronger than neutron sources. Hence, X-rays have the first rule in experiments.

Neutrons diffraction have preferred over X-rays in four general points:

1. Thermal neutrons have a wavelength (2Å) similar to inter-atomic distances, and energy (20 meV) similar to elementary excitations in solids.

Thus can simultaneously obtain information about the structure and dynamics of materials and e.g. measure dispersion relations (dependence of energy-wavelength) of excitations.

2. The neutron scattering cross section varies randomly between elements and even between different isotopes of the same element. Thus can use neutrons to study light isotopes. In particular, this is important for hydrogen, which is almost invisible with X-rays.

3. Since neutrons penetrate in matter easily, neutron scattering can be performed for the study very big samples up to 10 cm thickness, depending on its elemental composition.

4. With consider to property of the neutron magnetic moment , neutrons scatter from magnetic structures or magnetic field gradients. Unpolarized neutrons are used to determine the period and amount of the atomic magnetic moments, while scattering of spin-polarized neutrons can determine the direction them.

In most cases, neutron scattering is performed with other experimental techniques; often neutron scattering as one of the final techniques be used before conclusions.

1.3. Description of deformed space lattice with weak deformation

If crystal lattice is deformed continuously, operation of X-ray in the lattice is similar to the propagation of light waves in an inhomogeneous medium with continuously changing refractive index. This approach to the help of dynamical diffraction of x-rays has been developed for the first time in the work of Penning and Polder [15] and Kato [16] who considered the problem of X-ray trajectories of wave packets in a Bragg diffraction grating.

When the deformation is small enough, each small region of the crystal lattice can be considered as perfect with the effective local disorientation from the Bragg condition. Naturally, this

disorientation is a function of coordinates in the lattice. In this case, it is assumed that each point with the radius vector $\vec{r}$ simply shifted from its position to a new position (see Fig. 4)

$$\overrightarrow{r'} = \vec{r} + \vec{u}(\vec{r}), \tag{1.57}$$

where $\vec{u}(\vec{r})$ displacement vector, depending on the origin. It is assumed that during this displacement, distribution of the density of the scattering material (electron charge density for X-rays, the potential of nuclear forces for neutron beams or the potential of the Coulomb field of atoms in the electron waves) do not undergo changes during such a displacement, i.e. their values only shifting from $\vec{r}$ point to point $\overrightarrow{r'}$. Equation (1.57) can be rewritten as

$$\vec{r} = \overrightarrow{r'} - \vec{u}(\vec{r}) \quad , \tag{1.58}$$

if the coefficients of the stress tensor

$$\frac{\partial u_i}{\partial x_j} \ll 1 (i, j = 1,2,3), \tag{1.59}$$

With approximation can write

$$\vec{r} \simeq \overrightarrow{r'} - \vec{u}(\overrightarrow{r'}) \tag{1.60}$$

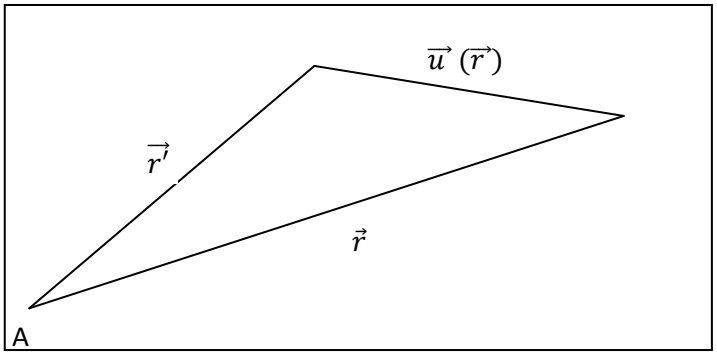

Fig .1.7 The relationship between the radius vectors $\vec{r}$ $and\overrightarrow{r'}$ and the displacement vector $\vec{u}(\vec{r})$

Before deformed crystal, equation of a plane of the family of direct lattice planes(hkl) is

$$H \equiv \overrightarrow{h}.\vec{r} = N \qquad (N = 0, 1, \ldots n), \tag{1.61}$$

reciprocal lattice vector $\vec{h}$ can be defined as the gradient of H.

$$\vec{h} = gradH \tag{1.62}$$

For the deformed crystal equation of atomic planes (1.61) and (1.62) are transformed into

$$H' = \overrightarrow{h}.\left(\overrightarrow{r'} - \vec{u}\left(\overrightarrow{r'}\right)\right) = N. \tag{1.63}$$

This equation determines the transformation of the atomic planes in the resulting deformation, and by analogy with (1.62) reciprocal lattice local vector can be defined as

$$\overrightarrow{h'} = grad\, H' = \vec{h} - grad\left(\vec{h}.\vec{u}\right) \ , \tag{1.64}$$

which naturally depends on the coordinates and represents the local reciprocal lattice vector.

Obviously, the local change of the reciprocal lattice vector

$$\overrightarrow{\Delta h} = \overrightarrow{h'} - \vec{h} = -grad\left(\overrightarrow{h}.\vec{u}\right) \ , \tag{1.65}$$

is also a function of the coordinates, and its small changes $\delta\left(\overrightarrow{\Delta h}\right)$will be determined by the second derivatives with respect to the coordinates in the form and its components are

$$\delta\left(\overrightarrow{\Delta h_j}\right) = -\frac{\partial^2(\vec{h}.\vec{u})}{\partial X_i \partial X_j}\delta x_i \ . \tag{1.66}$$

The dynamic theory is valid if this quantity be small with respect to the width of the dispersion surface, that is smaller than Λ^{-1}. If the spatial size of the wave packet be of the order of the extinction length

$$\delta x_i \sim \Lambda \ , \tag{1.67}$$

The condition of validity of the dynamic theory can be written as

$$\frac{\partial^2(\vec{h}.\vec{u})}{\partial X_i \partial X_j} \ll \frac{1}{\Lambda^2} \ , \tag{1.68}$$

and changes in the reciprocal lattice vector, must satisfy the condition:

$$\delta\left(\overrightarrow{\Delta h}\right) \ll \frac{1}{\Lambda^2} \ . \tag{1.69}$$

From the point of view of the Bragg diffraction, the lattice deformation leads to a local rotation of the atomic planes and local changes in the interplanar spacing. Rotate the atomic planes changes the

relative orientation of the beam and the planes. If before deformation, angular displacement from the exact Bragg condition is

$$\Delta\theta = \theta - \theta_B, \tag{1.70}$$

where θ is glancing angle of the beam relative to the planes, and θ_B is the angle at the exact Bragg condition, the Bragg angle after deformation $\theta_B$determined as follows:

$$\theta_B' = \theta_B - \frac{\Delta d}{d} tg\theta_B, \tag{1.71}$$

where $\Delta d$is amount of change in d-spacing. In turn, the angular displacement $\Delta\theta'$from the Bragg angle after deformation is defined as

$$\Delta\theta' = \theta' - \theta_B', \tag{1.72}$$

Where $\theta'$is the angle between the incident beam and planes after deformation, which obviously depends on the angle of rotation of the plane due to deformation.

From Figure 5 it is clear that in the general case

$$\theta' - \theta = \alpha \cos\varphi, \tag{1.73}$$

Where α is angle between the normal to the atomic planes before $(\vec{n})$ and after deformation $(\vec{n}')$, φ is the angle between the normal plane $(\vec{n}, \vec{n}')$ and the normal to the diffraction plane.

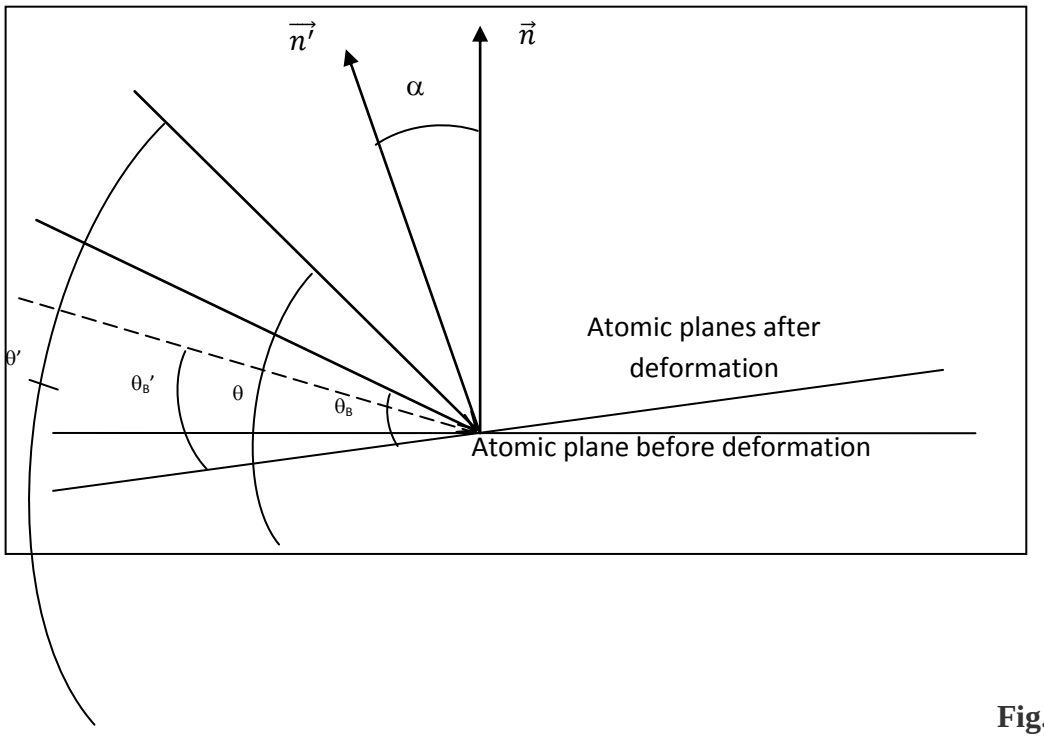

Fig.1.8 Effective disorientation beam with respect to the atomic planes before and after deformation

Thus, the effective local disorientation from the Bragg condition, due to the deformation of the determinant as follows:

$$\Delta\theta' - \Delta\theta = \alpha \cos\varphi + \frac{\Delta d}{d} tg\theta_B, \tag{1.74}$$

The main function the process of diffraction by a lattice is the distribution function of the scattering centers of the lattice. For x-rays,this characteristic function is three-dimensional periodic polarizability $\chi(\vec{r})$ and for neutron waves is the periodic potential of the nuclear in the lattice.Following is an example of X-rays, consider the features description of these functions in a continuously deformed crystal. Considering (1.60-1.62), and assuming that the deformation of the lattice not change electron charge density, i.e. charge density at the point $\vec{r}$ perfect crystal one by one into the point $\overrightarrow{r'}$ in a deformed crystal, it is possible for three-dimensional Fourier series of the function $\chi(\overrightarrow{r'})$ write

$$\chi(\overrightarrow{r'}) = \sum_h \chi_h \, e^{2\pi i \vec{h}.\left(\overrightarrow{r'} - \vec{u}\left(\overrightarrow{r'}\right)\right)}, \tag{1.75}$$

With consideration to the local reciprocal lattice vector which defined by (1.74) have

$$\chi(\vec{r}) = \sum_h \chi_h e^{2\pi i H'(\vec{r})}, \tag{1.76}$$

or

$$\chi(\vec{r}) = \sum_h \chi_h e^{2\pi i \overrightarrow{h \cdot r} \vec{r}}. \quad (1.77)$$

This means that the crystal itself is perfect, but the atomic planes turn or shift relative to each other.

Deformation of Crystal by temperature gradient

The condition (1.69) is a condition for the weak deformation. If the crystal be under influence of the constant temperature gradient, the vector function of the displacement $\vec{u}(\vec{r})$is given as[15]

$$\vec{u}(\vec{r}) = \vec{r}\left[\vec{r}\vec{\nabla}(\alpha T)\right] - \frac{r^2}{2}\vec{\nabla}(\alpha T), \quad (1.78)$$

where α is coefficient of linear thermal expansion of crystal. In this case, the plane perpendicular to $\vec{\nabla}(\alpha T)$are bent, and the radius of curvature is defined as:

$$R = \pm\left|\vec{\nabla}(\alpha T)\right|^{-1}, \quad (1.79)$$

where the sign of reduce of curvature is determined by the relative orientation of the vectors $\vec{h}$ and $\vec{\nabla}(\alpha T)$. The parallel plane to the temperature gradient remains flat but are distributed in the form of a fan relative to each other. As a result, if the reciprocal lattice vectors $\vec{h}$ and gradient $\vec{\nabla}(\alpha T)$be along the same line, i.e. or parallel or antiparallel and the scattering plane be y = 0, we have

$$\vec{\mathrm{h}}.\vec{\mathrm{u}} = \frac{\mathrm{h}}{2\mathrm{R}}(\mathrm{z}^2 - \mathrm{x}^2) \ . \quad (1.80)$$

In this case, conditionof validity of the dynamic theory (1.68) becomes:

$$\frac{h}{2R} \ll \frac{1}{\Lambda^2} \text{ or } R \gg \frac{\Lambda^2}{d}. \quad (1.81)$$

If the temperature gradient and the reciprocal lattice vector mutually perpendiculars have

$$\overrightarrow{h.\vec{u}} = h\frac{d(\alpha T)}{dz}xz, \quad ,\frac{\partial^2(\vec{h}.\vec{u})}{\partial s_0 \partial s_2} = 0 \quad (1.82)$$

where (s_0, s_h) are coordinate system associated with the Cartesian (x, z) in the case of symmetric Laue diffraction relations

$$z = (s_0 + s_h)\cos\theta_B \ , \ \ x = (s_0 - s_h)\sin\theta_B. \quad (1.83)$$

Equation (1.82) indicates that this lattice deformation does not affect the propagation of the X-ray wave field in the medium and wave field not feel strain field while reflecting atomic planes are not parallel, and the interplanar spacing varies from point to point.

Two types of deformation of the crystals are shown schematically in Fig.1.9.

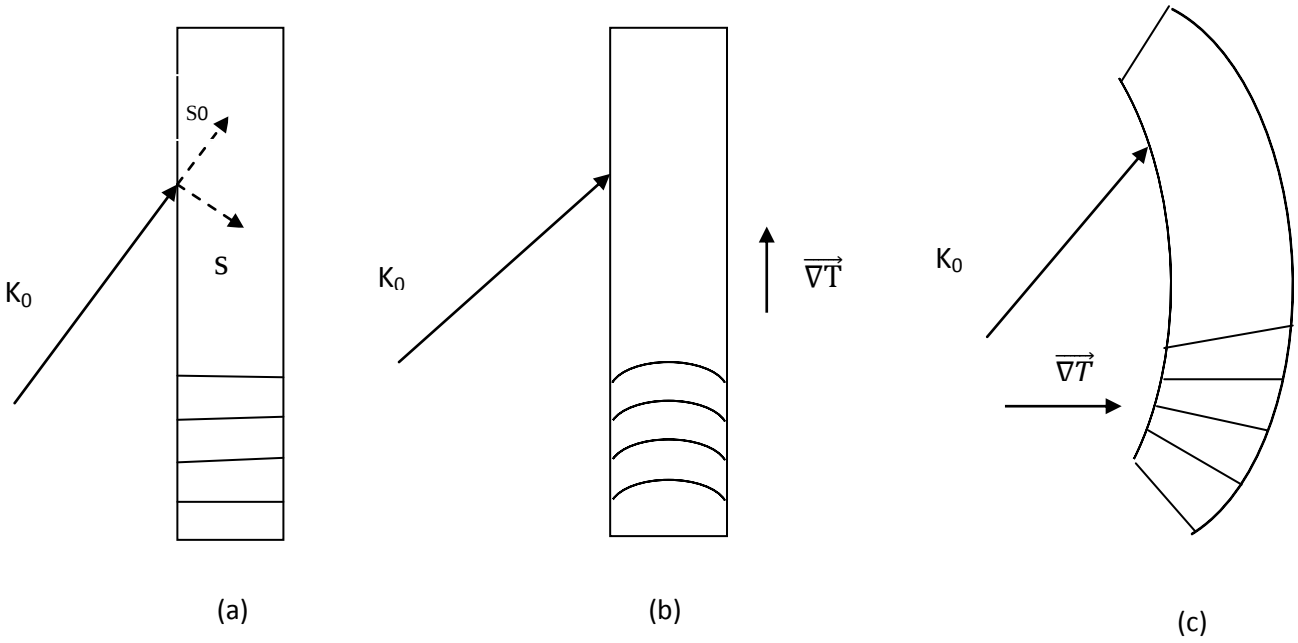

Fig. 1.9A schematic picture of the deformation of the crystal :a) undeformed crystal,

b) deformed crystal when$\vec{\nabla}(\alpha T)\|\vec{h}$,c)deformed crystal when$\vec{\nabla}(\alpha T) \perp \vec{h}$

1.3.1 Dynamic diffraction of X-ray beam in a crystal with weak deformation

We consider a symmetric Laue case with crystal oriented near the Bragg condition and the reflecting atomic planes are normal to the incidence surface of the crystal.The wave field of the crystal lattice is represented as a superposition of waves with the quasi-amplitudesψ_o(r) and ψ_h(r) [16]:

$$\psi\,(\mathrm{r})=\psi_o(\mathrm{r})\mathrm{e}^{-2\pi\mathbf{K_o}\mathrm{r}}+\psi_h(\mathrm{r})\mathrm{e}^{-2\pi\mathbf{K_h}\mathrm{r}}, \tag{1.85}$$

$$(\overrightarrow{k_h}=\overrightarrow{k_0}+\vec{h}), \tag{1.86}$$

$$\left|\overrightarrow{k_h}\right|=\left|\overrightarrow{k_0}\right|=\mathrm{K}\left(1+\frac{\chi_o}{2}\right), \tag{1.87}$$

where χ_o is the mean polarizability of the lattice. According to the Huygens–Fresnel principle [72], the quasi-amplitudes ψ_0 and ψ_h of wave field, stand for the transmitted and reflecting waves, are related by influence functions $G_j(x, z)$ (j= 0,h) determining the influence of primary radiation $\psi_j(\acute{x}, \acute{z})$ at the point $(\acute{x}, \acute{z})$ of the input surface plane (z = 0) of crystal on the field in observation point P(x, z) in the scattering plane:

$$\psi_j(x, z) = \int G_j(\mathrm{x} - \acute{x}, \mathrm{z} - \acute{z})\psi_j(\acute{x}, \acute{z})\, \mathrm{d}\acute{x}\, \mathrm{d}\acute{z}, \qquad (1.88)$$

Where the integration is on $\acute{z} = 0$ cross section coinciding with the incidence surface of the crystal. The x-axis of reference system is taken parallel to the incidence surface of crystal, and z-axis is directed along the internal normal to that surface. Besides that, oblique coordinate axes (s_o, s_h) shall be also used below with axes parallel to wave vectors K_o and K_h of the transmitted and diffracted waves in the lattice (fig.1.10).

The transition from one reference system to the other is made by means of transformations (1.83)

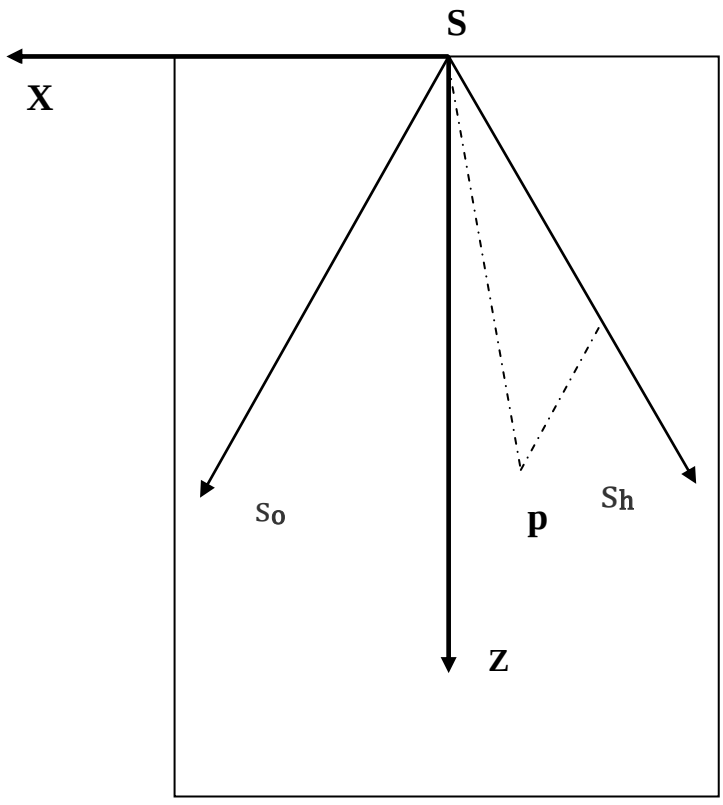

Fig .1.10 Diagram of reference systems, S is a point source of radiation, p is observation point

In the case of a constant strain gradient, the scalar product $\vec{h}.\vec{u}$ is a quadratic function of s_o and s_h

$\overrightarrow{h.\vec{u}} = \alpha\, s_o\, s_h$ (1.89)

The propagation of X-ray wave packages in the lattice is described by wave equations that follow as a consequence from the Takagi equations [73]. For the reflected beam with quasi-amplitude ψ_h this equation is described in the form:

$$\frac{\partial^2\psi_h}{\partial s_o\, \partial s_h} - i\beta_h \frac{\partial\psi_h}{\partial s_o} + (\sigma\bar{\sigma} - i\alpha)\psi_h = 0 \quad (1.90)$$

Where $\sigma = \pi k c X_h$, $\bar{\sigma} = \pi k c X_{\bar{h}}$, $\beta_h = \frac{\partial \vec{u}.\vec{h}}{\partial s_h}$ in fact β_h determines deviationfrom the Bragg angle that is due to the lattice deformation, c is the polarization factor equal to 1 or $\cos 2\theta_B$ for different polarization states of the radiation, χ_h and $\chi_{\bar{h}}$ are Fourier coefficients of crystal polarizability in the directs (h)and ($\bar{h}$) vectors of the reciprocal lattice, $k = 1/\lambda$ is the wave number of radiation in vacuum.

With substitution $Z = i\alpha\, s_o\, s_h$ in equation (1.90), that become to the well-known equation for confluent hypergeometrical function [74]

$$z\frac{d^2\psi_h}{dZ^2} + (1 - z)\frac{d\psi_h}{dZ} + \left(1 - \frac{\sigma\bar{\sigma}}{i\alpha}\right)\psi_h = 0. \quad (1.91)$$

Solution of this differential equation can presented in term of Whittaker function

$\psi_h(z) =$

$e^{\frac{z}{2}} Z^{-1/2} M_{a,0}(Z),$ $\qquad$ $e^{\frac{z}{2}} Z^{-1/2} M_{a,0}(Z),$

where $\qquad$ $a = \frac{\sigma\bar{\sigma}}{i\alpha} - 1/2.$

1.3.2 Asymptotic solution

We can note that the argument of the Whittaker function is written in the form [75]

$$aZ = (\sigma\bar{\sigma} - i\alpha/2)s_o\, s_h \quad (1.94)$$

From expression (1.94) it is clear that the parameter of crystal lattice deformation α introduces an additional imaginary part, which in its turn implies an additional attenuation or vice versa an amplification of the field amplitude which is not connected with the usual phenomena of radiation absorption in the crystal. This can be clearer if we consider the asymptotic behavior of solution

(1.92) far away from the edges of the Bormann delta ($s_o\ s_h = 0$) and weak deformations, i.e. under the following assumptions

$$\frac{\sigma\bar{\sigma}}{|\alpha|} \gg 1 \text{ and } \frac{\sigma\bar{\sigma}}{|\alpha|} \gg |\alpha s_o s_h| \tag{1.95}$$

After some calculation, the asymptotic of $M_{a,0}(z)$ obtain following

$$M_{a,0}(Z) \approx \pi^{-1/2}\left(\frac{Z}{a}\right)^{1/2} cos\left(2\sqrt{(\sigma\bar{\sigma} - i\,\alpha/2)s_o s_h} - \frac{\pi}{4}\right) \tag{1.96}$$

Expression of the quasi-ampitudes in terms of a cosine function is a result of the coherent superposition of two wave modes of weakly and strongly absorbing fields in the lattice [76],two beams which is characterized by two exponential functions with complex arguments:

$$\cos\left(2\sqrt{aZ} - \frac{\pi}{4}\right) = (e^{i\left(2\sqrt{aZ} - \frac{\pi}{4}\right)} + e^{-i\left(2\sqrt{aZ} - \frac{\pi}{4}\right)})/2 \tag{1.97}$$

Now, it is necessary we expand arguments of exponential functions,

$$\sqrt{s_o s_h} = \sqrt{\left(\frac{z^2}{cos\,\theta_B{}^2} - \frac{x^2}{sin\,\theta_B{}^2}\right)/4} = \frac{z}{2\,cos\,\theta_B}\sqrt{1 - P^2} \tag{1.98}$$

After some calculation have

$$\sqrt{s_o s_h} = \frac{\sqrt{1-P^2}}{2}(s_o + s_h) \tag{1.99}$$

where $P = tan\theta/tan\theta_B$ is a parameter determine the angular shift from the Bragg condition of the corresponding plane-wave component in the Fourier expansion of the incident beam[79,80] .

With notice to $X_h = X_{rh} + iX_{ih}$ and $X_{\bar{h}} = \chi\chi_{r\bar{h}} + iX_{i\bar{h}}$, For second part of argument have

$$\sqrt{(\sigma\bar{\sigma} - i\,\alpha/2)} = \sqrt{(\pi kc)^2[(\chi_{rh}\chi_{r\bar{h}} - \chi_{ih}\chi_{i\bar{h}}) + i(\chi_{rh}\chi_{i\bar{h}} - \chi_{r\bar{h}}\chi_{ih})] - i\frac{\alpha}{2}} \tag{1.100}$$

In usual cases, when the radiation frequency is much higher than to the natural frequencies of the absorption K-edge of the crystal substance, have

$$|\ \chi_{oi}| \ll |\chi_{or}|\ ,\ |\chi_{hi}| \ll |\chi_{hr}| \tag{1.101}$$

With approximation is obtained

$$\chi_{rh}\chi_{r\bar{h}} - \chi_{ih}\chi_{i\bar{h}} \cong \chi_{rh}\chi_{r\bar{h}} = |\chi_{rh}|^2 \tag{1.102}$$

Then for (1.100) have

$$\sqrt{(\sigma\bar{\sigma} - i\,\alpha/2)} = \sqrt{(\pi kc)^2[|\chi_{rh}|^2 + i(\chi_{rh}\chi_{i\bar{h}} - \chi_{r\bar{h}}\chi_{ih})] - i\frac{\alpha}{2}} = \left[\pi kc\,|\chi_{rh}| + i\pi kc|\chi_{ih}|\cos\varphi - i\alpha 4\pi kc\chi rh\right.$$

(1.103)

Where φ is phase difference between $X_{rh}\ and\ X_{i\bar{h}}$.

Finally, we obtain simplified argument of exponential functions of (1.97), following

$$2\sqrt{(\sigma\bar{\sigma} - i\,\alpha/2)s_o s_h} = \left[2\pi kc\,|\chi_{rh}| + i2\pi kc|\chi_{ih}|\cos\varphi - i\frac{\alpha}{2\pi kc|\chi_{hr}|}\right]\frac{\sqrt{1-P^2}}{2}(s_o + s_h) \tag{1.104}$$

Imaginary part of (1.104) represents the interference coefficient of attenuation with an additional term which is created by the lattice deformation

$$\mu_i = 2\pi kc|\chi_{ih}|\cos\varphi - \frac{\alpha}{2\pi kc|\chi_{hr}|}. \tag{1.105}$$

Note that the first terms of the interference attenuation (1.105) determines the Borrman effect and describes phenomenon of inelastic interaction of the wave with lattice atoms, while the second term does not contain dependent parameters to such phenomena.This term represented extinction phenomenon, i.e. screening of atomic planes of a given reflection, when some planes reflect the radiation so strong that they exclude the role of other planes in formation of the wave field in the crystal. Expression(1.105) represented to amplify or suppress the interference attenuation depend on the sign of α i.e. on the sign of curvature of atomic planes of the corresponding reflection.

CHAPTER2

Methods of working

2.1.Research devices and attachments

For the performance of this thesis, were used X-ray diffractometerURS-50 im, DRON-3m and X-ray source with a tungstenanodeRUP-120-5-1. Diffractometer URS-50im and DRON-3m were used for single-crystalline the reflecting position and recording the intensities of the diffracted and transmitted beams.

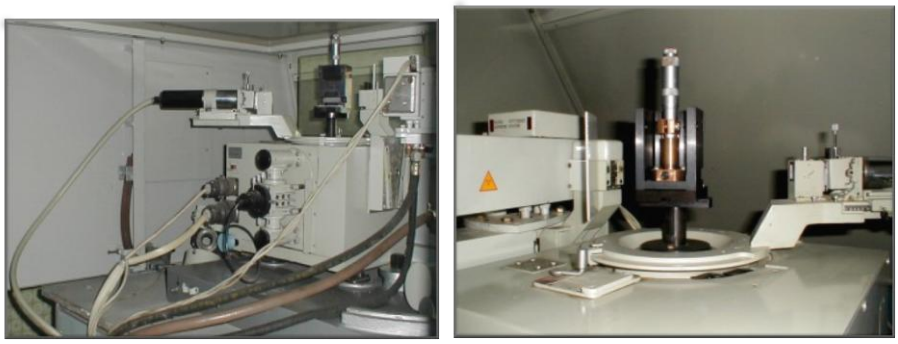

Fig.2.1 Photo of DRON-3m

In order to Set crystal in reflecting position, we used from goniometricheadGP-14(Fig.2.2) and GP-4.Goniometricheadprovideto rotate sample around the horizontal axis, andGUR-5 and GUR-8 provide to rotate sample around a vertical axis.

Fig.2.2 goniometricheadGP-14

Thus, the GP-14and GUR-8 made possible to rotate the crystal about two the perpendicular axes and to regulate reflected beam at the Bragg angle for any family of atomic planes such that detector ,which located in horizontal plane, could only register beam in the plane. We used from special chip carrier which fitted on goniometer head(Fig.2.3)

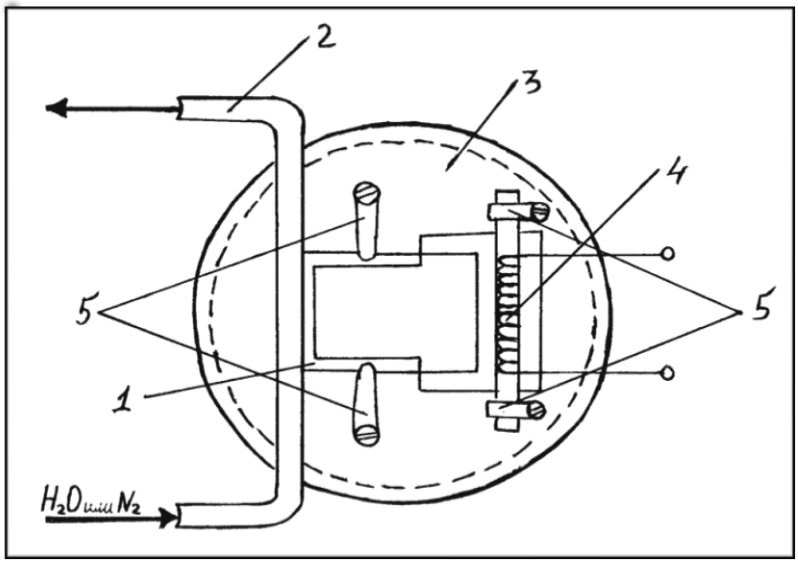

Fig.2.3 Chip carriers-crystal. 1-crystal, 2-cooling tube, 3- chip carrier,

4 –heater, 5clips.

The sample was rotated by GUR-8 around a vertical axis with accuracy twenty seconds of arc. A rectangular holder of slit is used in moving position of the horizontal and vertical planes and rotate around a horizontal (along the propagation direction of the primary beam) axis (Fig.2.4). This

mobility allows bringing the slit in the vertical position (i.e. parallel to the entrance slits, which placed before the monochromator and have size of 0.1x 10mm^2).This piece enables to separate $K_{\alpha 1}$ and $K_{\alpha 2}$ lines, as well as to reduce the background.

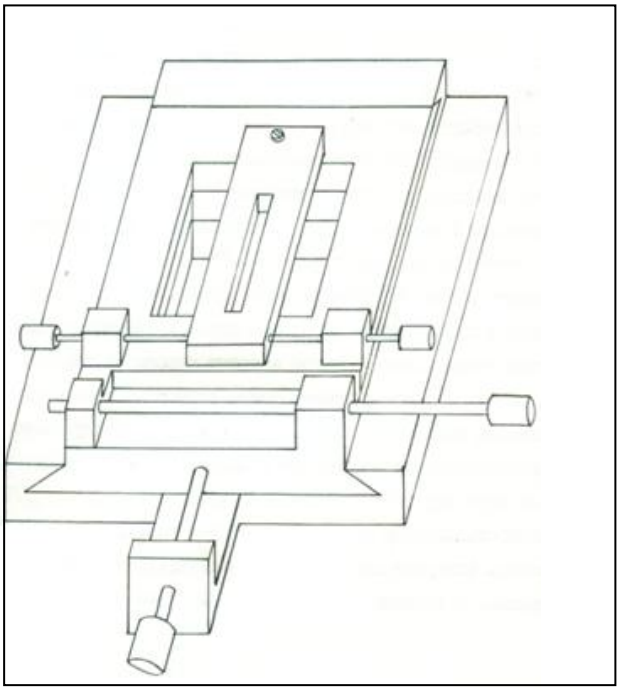

Fig.2.4 Diagram of movable slit.

Studies performed on samples of symmetric and asymmetric Laue reflections as the scheme (1.1), and in the scheme (1, -1).

The entrance slits are not enough lock on the monochromators of standard. This leads to frequent adjustment of the monochromator due to accidental vibrations. Overcoming this limitation was added an adjusted retainer to the entrance slit of the monochromator of goniometer GUR-8.The presence of this pace not only eliminates problem of the goniometer, but also allows the position of the entrance slit become mutable and obtain a beam of radiation from any part of the focus X-ray tube. Optimal location of entrance slit was determined by rocking curves(shown in Figure 2.5), which output be a maximum radiation.

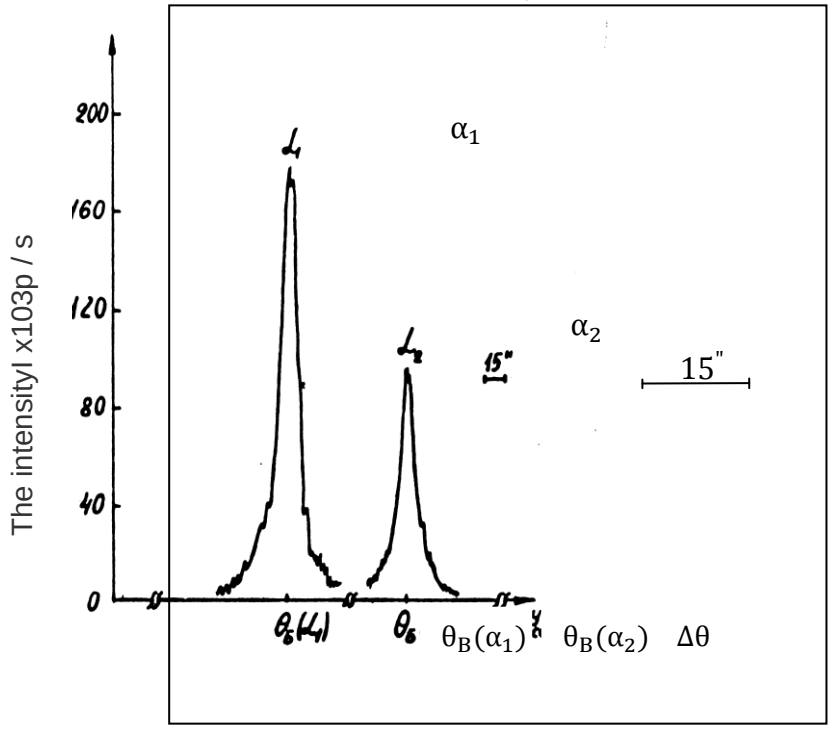

Fig.2.5 Rocking curveslines Mo$K_{\alpha 1}$andMo$K_{\alpha 2}$

The X-ray beam incident on the sample after the monochromator, has a cross-section of 0.1x 10mm^2(0.03x 10mm^2, 0.01 × 10mm^2) with a minimum angular divergence horizontally twenty seconds.

During the experiments used x-ray tubeBSV-6,BSV-29 with the anodes Mo and Ag on the diffractometerURS-50im, DRON-3m. The Tube voltageBSV-6 Mo varied from10 to30 kV and the anode current was a constant value 10 mA. The voltage and current of anode on the tube BSV-29 Ag were40 kVand20 mA, respectively. The characteristic lines and spectrum of X-ray tubes with the anodes Mo and Ag are shown in Table 2.We used from the scintillation counters for measuring intensity of the X-ray and the photographic method for registration ofthe x-ray beam. For obtaining topography of the diffracted x-ray beams, is used from x-ray films of RT-1, RT-2 and etc. (see Table 1).

During the work used from different monochromator such asquartzSiO2,silicon Si and germanium Gein Bragg and in the Laue geometry. Some property of these single crystals is given in Table 3.

The cross-section of incident X-ray beam on the sample was a rectangular shape with dimensions0,01 x10mm^2, 0,05 x10 mm^2, 0,1 x10 mm^2, 0,25 x10 mm^2.Distance from the focus of X-ray tube to the sample in the diffractometer URS-50 was 20 cm.

For creating the necessary value of the temperature gradient, we made a special microheater. It is formed from a nichrome wire of 0.3 mm diameter, which is wound around a porcelain core with uniform step. Moreover, the thickness of the porcelain core is of the order of the crystal thickness. Heater was located just in near of crystal (see Fig. 2.6).This piece connected to a variable voltage source. The required temperature gradient on the crystal is created by varying the output voltage. The temperature at different points of the crystal was measured by a copper-constantan thermocouple with accuracy 0.5 ° C.In addition, the chip carrier (Fig.2.3, Fig. 2.6)was equipped with a tube, which made it possible o cool opposite side of the crystal. This operation carried out by water, which flowed through tube.

Fig.2.6 Photo of Chip carriers-crystal

During the studies of the behavior of the diffracted and transmitted X-ray beams under the influence of the temperature gradient, for protection of x-ray film from the warm of heater was used from a suitable barrier(Figure 2.7).

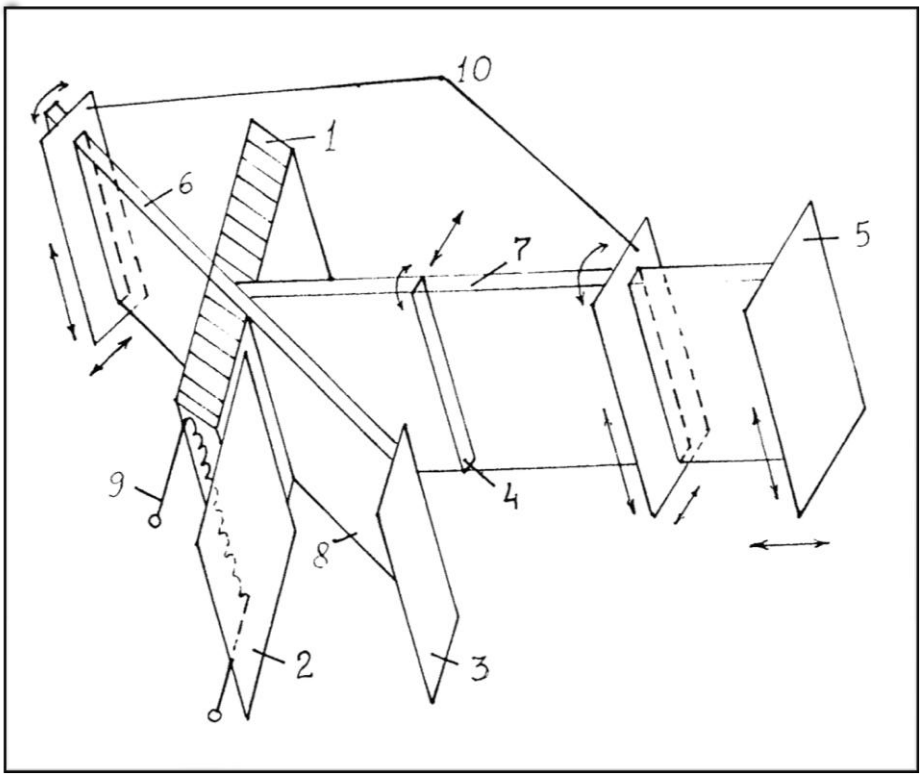

Fig.2.7 Diagramthe experiment on the effect gradient ton the X-ray diffraction in a quartz crystal: 1 - quartz crystal,2 -barrier, 3 - primary beam absorber, 4 – catch position of the reflections, 5 - screen (X-ray film), 6 - primary beam, 7 - diffracted beam, 8 - the transmitted beam, 9 - heater, 10 – movable slit.

Ultrasonic resonator

Figure 2.8 shows diagram of the experimentof the effectof ultrasonic vibrations on the intensity of the diffracted and transmitted X-ray beams. The ultrasonic vibrations are operated on crystal by means of high-frequency amplifier.

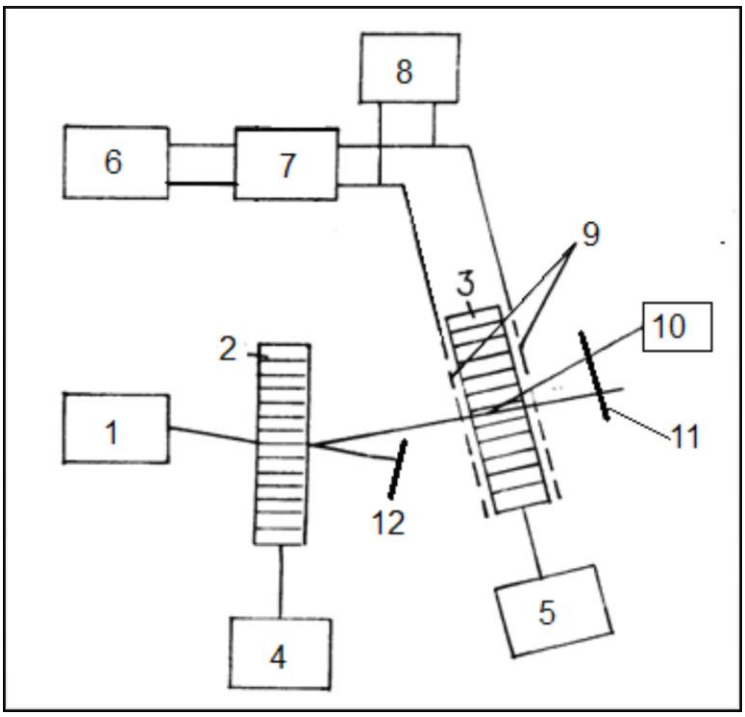

Fig.2.8 Diagramof the experiment of the effect ultrasonic vibrations on the quantitative and spatial distribution of the transmitted and reflected X-ray beams.

The numerals in diagram of Fig.2.8show1- the X-ray source, 2 - germanium crystal or quartz, 3 - ADP crystal,4,5 -goniometricconsoles,6 -high-frequency generator G4-158, 7- high-amplifier, 8 - a dual-trace oscilloscope C1-69, 9 - conductive electrodes, 10 - scintillation counter for record of diffracted and transmitted beams, 11 – x-ray film, 12 – absorber for the transmitted beam. This scheme with the use double-crystal spectrometer made it possible to study the effect of ultrasonic waves in the diffracted and transmitted of the X-ray beams.

The diagram crystal resonators shown in Fig. 2.9, which experiments were performed by it. The crystal is connected to the high-frequency amplifier by two electrical electrodes of the resonator. Figures 2.10-12 show photos of various ultrasonic resonators.

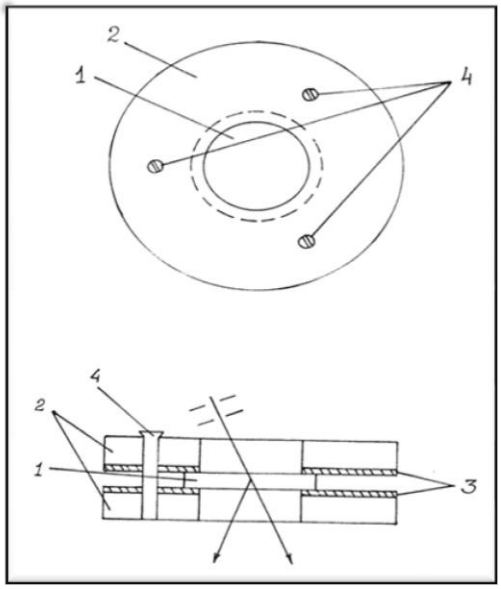

Fig. 2.9ultrasonicresonator: vertical and horizontal projection of the resonator.

1-crystal,2-crystal holder, 3- electrical contacts, 4 - screws.

Fig. 2.10 Photo of goniometric head with ultrasonic resonator

Fig.2.11 photos of Quartz ultrasonic resonators

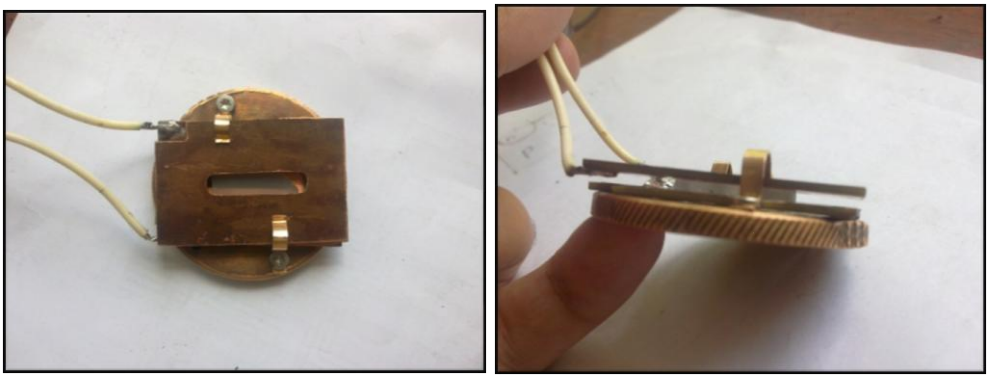

Fig.2.12photos of ADP ultrasonic resonators

Hot- air blower

In other the experiment, we needed to increase temperature of one of the two major surface crystal uniformly. We made a hot- air blower handmade. As Fig2.13 shows, flow of air is produced by afan and air passes through a glass tube. Inside tube, there is a metallic filament that connects to a voltage source. The air temperature of around filament rises when the electric current crosses from filament and hot air exits from the other end of the tube. We were able to change the air temperature of flowing by changing voltage. With impacting hot air to crystal, front surface of crystal uniformly heated.

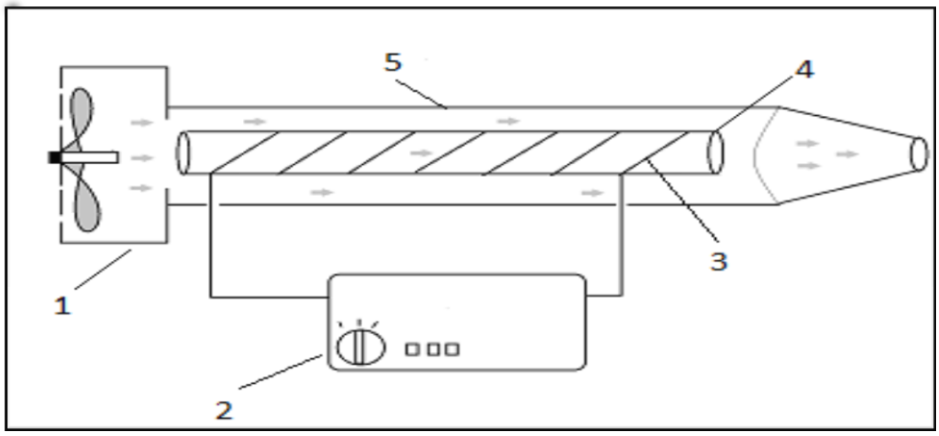

Fig.2.13 hot- air blower,1-electrical fan, 2-voltage source, 3-filament, 4-base of filament,5-glass tube

2.2. Preparing and improving samples

We were used large crystal piece for preparing of samples (ADP, SiO_2).The crystals were polished so that geometric surface of them was coincided to lattice planes with matching thirty seconds of arc. The work is done by the following way:

First, the orientation of the crystal was determine, then the crystal was polished to parallel of the desired atomic planes next with the rotation of the crystal around the normal to the geometry surface of the sample (the horizontal axis) conditions for reflection of x-ray was provided and was obtained different of angles diffraction from θ+φ to θ- φ, where φ is angle between the geometric and the atomic planes and θ is Bragg angle for the atomic plane. The process of polishing and checking of sample was continued until the angle φ tends to zero. As the sample was rotated around the horizontal axis at all the situations there was a reflection. Then the crystal was cut with the appropriate thickness by machine K-4 with a rotating diamond disc to thickness of 0.1 mm. The thickness of the crystal was selected for a given wavelength of radiation so that the product μt takes the necessary value.

In the study of diffraction effects in the Laue case must take into account the absorption of single crystals. For qualitative and quantitative evaluation of changes in the intensity of the reflected and transmitted beams under the influence external force must was define the product μt, where μ is linear absorption coefficient for given wavelength of the radiation and t is thickness of crystal. The absorption coefficients are calculated for composite substances by formula following

$$\frac{\boldsymbol{\mu}}{\boldsymbol{\rho}}=\frac{\mathbf{1}}{\sum_{j=1}^{K}\boldsymbol{A_j m_j}}\cdot\left[\mathrm{m_1A_1}\left(\frac{\boldsymbol{\mu_1}}{\boldsymbol{\rho_1}}\right)+\mathrm{m_2A_2}\left(\frac{\boldsymbol{\mu_2}}{\boldsymbol{\rho_2}}\right)+\cdots+\mathrm{m_KA_K}\left(\frac{\boldsymbol{\mu_K}}{\boldsymbol{\rho_K}}\right)\right] \quad (2.1)$$

In the formula,$m_1, m_2, \ldots . m_K$ are number of atoms from a kind in the compound, k is number of different kinds of atoms, $A_1, A_2, \ldots A_K$ are atomic weights of the chemical elements that make up the compound,$\left(\frac{\mu_K}{\rho_K}\right)$is mass absorption coefficient of elements. The mass absorption coefficient$\left(\frac{\mu_K}{\rho_K}\right)$ for some chemical elements is given in the book Guinier [58].Table 4 shows the linear absorption coefficients of some crystals for radiation of W$K\alpha_1$, Ag$K\alpha_1$, Mo$K\alpha_1$, Cu$K\alpha_1$ andFe$K\alpha_1$.The value of μt depends on the nature of the effect of external factors [17, 82].According to Ref. [83], the optimum of thickness for which we obtain the maximum intensity of the diffracted beam, that is which the intensity due to the absorption reduce to half. So the thickness o the crystal is determined by μt = 0.69.

2.3-characteristics of crystals used

A) Quartz samples

Quartz is a crystalline form of silicon dioxide (SiO_2). It is a hard, brittle, transparent material with a density of 2649 kg/m^{3}and melting point of 1750° C. Quartz is insoluble in ordinary acids, but soluble in hydrofluoric acid and in hot alkalis. If quartz is heated up to 573° C, its crystalline form changes. The stable form above this temperature is known as high-quartz or beta-quartz, while the stable form below 573° C is known as low-quartz or alpha-quartz. For resonator applications, only alpha-quartz is used. When it is said quartz, it refers to alpha-quartz.

Today, quartz is grown artificially to specified dimensions. Crystal orientation is controlled and purity is uniformly high.

Alpha-quartz belongs to the crystallographic class 32, and it is a hexagonal prism with six cap faces at each end. The prism faces are designated m-faces and the cap faces are designated R and r-faces. The R-faces are often called major rhomb faces and the r-faces are minor rhomb faces. Both left-hand and right-hand crystals occur naturally and can be distinguished by the position of the S and X faces.

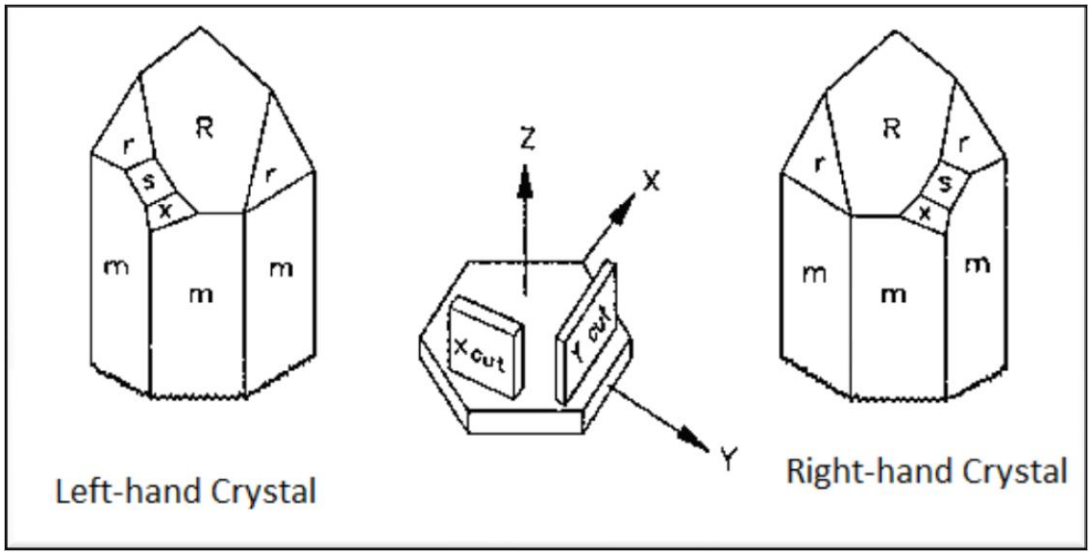

Fig.2.13schematic of quartz

As shown in Fig.2.13 alpha-quartz crystal has a single axis of three-fold symmetry (trigonal axis), and it has three axes of two-fold symmetry (diagonal axes) that is perpendicular to that trigonal axis. The digonal axes have 120° angel with each other and are polar axes, that is, a definite sense

can be assigned to them. The presence of polar axes implies to absence of a center symmetry which it is necessary condition for the existence of the piezoelectric effect. The digonal axes are also known as the electric axes of quartz (x-, y-axis). In crystal with fully developed natural faces, the two ends of each polar axis can be differentiated by the presence or absence of the S and X faces. When pressure is applied in the direction of the electric axis, a negative charge is developed at that end of the axis modified by these faces. The trigonal axis, also known as the optic axis (z axis), is not polar, since the presence of digonal axes normal to it implies that the two ends of the trigonal axis are equivalent. Thus, no piezoelectric polarization can be produced along optic axis. In the rectangular coordinate systems, the z-axis is parallel to the m prism faces.

A plate of quartz which its major surface is perpendicular to the x-axis, is called an X-cut plate. Rotating the cut 90 degrees about the z-axis gives a Y-cut plate with the y-axis now perpendicular to the major surface. Since a quartz crystal has six prism faces, three choices exist for the x- and y-axis. The selection is arbitrary becausethey have identical behaves.

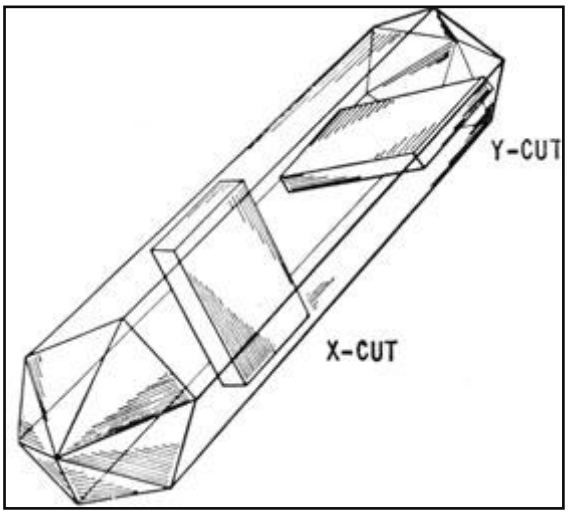

Fig .2.14 x-cut and y-cut Quartz plates

Quartz is an optically active material. When a beam of polarized light passes along the optic axis, rotation of the plane of polarization occurs which the amount the rotation depends on the traversed distance in the material. The concept of the rotation can be used to distinct between the two forms of left quartz and right quartz. In left quartz the plane of polarization rotates anti-clockwise when seen by an observer looking towards the source of light, and in right quartz it rotates clockwise. The most grown quartz crystals are right quartz, whereas in natural left- and right- quartz crystals areabout equally. The either form can equally well be used in the manufacture of resonators, but material which left and right forms are mixed, which is called optically twinned material, cannot be

used. On the other hand, electrically twinned material is all of the same hand, but contains regions where the sense of the electric axis is reversed, thus reducing the overall piezoelectric effect. Such material is also not suitable for resonator application. The presence of twinning and other defects in natural quartz crystal is the major reason for the shortage of suitable natural material, and the absence of twinning in grown quartz is one of its main advantages. If alpha-quartz is heated to above 573° C, the crystalline form changes to beta-quartz, which has hexagonal instead trigonal symmetry. With cooling to down 573° C, the material reverts to alpha-quartz, but in general will be found to electrically twinned. By the same token, the application of large thermal or mechanical stresses can induce twinning, so it is necessary in resonator processing to avoid any such thermal or mechanical shocks.

Reflecting relative power of the atomic planes of quartz is shown in Table3. The atomic plane$(10\bar{1}1)$has maximum value reflectivity .For obtaining diffraction in case of symmetric Laue fromt he atomic plane$(10\bar{1}1)$,it is necessary to take a slice of crystal which the atomic plane $(10\bar{1}1)$ be perpendicular to the large surface of plate. The X-cut one of these planes, which is perpendicular to the plane of the atomic $(10\bar{1}1)$, is shown in (Fig.2.15).

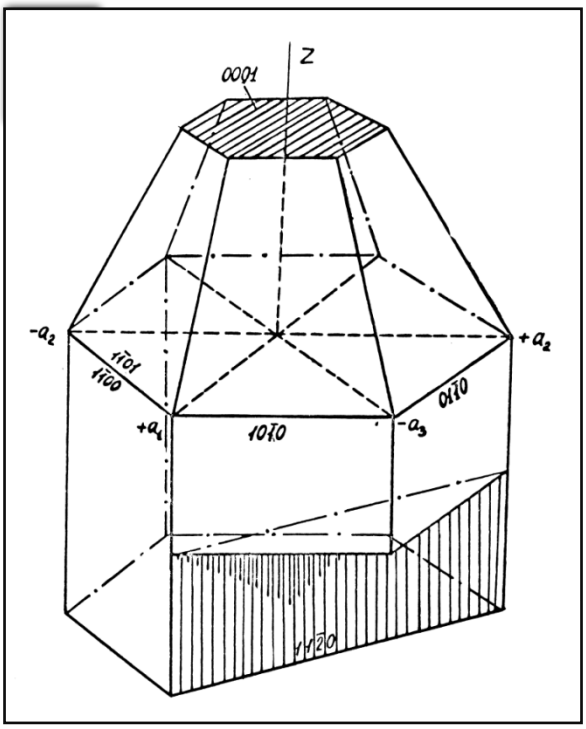

Fig .2.15 Faces of the quartz crystal

For the study of diffraction of quartz, the crystal shape must be direct parallelepiped and large surface coincide with the X-cut. In Figure2.16 is shown relative position of the planes perpendicular to the X-cut.

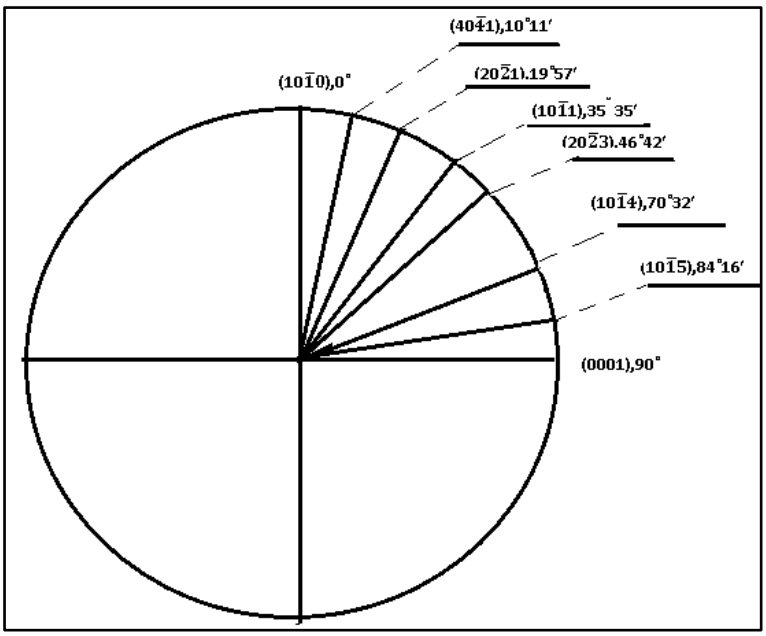

Fig.2.16diagrammatic representation of the relative position of the planes perpendicular to the X-cut.

After cutting crystal with diamond disc, for smoothing rough edges the parallelepiped we have to polish all its facets. As a result of these operations on the face of the crystal arise mechanical tensions. These tensions were removed with assistance of concentrated hydrofluoric acid (HF)at room temperature for several hours. After the chemical processing, the crystal was washed by water and was dried. The crystal dimensions were adjusted to optimal values by polishing and etching. the crystal thickness was measured by a micrometer.

B) ADP crystal

Ammonium dihydrogen phosphate (ADP), or monoammonium phosphate, $NH_4H_2PO_4$, belongs to system of tetragonal crystal with $\bar{4}2m$ symmetry. It has the tetramolecular unit cell with parameters, a = b = 7.510Å and c = 7.564Å [59].

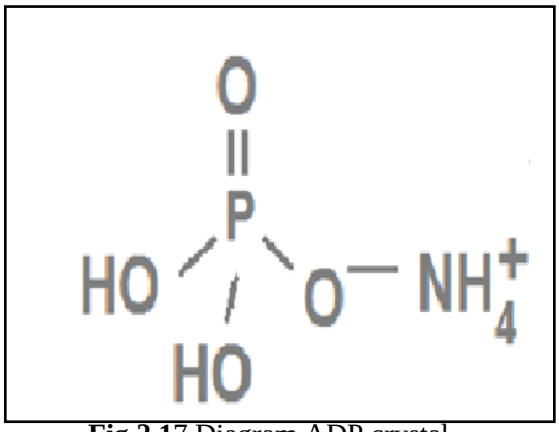

Fig.2.17 Diagram ADP crystal

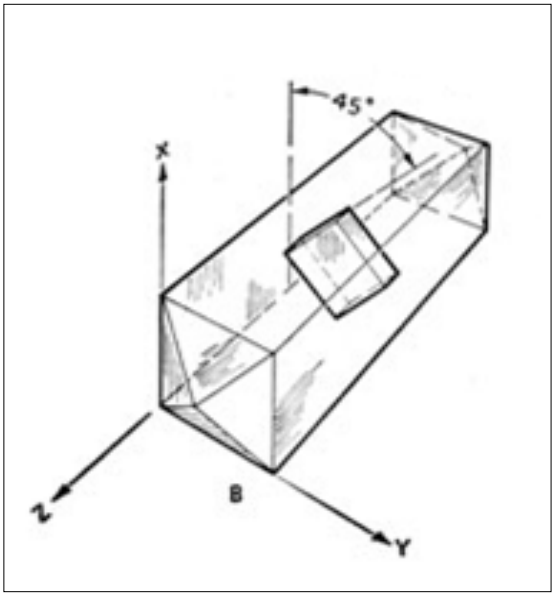

Fig.2.18 Schematic ADP crystal with 45^0 z-cut plate

We used from ADP crystals with x-cut; Figure2.19 shows relative position ofthe planes perpendicular to theX-cut.

At room temperature ADP crystals are piezoelectric. Piezoelectric crystals have been thoroughly investigated for more than 120 years, for applications their actuator and sensor. In the 1950s,the ADP crystals largely replaced with quartz and Rochelle Salt crystals in transducers. The ADP crystal has nonlinear optical and electro-optical properties and also it is widely used in X-ray monochromators [60] and also in the field of optics due to its birefringence properties.

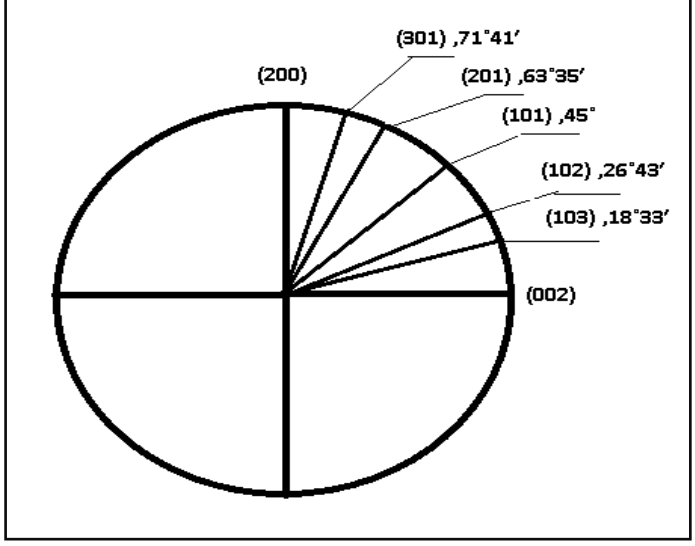

Fig. 2.19diagrammatic representation of the relativeposition of the planes perpendicular to the X-cut.

This material has negative uniaxial optical symmetry with typical refractive indices n_o=1.522 and n_e=1.478 at optical wavelengths [61].

C) Other crystals

In separate studies were used perfect single crystals of Si, Ge, for monochromatic beams of anomalous transmission. Methods of processing these crystals are similar to the method of processing of quartz.

2.3.1Some information about the used substances and the radiations

In this work often required different parameters of the used substances. The tables and figures following are the information about the substances which are used for the work.

Table. 1 Characteristics of X-ray films used [63].

Type of film	Relative sensitivity			Sensitivity to visible light	contrast	Resolution of the lines mm	Sensitivity when working with screen
	λ=0.45Å	MoKα 0.7Å	CuKα 1.54Å				
PT-1	100	100	100	100	3.0	70	100
PT-2	33	38	41	450	3.0	75	350
PM-1	26	30	37	400	2.5	75	300
PM-2	40	44	52	500	2.8	75	400

PM-3	39	47	60	350	2.7	78	300

Table.2 X-ray spectral characteristics of some metals[62].

element	**emission line**	**The relative intensity from the intensity of theKα1in %**	**Wavelength, mÅ**	**The excitation energy keV**	**Wavelength difference$\Delta\lambda' = \lambda_{K\propto 1} - \lambda_{K\propto 2}$mÅ**	**The difference between the excitation energy ofKα1, Kα2eV**	**The line width,Δλ mÅ**
W	K_β	24.8	185. 181	67. 2443	4,818	1337	43,2
	$K_{\alpha 1}$	100	209. 010	59. 31824			
	$K_{\alpha 2}$	57.8	213. 828	57. 9817			37,4
Ag	K_β	28.4	497.685	24.94	4,39	172	8,6
	$K_{\alpha 1}$	100	559.407	22.16			
	$K_{\alpha 2}$	52.2	563.798	21.99			8,7
Mo	K_β	26.5	632.288	19.608	4,29	105	5,86
	$K_{\alpha 1}$	100	709.3	17.479			
	$K_{\alpha 2}$	52.5	713.59	17.374			6,18
Cu	K_β	20	1392. 218	8. 90529	3,84	20	2,31
	$K_{\alpha 1}$	100	1540. 562	8. 04778			
	$K_{\alpha 2}$	50.7	1544. 398	8. 02779			3,21
Fe	K_β	16.7	1756. 61	7. 05798	3,94	13	2,653
	$K_{\alpha 1}$	100	1936.042	6.40384			
	$K_{\alpha 2}$	50.6	1939. 98	6.39084			

Table. 3 Bragg angles of some of the atomic planes of single crystals ofSiO2, Si, Ge, and the coefficients of thermal expansion in the direction perpendicular to these planes, the used crystals [62].

Material	Indices of reflection(hkil)	Distance between planes d, Å	The relative intensity	Bragg angle			Thermal expansion coefficient $x10^{-6}$ cm / ° C
				Ag $K_{\alpha 1}$	Mo $K_{\alpha 1}$	Cu $K_{\alpha 1}$	
1	2	3	4	5	6	7	8
SiO_2	$(10\bar{1}0)$	4.24	5	3°47′	4°47′	10°28′	7.8
	$(10\bar{1}1)$	3.34	10	4°48′	6°6′	13°20′	10.3970
	$(20\bar{2}0)$	2.12	5	7°35′	9°37′	21°16′	7.8
	$(40\bar{4}1)$	1.042	5	15°34′	15°55′	47°39′	8.0527
	$(20\bar{2}1)$	1.975	5	8°8′	10°21′	22°57′	8.7094
	$(30\bar{3}2)$	1.254	7	12°53′	16°27′	37°54′	10.9525
	$(20\bar{2}3)$	1.372	9	11°45′	15° ′	34°08′	11.7535
	$(10\bar{1}2)$	2.28	5	7°3′	8°57′	19°44′	12.6404

	$(10\bar{1}3)$	1.656	-	9°43′	12°23′	27°52′	13.56303
	$(10\bar{1}4)$	1.285	6	12°34′	16°02′	36°08′	14.0082
	$(10\bar{1}5)$	1.046	6	15°30′	19°50′	47°23′	14.1849

Table 3.

1	2	3	4	5	6	7	8
SiO_2	$(3\bar{4}10)$	1.1779	7	13°43′	17°32′	40°49′	7.8
	$(1\bar{2}10)$	2.45	5	6°33′	8°20′	18°19′	7.8
	$(2\bar{4}20)$	1.226	5	13°11′	16°50′	38°54′	7.8
	$(3\bar{6}30)$	0.82	-	19°56′	25°35′	69°53′	7.8
	$(2\bar{2}02)$	1.67	5	9°38′	12°17′	27°30′	10.4
	(0001)	5.405	-	2°58′	3°45 ′	8°18′	14.6
	(0002)	2.7	-	5°57′	7°32′	16°34′	14.6
	(0006)	0.9	-	18°6′	23°10′	58°48′	14.6
		0.81	-	20°11′	25°55′	71°55′	8.4

	$(50\bar{5}2)$ (0003)	1.8	-	8°56′	11°21′	25°20′	14.6
Si	(220) (111)	1.902 3.111	10 10	8°27′ 5°9′	10°46′ 6°33′	23°55′ 14°21′	- -
ADP	(001) (101) (020) (111) (102) (112) (103) (230) (410) (411)	7.55 5.32 3.75 4.34 3.37 3.07 2.38 2.08 1.82 1.77		2 ° 7′ 3° 1′ 4 ° 16′ 3° 42′ 4° 45′ 5° 13′ 6° 43′ 7° 43′ 8° 50′ 9° 6′	2° 41′ 3° 49′ 5° 25′ 4° 41′ 6 ° 2′ 6° 37′ 8° 32′ 9° 49′ 11° 14′ 11° 34′	5° 51′ 8° 19′ 11 ° 51′ 10° 13′ 13° 12′ 14° 30′ 18° 50′ 21° 44′ 25° 2′ 25° 49′	
Ge	(220)		10 10	7°56′ 4°54′	10°07′ 6°14′	23°26′ 13°38′	- -

	(111)						

Table. 4 The coefficient of linear absorption of X-rays with different wavelengths[58].

Radiation line	**Linear absorption coefficientμ (cm^{-1})**				
	Si	**SiO_2**	**Ge**	**ADP**	**Air: N_2 -78% , O_2 -22% x10^{-3}**
W$K\alpha_1$	0.745	0.665	11.186		0.24
Ag$K\alpha_1$	7.823	5.1	181.1	2.47	0.68
Mo $K\alpha_1$	15.61	10.4	339.83	5.0	1.17
Cu $K\alpha_1$	140.5	92.6	371.98	50.4	10.87
Fe $K\alpha_1$	270.28	175.2	686.08	89.5	21.16

Table. 6 Elasticitymodules of single crystals[64].

Material	**Elastic module ×10^{10} , dyn/cm^2**
SiO_2	C_{11} 86,80 C_{14} -18,04
Si	C_{11} 130,0 C_{12} 49,0
Ge	C_{11} 165,0 C_{14} 64,0
ADP	C_{11} 61.17 C_{33} 32.8 C_{12} 7.2

Table. 7 Some of used parameters of crystals [64].

	silicon	**quartz**	**ADP**	**Germanium**
Formulas	Si	SiO_2	$NH_4H_2PO_4$	Ge
Density g/cm^3	2,3283	2,65	1.8	5,32674
Space Group	Fd3m	D_3-32 P_{31}-21	$\bar{4}2m$	Fd3m
Unit cell parameters	5,4307	a=4,9138 c=5,4052	a=7.50 b=7.58	5,65749
Melting temperature^{0}C	1412	1470	190	958,5
Warm.expansion $10^{-6}K^{-1}$	15,6	8,6		2,6
Cleavage	111	$10\bar{1}1$		111

Table. 8 The value of extinction depth τ_0 (in mm) in the diffraction of different radiation (symmetrical reflection). [65]

Material	**Reflection (hkl)**	**Radiation**		
		AgK_α	**MoK_α**	**CuK_α**
Si	111	54,1	42,4	18,4
	220	46,5	36,6	15,4
	422	62,4	48,2	16,4
	333	92,8	71,5	23,2
	444	88,7	66,9	6,43
Ge	111	23,6	18,6	8,64
	220	19,25	15,2	7,0
	422	26,2	30,6	8,1
	333	39,8	29,1	11,2
	444	36,8	29,1	5,8

Table. 9 Some characteristics of the x-ray tubes [63].

Tube type	**Number of windows**	**Exit angle, degrees**	**Focusmm^2**		**Anode voltage, kV max**	**Current mAmax**	**Power kW**
			actual	**projection**			
BSV-6	2	2	2,5x5	2,5x0,2	45	15	0,45
BSV-7	2	3	0,1x2	0,1x0,1	45	2,5	0,11
BSV-21	3	3	0,4x10	0,1x10	60	40	0,8
BSV-25	3	3	0,4x10	0,1x10	60	40	0,8
BSV-27	3	3	0,4x10	0,1x10	60	40	0,8
BSV-29	3	3	0,4x10	0,1x10	60	40	0,8

Chapter 3

The x-ray diffraction from single crystals under the influence of temperature gradient

Investigationsinto features of the x-ray diffraction under the influences of external factors such as temperature gradient and acoustic wave are of interest to solid state Physics, and particularly, crystallography because they make it possible to obtain highly monochromatic and intense x-ray beams controllable in space and time.

3.1 The x-ray diffraction from ADP crystal under the influence of temperature gradient applied perpendicular to reflecting atomic planes

In the first part of the work, we investigated the dependence of the intensity of the diffracted x-rays from single crystal of ammonium dihydrogen phosphate (ADP) with different thickness in the Laue geometry while direction of temperature gradient was perpendicular to reflecting atomic plane[110, 113].

Ammonium dihydrogen phosphate (ADP) and potassium dihyrogen phosphate (KDP) are piezoelectric and their structure is tetragonal with $\bar{4}2m$ symmetry, but ADP has some properties which is qualitatively different from KDP .The low temperature transitions ADP is ant ferroelectric while KDP is ferroelectric. At room temperature the elastic stiffness constants c_{11} and c_{33} of ADP are in the ratio of 2:1 while they are almost equal for KDP. The most interesting difference is between the coefficients of thermal expansion. In the KDP, the coefficient along the c axis is greater than that in a perpendicular plane while in ADP is reverse [114]

3.1.1 Experimental methods

The experiments were performed by the X-ray diffractometer DRON-3M ,x-ray tubes used BSV-29 with anodes Ag or Mo. Focal spotsizeswerehorizontally0.4mmandvertically8mm. Fig.3.1 shows scheme of experiment.

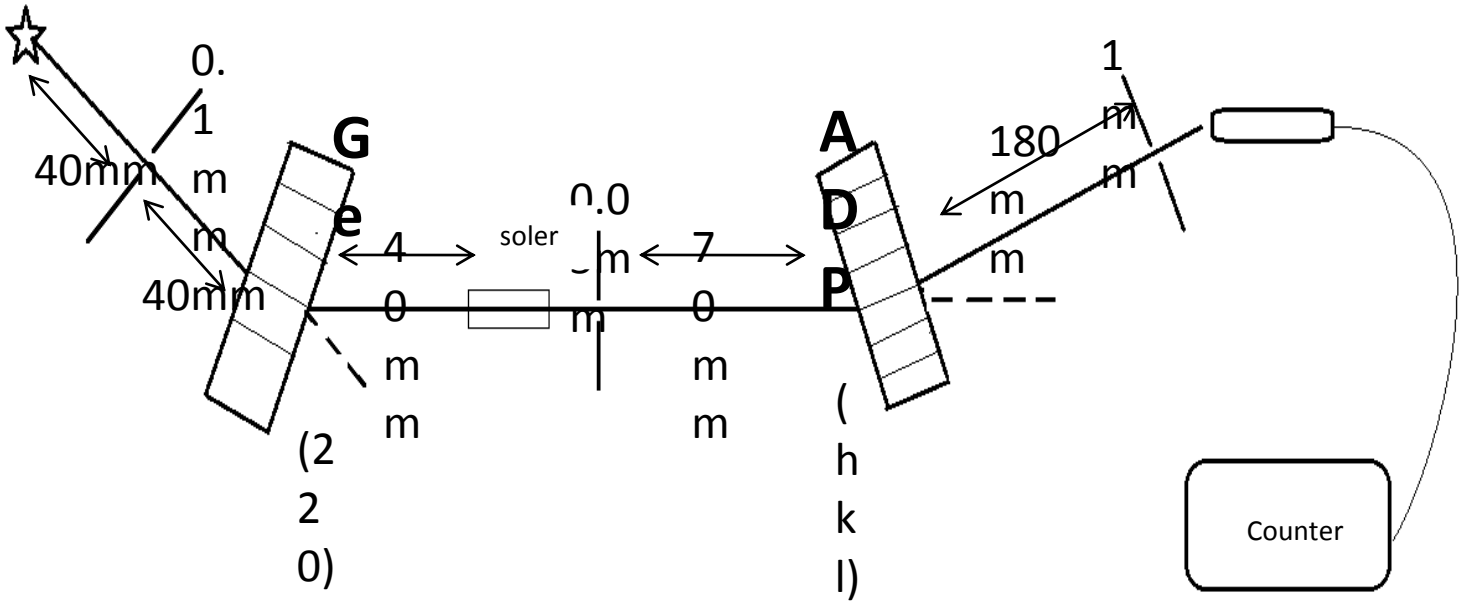

Fig.3.1 The experimental scheme.

The monochromized beam of x-ray radiation was produced by anomalous transmission from atomic planes (220) of a perfect Ge single crystal with the thickness 0.6 mm and coefficient of linear absorption 181cm^{-1} for AgKα line and 340 cm^{-1} for MoKα line, respectively.The monochromatic x-ray beam had horizontal angular divergence 3" and the vertical collimation was performed by Soler slits. Monochromized and collimated x-ray radiation passes through a special slit with size ≈0.05×10 mm^2, which placed at the distance of 10 mm from the Soler slit and enabled to separate (in Bragg geometry) monochromized lines $K\alpha_1$ and $K\alpha_2$ .The thickness of studied crystal ADP selected 1.3 and 2.5 mm with a linear absorption coefficient of 2.75 cm-1 and 5.4 cm-1 for AgKα and MoKα lines, respectively.

We used a variable hot filament for producing temperature gradient. Filament located near and parallel to small surface of crystal. The temperature of surface of the single crystal is measured by a copper-constantan thermocouple with accuracy of $\pm$ 0.5 ℃.

The direction of the temperature gradient was opposite direction of vector diffraction.However, we note that the value of the integrated intensity of the reflected beam is independent of the direction of the temperature gradient [67, 77]. When diffraction vector is inverse direction of the vector of the temperature gradient, diffracted beam would be focusing and if they be same direction, reflected beam would be defocusing.

Integral intensity of the diffracted X-ray beam was measured with use of scintillation counter with FEU-85 and standard recording block BR-1 available in the collection of X-ray diffractometer DRON-3M.

3.1.2 Experimental results

We studied experimentally the variations of the integrated intensity of reflected beams from different atomic planes such as (100), (110),(101), (002), (420) and (220) of ADP crystal under the influence temperature gradient for two different thickness 2.5 mm and 1.3mm. The results of the experiment are shown in Table 3.1 .

Table 3.1 Dependence of the integrated intensity of reflected beam from the atomic planes (hkl) single crystal of ADP on the thickness of the crystal and on the temperature gradient ,K : coefficient of amplification

$\Delta T/\Delta x$ $(deg\ /\ cm)$	Intensity $(pulse/sec)$						
	t=2.5mm					t=1.3mm	
	(100)	(110)	(101)	(002)	(420)	(220)	(002)
0	1400		4400	7000	3300	11000	6300
1.5	1100		3900			10000	
3	1200	1600	4000			9500	6600
4.5	2100		5300			9600	
6	3400	2500	6700	10000	4500	10000	7200
12	5000	3600	12000	15000	5900	17000	9500
18	6600	4200	17000	21000	7000	24000	11100
24	9700	5800	22000	25000	9500	35000	12500
30	13000	7500	24000	30000	11000	42000	14900
36	17000	9000	26000	35000	12500	47000	15400
42	20000	10200	30000	39000	14000	55000	16000
48	26000	11500	33000	44000	14800	62000	
54	28000	14000	32000	48000	16800	68000	
60	30000	15000		67000	17500	74000	
66	34000	18000		77000	18300		
72	36000	20000		80000	19000		
78	38000	27000		81000	20000		
84	40000	29000		66500	20800		
90		32000		88500	21500		
96				90000			
K	28.6	20	7.3	12.9	6.5	6.7	2.5

We obtained coefficient of amplification of the intensity of the beam reflected from atomic planes. The amplification coefficient, K, is defined as the ratio of the reflected beam intensity in the presence of temperature gradient, in the point where intensity saturation begins, to the intensity in the absence temperature gradient [109]. The value of this coefficient is various for different atomic planes and different thickness. The coefficient of amplification at reflection from the planes (100) had the highest value and reflection from the planes (420) with thickness of 2.5 mm had the lowest value.

With usage of experimental data of Table 3.1, graphs of intensity of reflected radiation versus the temperature gradient are plotted for different reflecting atomic planes (Figures 3.2 – 3.8).

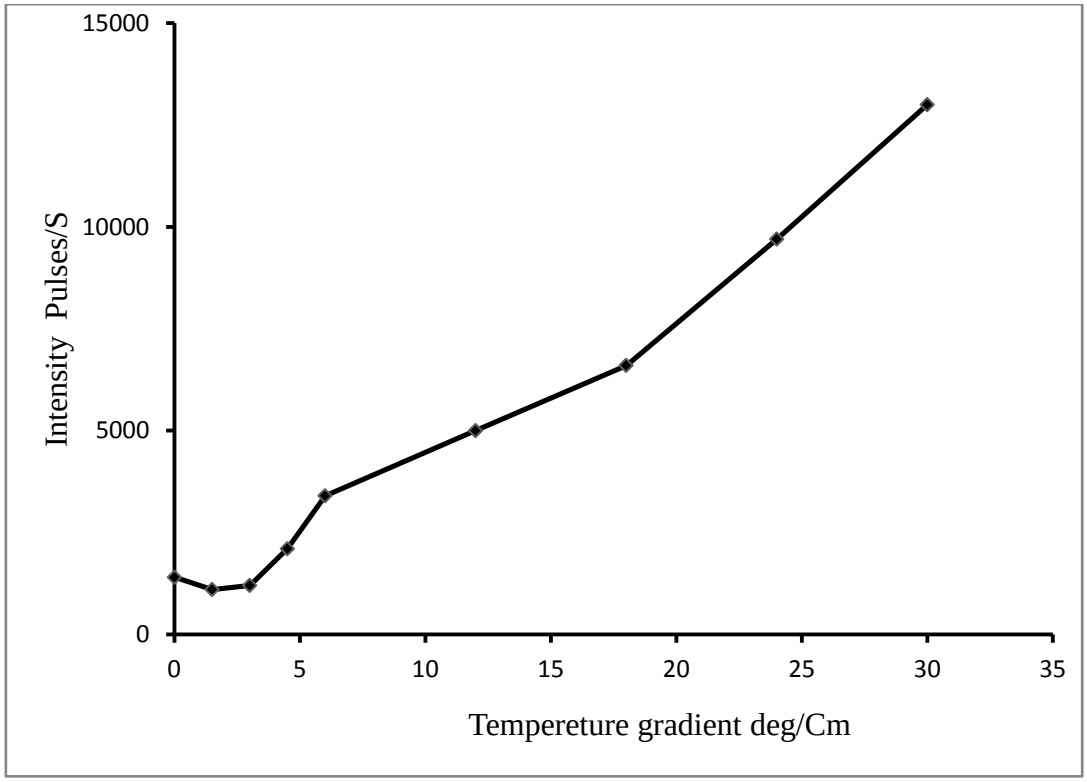

Fig.3.2 Dependence of the integrated intensity of reflected beam on the temperature gradient for the atomic plane (100),t= 2.5 mm.

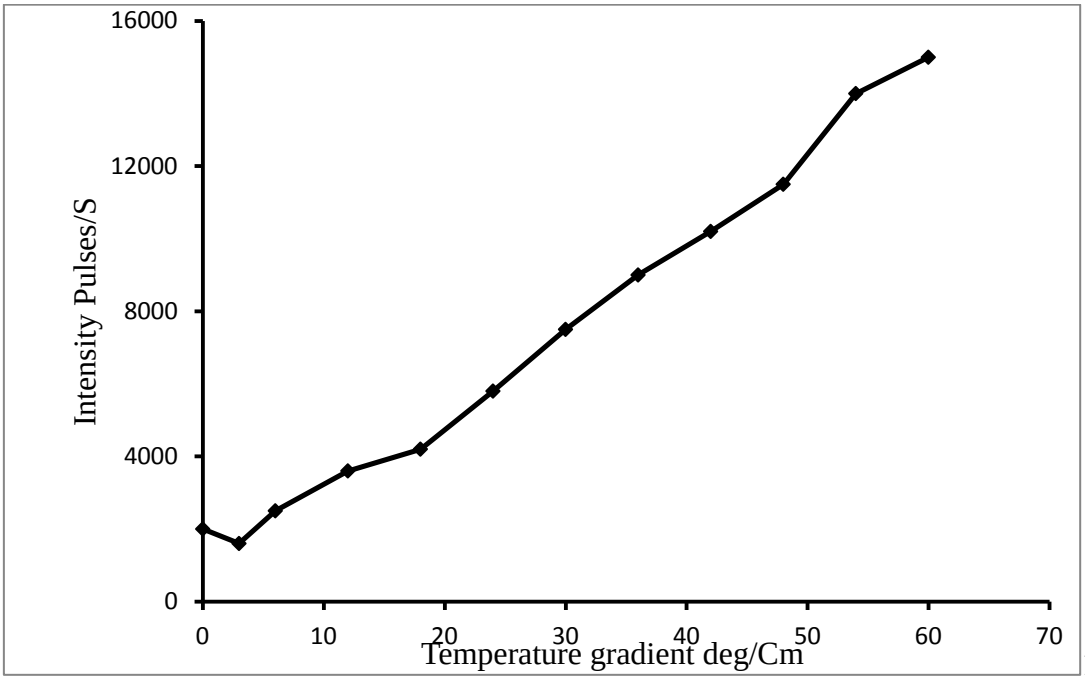

Fig.3.3 Dependence of the integrated intensity of reflected beam on the temperature gradient for the atomic plane (101),t= 2.5 mm.

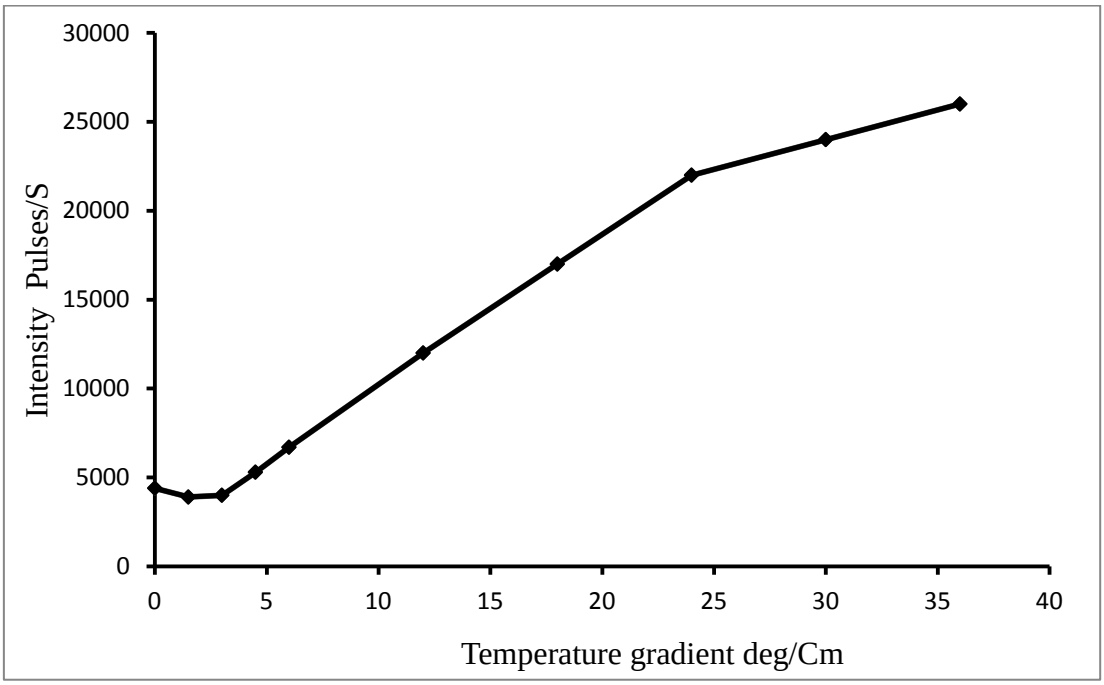

Fig.3.4 Dependence of the integrated intensity of reflected beam on the temperature gradient for the atomic plane (101), t= 2.5 mm.

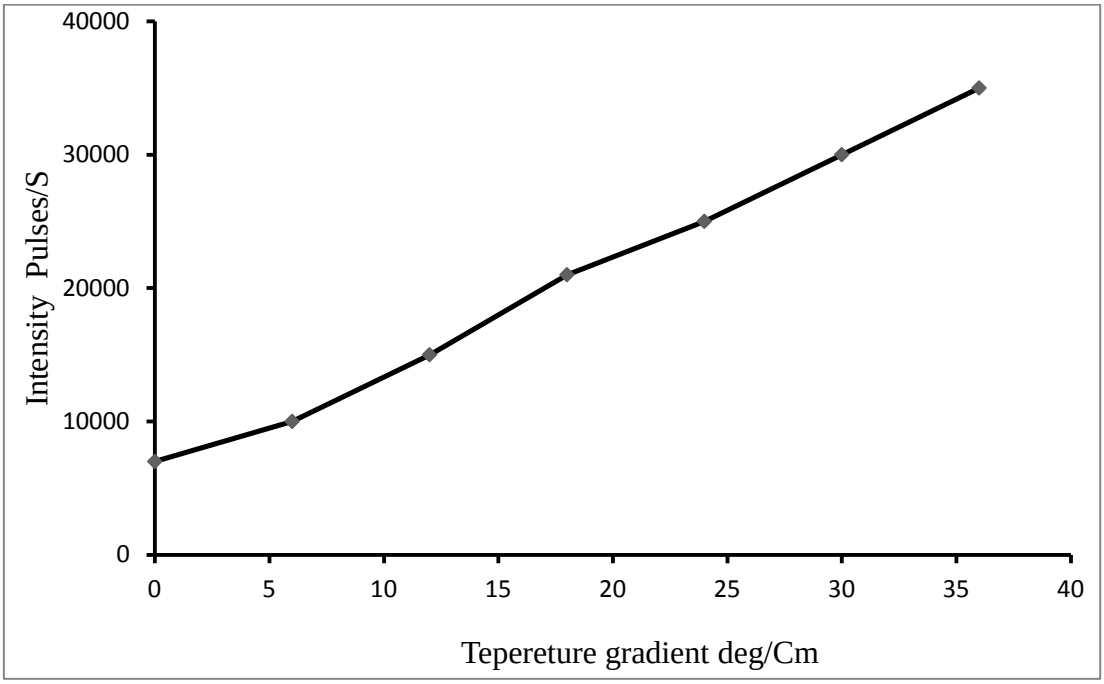

Fig.3.5 Dependence of the integrated intensity of reflected beam on the temperature gradient for the atomic plane (002), t= 2.5 mm.

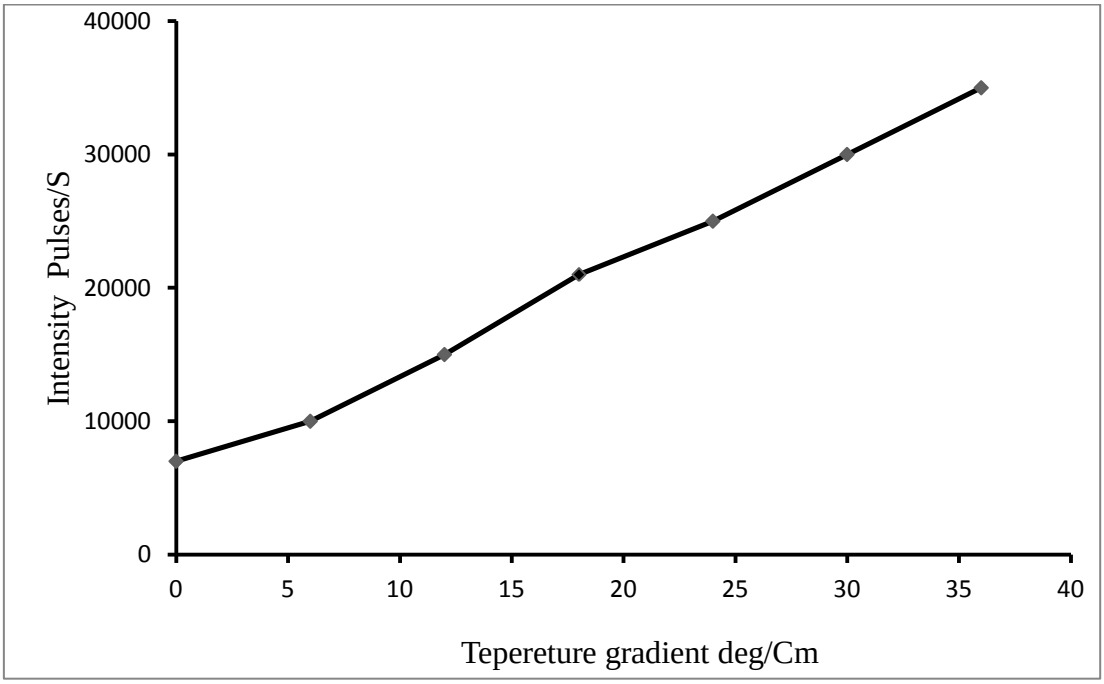

Fig.3.6 Dependence of the integrated intensity of reflected beam on the temperature gradient for the atomic plane (420), t= 2.5 mm.

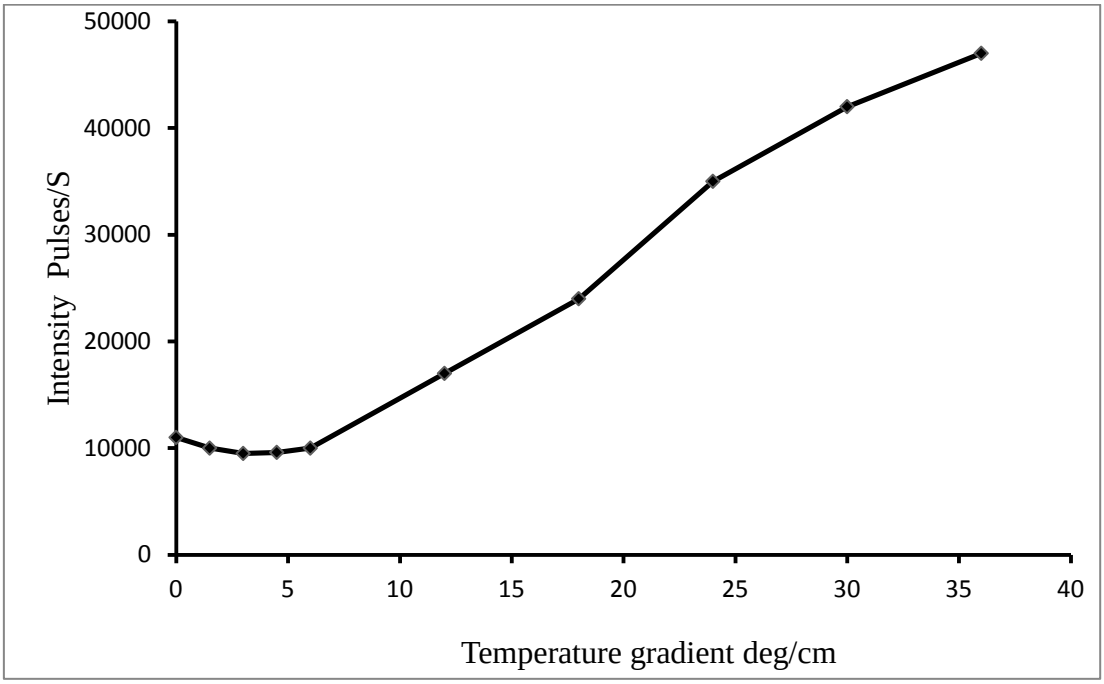

Fig.3.7 Dependence of the integrated intensity of reflected beam on the temperature gradient for the atomic plane (220), t=1.3 mm.

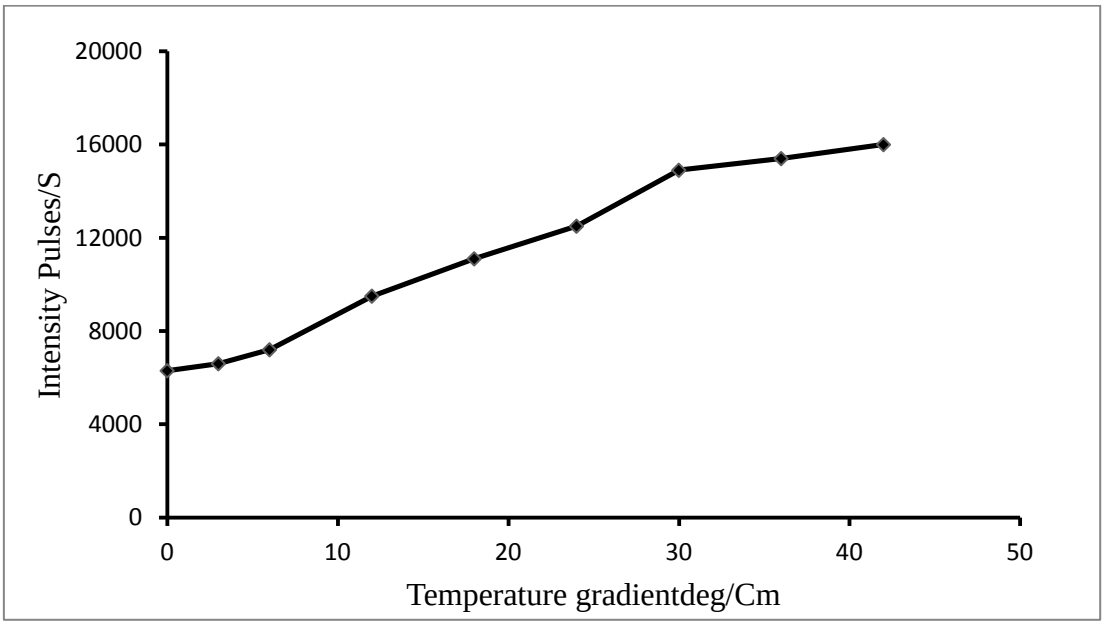

Fig.3.8 Dependence of the integrated intensity of reflected beam on the temperature gradient for the atomic plane (002),t=1.3 mm.

As in Fig.3.2, Fig.3.3, Fig 3.4 and Fig3.7 are seen, first intensity of the reflected beam reduces by about 10%, and then uniformly increases with increasing temperature gradient. We will theoretically explain this phenomenon in the next section.

Fig.3.9 shows topography Picture of diffraction from the reflecting atomic plane (100) in absence and presence of temperature gradient.

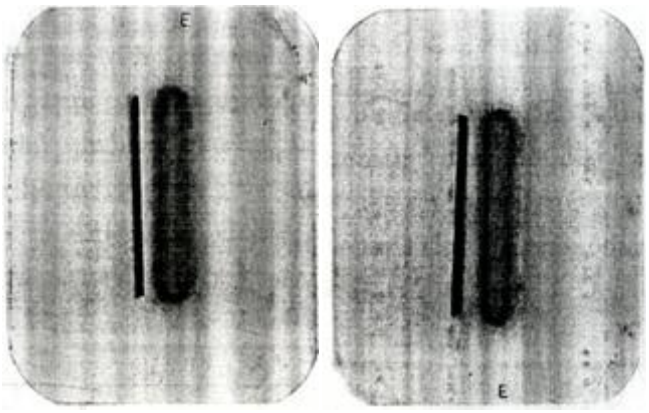

a b

Fig.3.9 Topography of diffraction from the reflecting atomic plane (100),
a) Absence of temperature gradient, b) presence of temperature gradient

As can be seen in conditions absence of temperature gradient, intensity of diffracted beam is low while with applying temperature gradient to crystal, the intensity of diffracted beam increases. Also Fig.3.10 and Fig.3.11 show topography of diffraction for reflecting atomic planes (110) and (200).

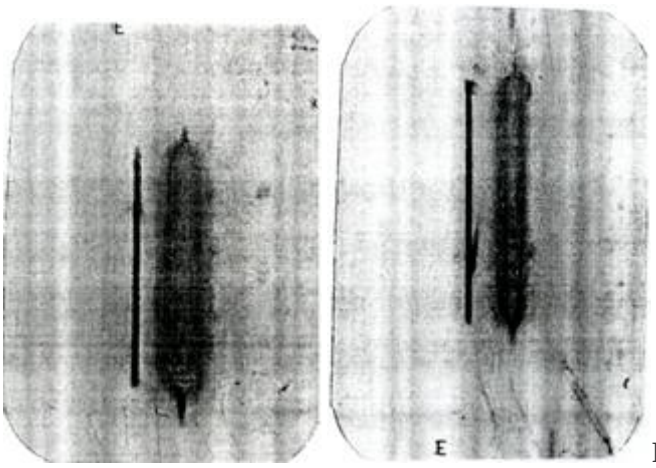

Fig.3.10 topography of diffraction from reflecting atomic plane (11(a b

a) absence of temperature gradient, b) presence of temperature gradient

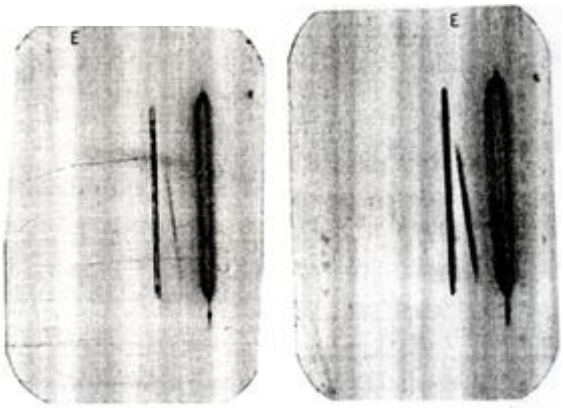

a b

Fig.3.11 Topography of diffraction from reflecting atomic plane (200),

a) absence of temperature gradient, b) presence of temperature gradient

3.1.3 Theoretical analysis of experiment

A crystalline the absence of internal stresses, under the influence o fa uniform temperature

gradient ∇T, will deform and the lattice planes perpendicular to $\nabla T$are curved with radius of curvature which given by

$$R = \pm|\boldsymbol{\nabla}(aT)|^{-1} \tag{3.1}$$

Where a islinear coefficientof thermal expansion. The sign of the curvature of the planes is determined by the relative orientation of the diffraction vector and $\vec{\nabla}(\alpha T)$).Atomic planes parallel with vector of∇T remains flat, but distributed in the form of a fan with respect to each other.

The vector function ***u(r)*** of displacement of atoms of deformation field is given in the form

$$\boldsymbol{u}(\boldsymbol{r}) = \boldsymbol{r}[\boldsymbol{r}.\boldsymbol{\nabla}(aT)] - \frac{1}{2}(\boldsymbol{r}.\boldsymbol{r})\boldsymbol{\nabla}(aT) \tag{3.2}$$

Where **r** is the position vector of the considered point. Obviously, the displacement function is a quadratic function of position.

As it is seen in figure 3.12, the coordinate system is chosen as the axis x is opposite diffraction vector h and the axis z is in along of normal to input surface of the crystal.

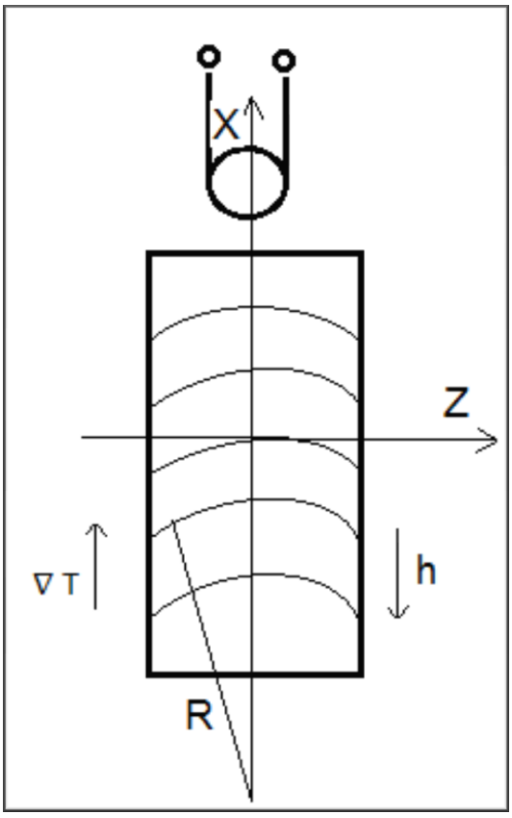

Fig.3.12 bending reflecting atomics plane due to temperature gradient

Curved radius of reflecting atomic planes of lattice, perpendicular to temperature gradient, is obtain by (1.79)

$$\boldsymbol{\nabla}(aT)=\frac{1}{\mathrm{R}}. \tag{3.3}$$

Also have

$$\boldsymbol{r} = x\vec{\imath}+y\vec{j}+z\vec{k} \tag{3.4}$$

Now with Substituting above quantities in (3.2), parameter localdeviation from theBragg scattering in plane (y=0) obtain

$$\boldsymbol{h}.\boldsymbol{u}(\boldsymbol{r}) = \frac{h}{2R}\,(z^2 - x^2) \tag{3.5}$$

Where $\boldsymbol{h}= h(-\vec{\imath})$ is vector of the reciprocal lattice of the crystal .

In section1.3.2, an asymptotic solution of the dynamical theory has been explained based on the Takagi's approach in weakly deformed crystals. Our experimental conditions with presence of temperature gradient make it possible, using from asymptotic solution [80,110]. In according (1.68), condition of validity dynamical theory is

$$\frac{\partial^2(\boldsymbol{h}.\boldsymbol{u})}{\partial S_0 \partial S_h} \ll \frac{\pi^2}{\lambda^2}|\chi_h|^2 \tag{3.6}$$

Where χ_h ($\equiv$ χ_{hkl}) is Fourier – expansion of the microscopic polarizability of the crystal for atomic plane hkl. With notice (3.5), we have

$$\frac{\partial^2(\boldsymbol{h}.\boldsymbol{u})}{\partial S_0 \partial S_h} = \frac{h}{2R} \tag{3.7}$$

After some calculation, maximum of curvature radius of atomic planes according to (3.6) is

$$R \gg \frac{\mathrm{h}\lambda^2}{2\pi^2|\chi_h|^2} = \frac{\lambda^2}{2\pi^2 d|\chi_h|^2}\,, \tag{3.8}$$

Where$d = h^{-1}$ is interplanar spacing of the reflecting planes. With assumption $\lambda \sim 10^{-8}cm$, $d \sim 10^{-8}cm$ and $|\chi_h| \sim 10^{-6}$have

$$R \gg 10^3\mathrm{cm}, \tag{3.9}$$

On the other hand, if the maximum value of the applied temperature gradient be $\Delta T / \Delta X \approx 100 deg/cm$ for ADP crystal with coefficient of linear thermal expansion $\simeq 10^{-6}°C^{-1}$, the radius of curvature of the reflecting planes will obtain following

$$R \simeq \left|\frac{d(aT)}{dx}\right|^{-1} \simeq 10^4 cm\,, \tag{3.10}$$

From comparison of the Expressions (3.9) and (3.10), we conclude that inour experimental conditions can start from the assumption of a weak the deformation field and use the theoretical results obtained in [80,110] (see 1.3.2).

According to dynamical theory, the integrated intensity of reflection in the symmetric Laue-diffraction geometry may be represented by the formula following [2]

$$I_h = I_i \frac{\pi|\chi_{hr}|}{2\sin 2\theta_B} e^{-\frac{\mu t}{\cos\theta_B}} I_0\left(\frac{t}{\cos\theta_B}(2\pi k|\chi_{hi}|)\right), \tag{3.11}$$

Where I_i is intensity of incident beam, μ is the linear absorption coefficient of the crystal for the given radiation, θ_B is the Bragg angle, $I_0(y)$ is the modified Bessel function, χ_{hr} and χ_{hi} are the real and imaginary parts of the Fourier expansion coefficient of polarizability, respectively. Under conditions of weak deformation in crystals and relation (105), it should replace term $2\pi k|\chi_{hi}|$ by $\left(2\pi k|\chi_{hi}| - \frac{\alpha}{2\pi k|\chi_{hr}|}\right)$ in formula of integrated intensity. Then (3.11) become to

$$I_h = I_i \frac{\pi|\chi_{hr}|}{2\sin 2\theta_B} e^{-\frac{\mu t}{\cos\theta_B}} I_0\left(\frac{t}{\cos\theta_B}\left(2\pi k|\chi_{hi}| \mp \frac{|\alpha|}{2\pi k|\chi_{hr}|}\right)\right), \tag{3.12}$$

Hereα is parameter of crystal deformation. The value ofαunder the influence of temperature gradient is equal with

$$\alpha = \frac{ha}{2}\frac{\Delta T}{\Delta x}\,, \tag{3.13}$$

Where a is the linear coefficient of thermal expansion and h is the vector magnitude of the reciprocal lattice of the crystal. The sign of α is determined by the sign of R in (3.3).

The expression (3.12) represents the integrated intensity $I_h$depends on the temperature gradient. In the case $\alpha > 0$, the integrated intensity initially decreases with increasing value of α (or $\frac{\Delta T}{\Delta x}$) until reaches to a minimum and then begin to increase, Figure 3.13 shows variations integrated intensity versus temperature gradient in this case.

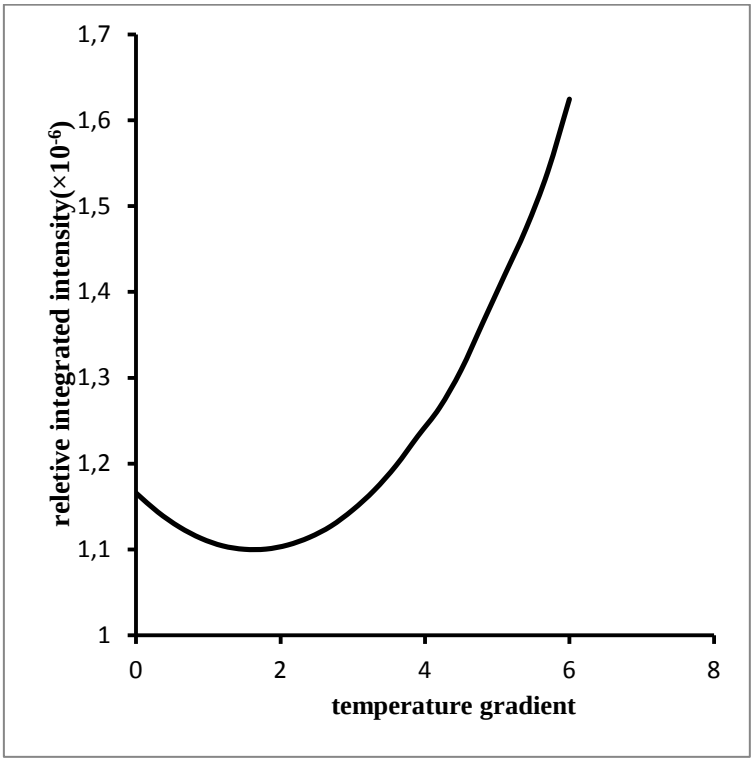

Fig.3.13 variations relative integrated intensity with temperature gradient, $\alpha > 0$,(101) ADP crystal, theoretical

According to (3.12) in the case $\alpha < 0$, the integrated intensity increases with increasing value of α(or $\frac{\Delta T}{\Delta x}$). Figure 3.14 shows dependence integrated intensity on α in this case.

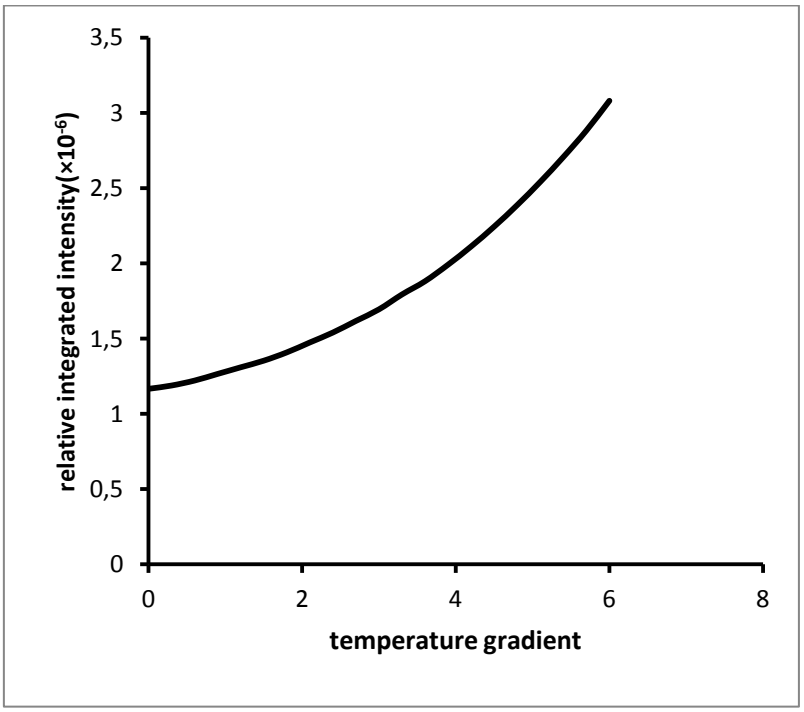

Fig. 3.14 variations the relative integrated intensity with temperature gradient, $\alpha < 0$, theoretical

As be seen theoretical results obtained by relation (3.12) are consistent with practical observations for ADP crystal in condition weak deformation.

3.1.4 Calculation of χ_{hr} and χ_{hi}, real and imaginary parts of Fourier-coefficients of polarizability, of ADP crystal

In section 3.1.2,the practical results of the variations of the integrated intensity of reflected beams from different atomic planes of ADP crystal under the influence temperature gradient were represented. As can be seen, there are a minimum in graph of the integrated intensity some atomic planes such as (100), (101) and (220). In the other hand, in case $\alpha>0$formula (3.12) represents which the integrated intensity has a minimum and this inconsistent with practical observations above mentioned. The modified Bessel function in (3.12) will be minimum when its argument is equal to zero i.e.

$$2\pi k|\chi_{hi}| - \frac{\alpha}{2\pi k|\chi_{hr}|} = 0, \tag{3.14}$$

$$|\chi_{\mathrm{hi}}||\chi_{\mathrm{hr}}| = \frac{\alpha}{(4\pi \mathrm{K})^2}, \tag{3.15}$$

And with usage of (3.13) have

$$|\chi_{\mathrm{hi}}||\chi_{\mathrm{hr}}| = \frac{\mathrm{ha}}{2(4\pi \mathrm{K})^2}\left(\frac{\Delta \mathrm{T}}{\Delta \mathrm{x}}\right)_{\mathrm{min}}, \tag{3.16}$$

$\left(\frac{\Delta \mathrm{T}}{\Delta \mathrm{x}}\right)_{\mathrm{min}}$ is value of temperature gradient which causes the integrated intensity be minimum.

Now we can extract values of χ_{hr} and χ_{hi} by usage from relations (3.16), (3.13) and experimental data which obtained in section 3.1.2 .Table 3.2 shows summery practical results of integrated intensity for some reflecting atomic planes ADP crystal [115]

Table 3.2 Dependence of the integrated intensity of reflection from atomic planes of ADP crystal on the applied temperature gradient and thickness of crystal

$\Delta T/\Delta x$ (deg/cm)	Intensity $(pulse/sec)$		
	t=2.5mm		t=1.3mm
	(100)	(101)	(220)
0	1400	4400	11000
1.5	1100	3900	10000
3	1200	4000	9500
4.5	2100	5300	9600
6	3400	6700	10000
12	5000	12000	17000
18	6600	17000	24000

For atomic plane (101), the value of the integrated intensity will be minimum when the temperature gradient is equal to $1.5\,\frac{deg}{cm}$ .With substituting amounts $\lambda=k^{-1}=0.56\times10^{-8}cm$, $d=h^{-1}=5.3\times10^{-8}cm$, $a=1.97\times10^{-5}K^{-1}$ and $\left(\frac{\Delta T}{\Delta x}\right)_{min}=1.5\,\frac{deg}{cm}$ in relation (3.16) have

$$|\chi_{hi}||\chi_{hr}| = 2.2\times10^{-16}, \tag{3.17}$$

Now, we obtain ratio between intensities in $\frac{\Delta T}{\Delta x}=6\,\frac{deg}{cm}$ and $\frac{\Delta T}{\Delta x}=4.5\,\frac{deg}{cm}$

$$\frac{I_0\left(\frac{t}{\cos\theta_B}\left(2\pi k|\chi_{hi}|-\frac{ha\times6}{4\pi k|\chi_{hr}|}\right)\right)}{I_0\left(\frac{t}{\cos\theta_B}\left(2\pi k|\chi_{hi}|-\frac{ha\times4.5}{4\pi k|\chi_{hr}|}\right)\right)}=\frac{6700}{5300}=1.26, \tag{3.18}$$

For solving the equation (3.18),it was used Taylor series expansion of modified Bessel function about the point zero.

$$I_0(x)=1+\frac{x^2}{4}+\frac{x^4}{64}+\frac{x^6}{2304}+\cdots \tag{3.19}$$

Using first two term of modified Bessel function, equation (3.18) become to

$$1+\frac{\left(\frac{t}{\cos\theta_B}\left(2\pi k|\chi_{hi}|-\frac{ha\times 6}{4\pi k|\chi_{hr}|}\right)\right)^2}{4}=1.26+\frac{1.26\left(\frac{t}{\cos\theta_B}\left(2\pi k|\chi_{hi}|-\frac{ha\times 4.5}{4\pi k|\chi_{hr}|}\right)\right)^2}{4} \quad (3.20)$$

Solving the system of two equations (3.17) and (3.20) have

$$|\chi_{hr}|=0.14\times10^{-6},\ |\chi_{hi}|=0.16\times10^{-8}, \quad (3.21)$$

We repeat the same way for atomic plane (100).The integrated intensity of the atomic plane (100)will be minimum when the temperature gradient be equal to $1.5\frac{\deg}{cm}$. With substituting amounts $\lambda=k^{-1}=0.56\times10^{-8}$cm, $d=h^{-1}=7.5\times10^{-8}$cm, $a=1.97\times10^{-5}K^{-1}$ and $\left(\frac{\Delta T}{\Delta x}\right)_{min}=1.5\ \frac{deg}{cm}$ in relation (3.16) have

$$|\chi_{hi}||\chi_{hr}|=1.6\times10^{-16}, \quad (3.22)$$

Ratio of the intensities in $\frac{\Delta T}{\Delta x}=6\frac{\deg}{cm}$ and $\frac{\Delta T}{\Delta x}=4.5\frac{\deg}{cm}$ is equal to

$$\frac{I_0\left(\frac{t}{\cos\theta_B}\left(2\pi k|\chi_{hi}|-\frac{ha\times 6}{4\pi k|\chi_{hr}|}\right)\right)}{I_0\left(\frac{t}{\cos\theta_B}\left(2\pi k|\chi_{hi}|-\frac{ha\times 4.5}{4\pi k|\chi_{hr}|}\right)\right)}=\frac{3400}{2100}=1.62, \quad (3.23)$$

By doing the similar calculation of above mentioned have

$$|\chi_{hr}|=0.44\times10^{-7},\ |\chi_{hi}|=0.35\times10^{-8}, \quad (3.24)$$

Finally for atomic plane (220), the integrated intensity will be minimum when the temperature gradient be equal to $3\frac{\deg}{cm}$.With substituting amounts $\lambda=k^{-1}=0.56\times10^{-8}$cm, $d=h^{-1}=2.65\times10^{-8}$cm, $a=1.97\times10^{-5}K^{-1}$and $\left(\frac{\Delta T}{\Delta x}\right)_{min}=3\frac{deg}{cm}$ in relation (3.16) have

$$|\chi_{hi}||\chi_{hr}|=8.8\times10^{-16}, \quad (3.25)$$

Ratio of intensities in $\frac{\Delta T}{\Delta x}=6\frac{\deg}{cm}$ and $\frac{\Delta T}{\Delta x}=4.5\frac{\deg}{cm}$

is equal to

$$\frac{I_0\left(\frac{t}{\cos\theta_B}\left(2\pi k|\chi_{hi}|-\frac{ha\times 6}{4\pi k|\chi_{hr}|}\right)\right)}{I_0\left(\frac{t}{\cos\theta_B}\left(2\pi k|\chi_{hi}|-\frac{ha\times 4.5}{4\pi k|\chi_{hr}|}\right)\right)}=\frac{10000}{9600}=1.04, \quad (3.26)$$

By doing the similar calculation of above mentioned have

$$|\chi_{hr}|=0.28\times10^{-6},\ |\chi_{hi}|=0.32\times10^{-8}, \quad (3.27)$$

Table 3.3 shows obtained values of χ_{hr} and χ_{hi}.

Table 3.3. The values of χ_{ih} and χ_{rh} of different atomic planes for ADP crystal .

ADP	$\|\chi_{hr}\|$	$\|\chi_{hi}\|$
(100)	0.44×10^{-7}	0.35×10^{-8}
(101)	0.14×10^{-6}	0.16×10^{-8}
(220)	0.28×10^{-6}	0.32×10^{-8}

3.2 Investigation of rocking curve of ADP single crystal under the influence of temperature gradient applied perpendicular to reflecting atomic planes

In this section, we present the rocking curve of reflection, transition and total intensity of ADP crystal under influence of temperature gradient applied perpendicular to reflecting atomic plane in Laue-case geometry[116]. Practical results of reflectivity are compared with theoretical results which have been obtained based on the asymptotic solution of dynamical diffraction of X-ray wave in crystals with weak deformation.

3.2.1 Experimental results

Experimental studies were performed with the scheme of two crystals. The x-ray tube BSV-Mo 27 was used as a source radiation. Experiment carried out for reflecting atomic plane (002) of ADP crystal with thickness of 1.9 mm in presence of a temperature gradient of perpendicular to the reflecting atomic planes. The intensity of passing beams of x-ray was recorded by a scintillation counter. Figures3.15up to 3.18 show the rocking curves of reflectivity from atomic plans (002) of ADP crystal for different values of the temperature gradient.

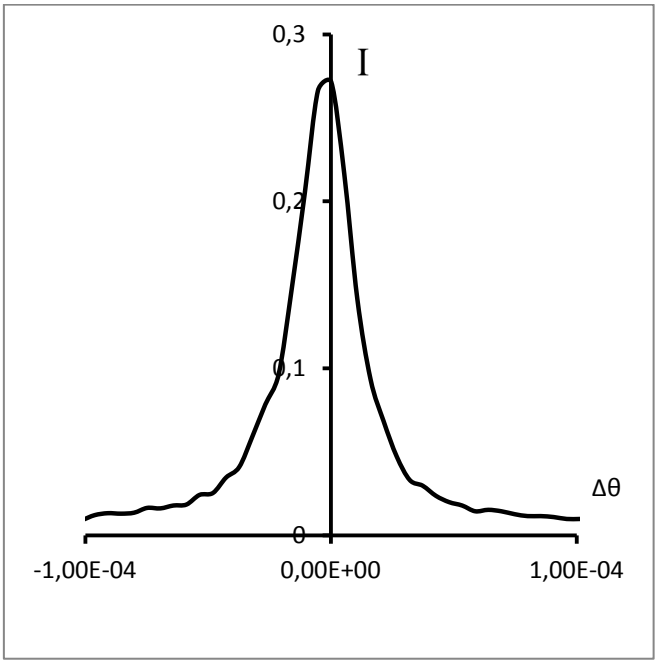

Fig. 3.15 The rocking curve of reflectivity from (002) ADP crystal in absence of temperature gradient.

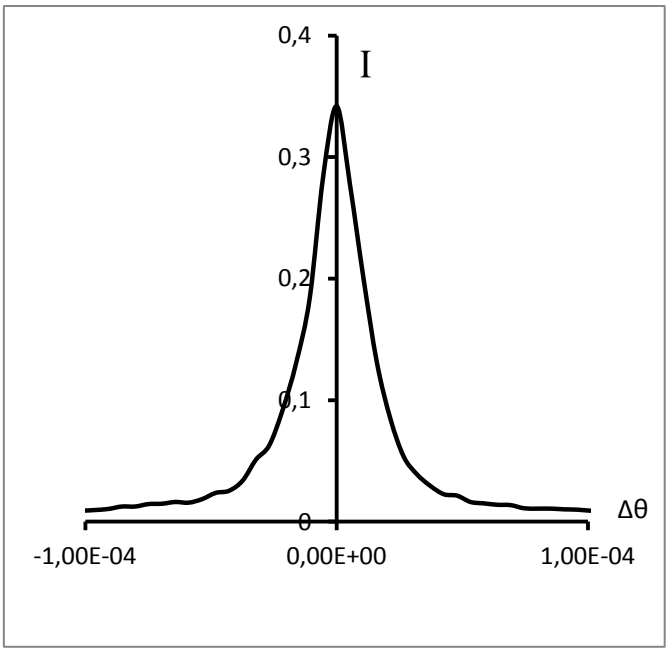

Fig. 3.16 The rocking curve of reflectivity from (002) ADP crystal in presence of temperature gradient, $\Delta T/\Delta x=6$ deg/cm

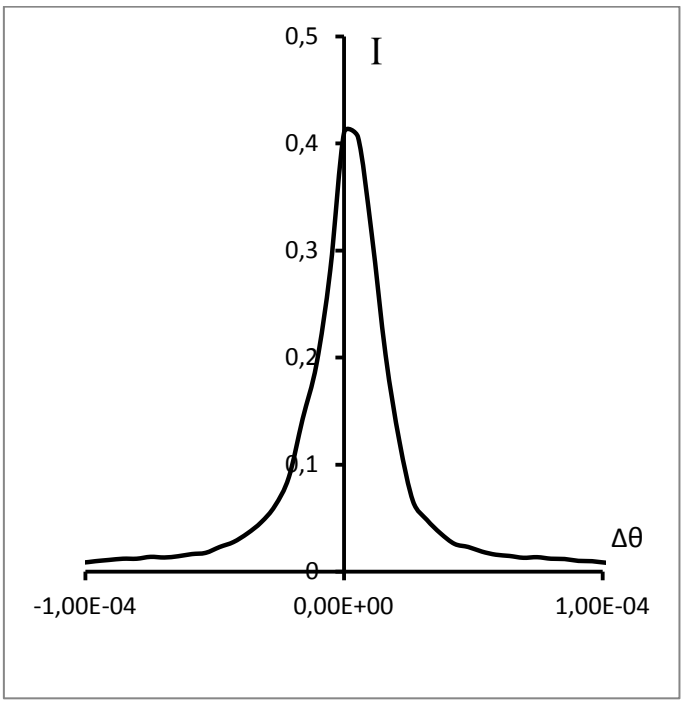

Fig. 3.17. The rocking curve of reflectivity from (002) ADP crystal in presence of temperature gradient, ΔT/Δx=12 deg/cm.

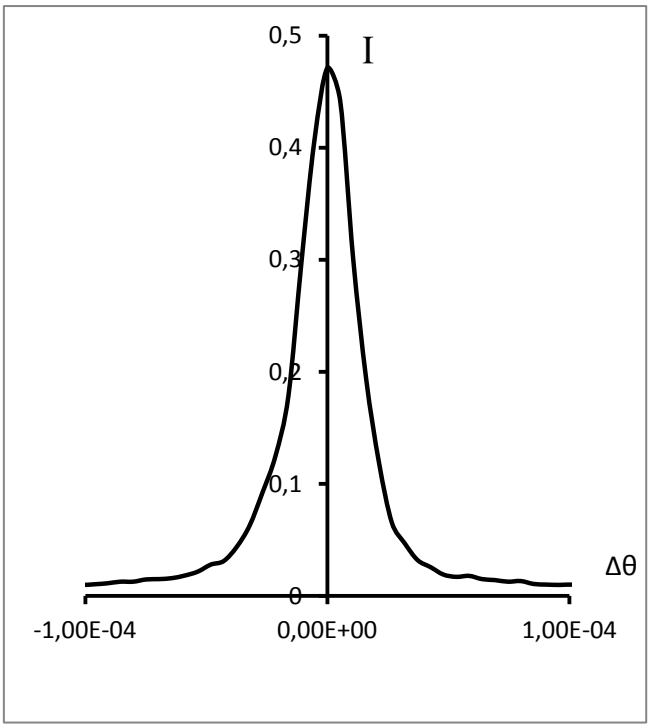

Fig. 3.18 The rocking curves of reflectivity from (002) ADP crystal in presence of temperature gradient, ΔT/Δx=18 deg/cm

As be seen, the reflectivity increases with increase of the value of the temperature gradient, but the width of rocking curve slightly increases. Table 3.4 shows the value of intensity at Bragg angel *(Δθ= 0)* and FWHM of rocking curves.

Table 3.3T

he values of maximum intensity and FWHM of rocking curves for different temperature gradient

ΔT/Δx (deg/cm)	0	6	12	18
I_{max}	0.27	0.34	0.41	0.47
FWHM ($\times 10^{-5}$rad)	4.6	5	5.2	5.6

We also measured the rocking curves of transmitted intensity beam and the total intensity of the transmitted beams.

The intensity of transmitted X-ray was recorded by scintillation counter. Figures3.19 up to 3.22 show the rocking curves of transmitted beam of ADP crystal for different values of the temperature gradient applied to the crystal.

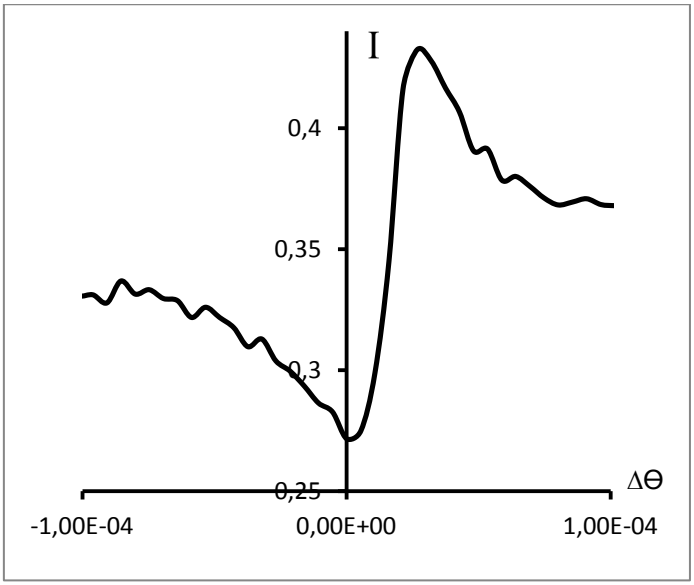

Fig. 3.19 The rocking curves of transmitted beam from ADP crystal in absence of temperature gradient

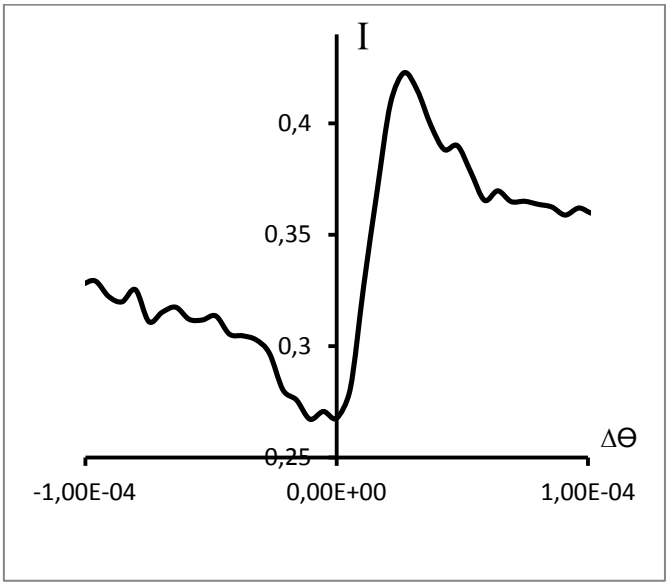

Fig. 3.20 The rocking curves of transmitted beam of ADP crystal in presence of temperature gradient, ΔT/Δx=6 deg/cm

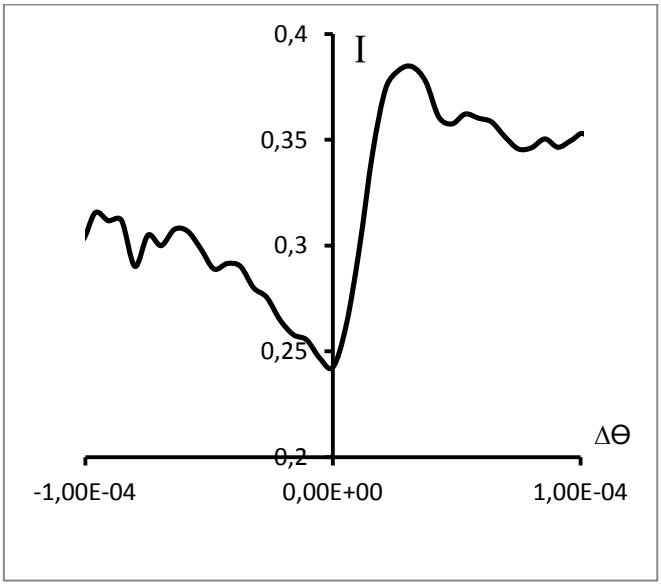

Fig. 3.21 The rocking curves of transmitted beam of ADP crystal in presence of temperature gradient, ΔT/Δx=12 deg/cm

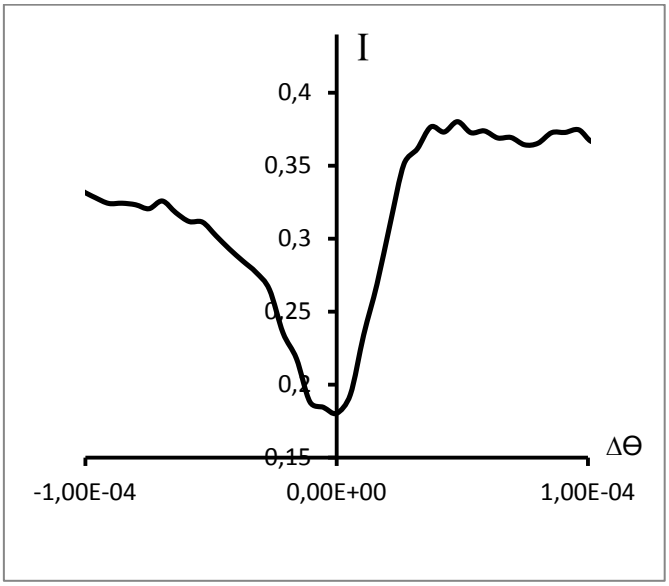

Fig. 3.22 The rocking curves of transmitted beam of ADP crystal in presence of temperature gradient, $\Delta T/\Delta x$=30 deg/cm

As be seen, the intensity of transmitted beam at Bragg angel ($\Delta\theta$ =0) decreases with the increase of the temperature gradient, which indicate the phenomena of transfer of the X-ray intensity from the transmission direction to the reflection direction in Laue geometry.

For measurement of the total intensity of transmitted and reflected beams, we put counter near the crystal in order to both reflected and transmitted beam at the same time arrived in counter (fig 3.23).

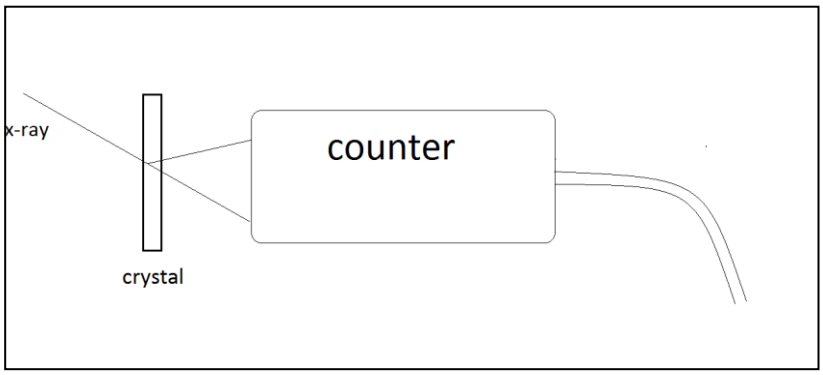

Fig. 3.23 scheme of measurement of total intensity

Figure 3.24 shows the dependence of the total intensity of X-ray on the deviation from the Bragg angle for different values of temperature gradient applied to the crystal.

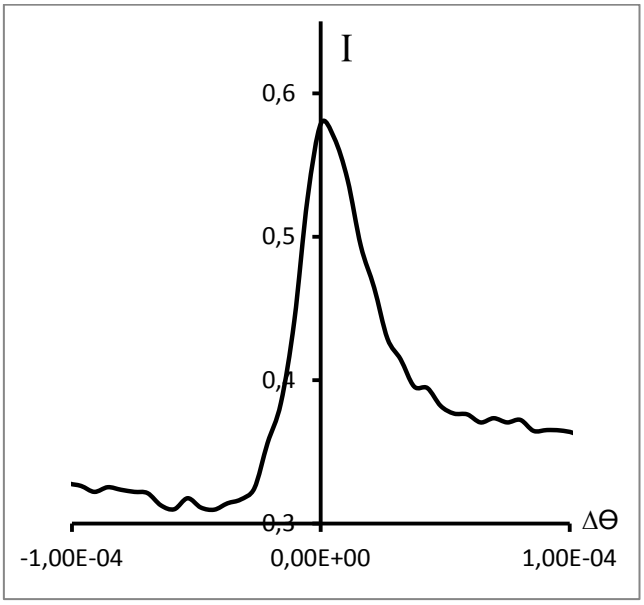

Fig. 3.24 The rocking curve of passing the total intensity from (002) ADP crystal in absence temperature gradient

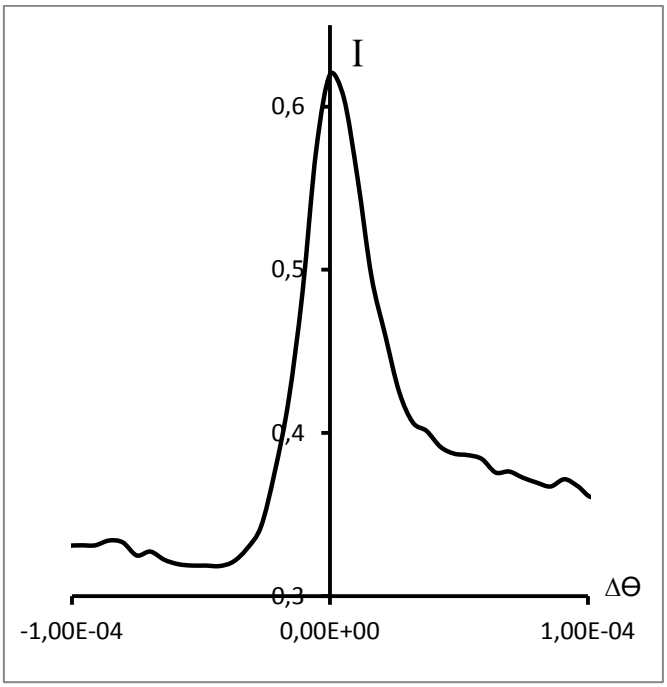

Fig. 3.25 The rocking curve of the passing total intensity of (002) ADP crystal in presence temperature gradient, $\Delta T/\Delta x$=6 deg/cm

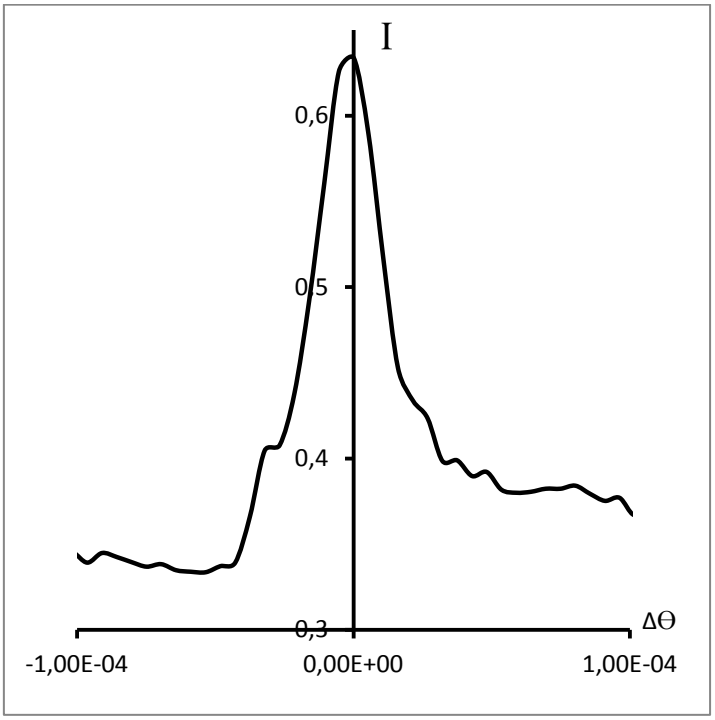

Fig. 3.26 The rocking curve of the passing total intensity of (002) ADP crystal in presence temperature gradient, ΔT/Δx=12 deg/cm

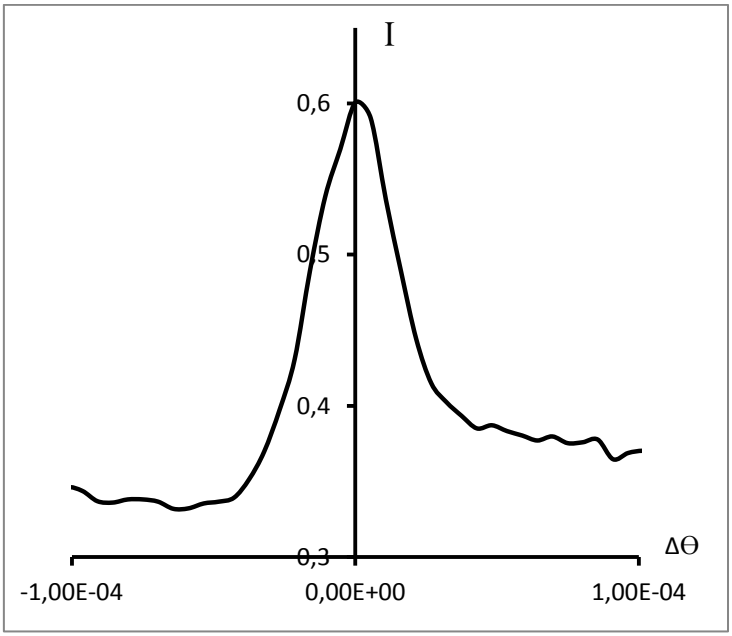

Fig. 3.27 The rocking curve of the passing total intensity of (002) ADP crystal in presence temperature gradient, ΔT/Δx=30 deg/cm

As be seen in figures 3.24 to 3.27, with the increase of the temperature gradient, the passing total intensity initially increases until reaches a maximum value at certain temperature gradient *(ΔT/Δx =12 deg/cm)*and then begins to decrease. This behavior is caused by the variations of

the absorption interference coefficient of X-rays in ADP crystals under effect of temperature gradient. This phenomenon also observed for quartz single crystal. Ref. [81] showed for quartz single crystal with the increase of the temperature gradient, the interference coefficient of absorption of X-ray at certain value of temperature gradient has a minimum value.

3.2.2 Theoretical analysis of reflectivity

The reflectivity of symmetric Laue geometry without influences of external force is defined by the formula following [2]:

$$I_R = \frac{e^{\frac{-\mu z}{\cos\theta_B}}}{2(1+p^2)} \times \left[cosh\left(G_i \frac{z}{\cos\theta_B}\right) - cos\left(\frac{2\pi kc|X_{hr}|}{sin\theta_B}\sqrt{1+p^2}z\right)\right], \quad (3.28)$$

$$G_i = (2\pi k|X_{hi}|) \times \frac{1}{\sqrt{1+p^2}}, \quad (3.29)$$

Where θ_B is the Bragg angle, μ is the linear absorption coefficient of the crystal, p is deviation parameter from Bragg angel, χ_{hi} and χ_{hr} the imaginary and real parts of Fourier coefficient of crystal polarizability, respectively. We already described that in our experimental conditions can start from the assumption of a weak deformation field and use the theoretical results obtained in [110](see 1.2.2). Under conditions weak deformation in crystals, it should replace term $2\pi k\chi_{hi}$ by $2\pi k\chi_{hi} - \frac{\alpha}{2\pi k|X_{hr}|}$ in reflectivity formula. Here α is parameter of crystal deformation and under the influence of the temperature gradient is equal to

$$\alpha = \frac{h}{2R} = \pm\frac{ha}{2}\frac{dT}{dx}, \quad (3.30)$$

Where $h$is the magnitude of diffraction vector of corresponding with reflecting atomic plans. Expression (3.29) under the influences of the temperature gradient is converted to

$$G_i = (2\pi k|\chi_{hi}| \mp \frac{|\alpha|}{2\pi k|\chi_{hr}|}) \times \frac{1}{\sqrt{1+p^2}}, \quad (3.31)$$

The sign of α is determined by the sign of R in (3.3). The behavior of reflectivity dependence on sign of α. with considering of (3.28) and (3.31), It is obvious in case $\alpha>0$, with increase of temperature gradient, reflectivity initially drops to a minimum and then begins to increase. This phenomenon was explained in section 3.1.3. In case $\alpha<0$, reflectivity increases with the increase of the temperature gradient. The experimental results of reflectivity obtained from atomic planes (002) ADP crystal correspond to the latter case.

Calculation of χ_{hi} and χ_{hr}

We measured the value of reflectivity in absence temperature gradient at exact Bragg angel (p=0) and then substituted the obtained value in the equation (3.28) and calculated the value of χ_{hi} following

$$\chi_{hi} = 0.6 \times 10^{-8},$$

Also with measurement of Darwin width and usage of definition below

$$\delta_{0s} = \frac{\sqrt{\chi_h \chi_{\bar{h}}}}{\sin 2\theta_B}, \tag{3.32}$$

Value of χ_{hr} was estimated

$$\chi_{hr} = 0.2 \times 10^{-5},$$

Attaining rocking curve of reflectivity in presence temperature gradient-theoretically

For simplicity, we ignored from term of cosine in (3.28). Theoretical formula of reflectivity was obtained by Relations (3.28) and (3.21) for atomic plane (002) of ADP crystal with thickness 1.9mm under the influences of temperature gradient. Figures 3.28 up to 3.31 show theoretical and experimental Rocking curves of reflectivity for different values of temperature gradient.

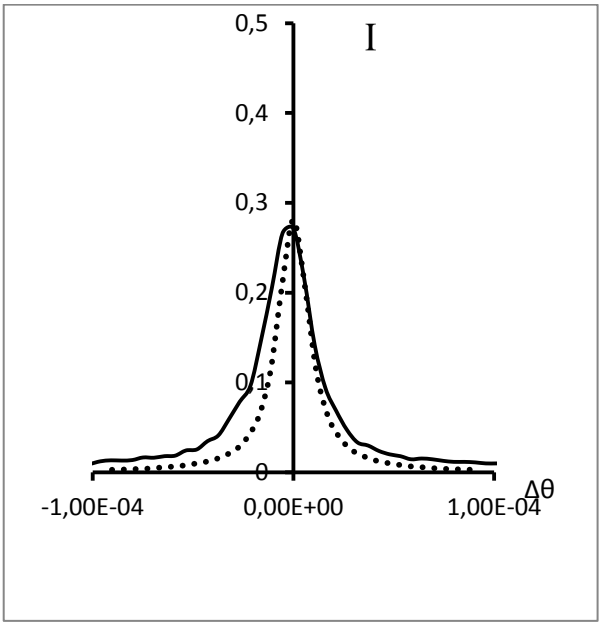

Fig. 3.28 The rocking curves of reflectivity from (002) of ADP crystal in absence temperature gradient, solid curve: Experimental, dotted curve: theoretical

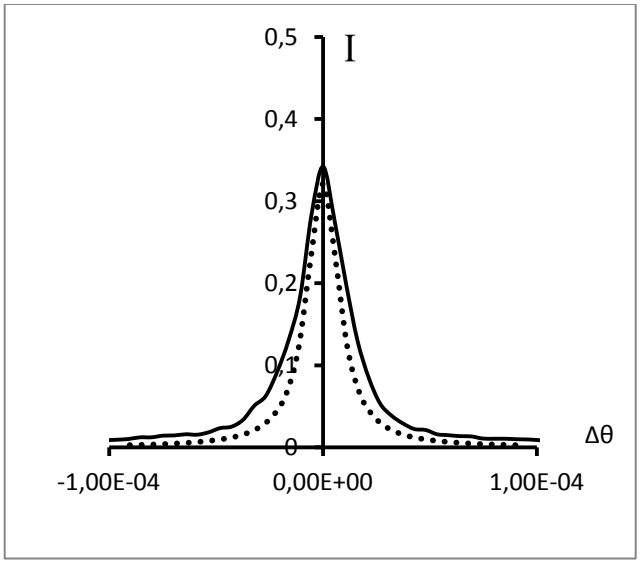

Fig.3.29 The rocking curves of reflectivity from (002) of ADP crystal in presence gradient dT/dx=6 deg/cm, solid curve: experimental, dotted curve: theoretical

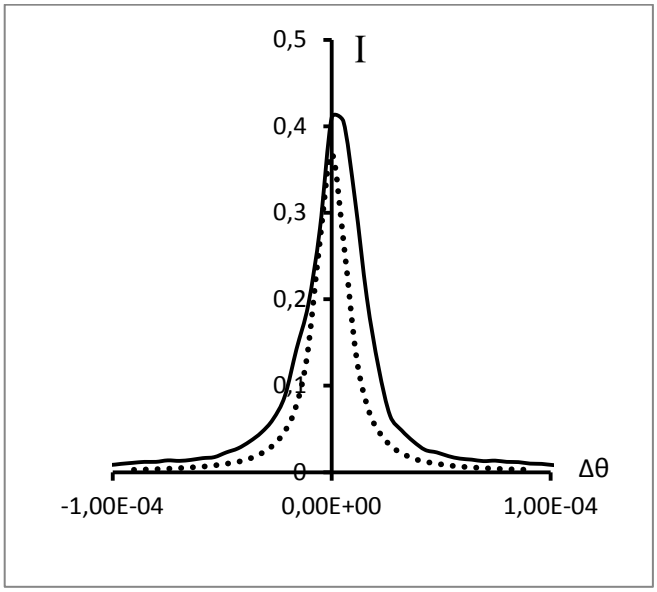

Fig.3.30 The rocking curves of reflectivity from (002) of ADP Crystal in presence temperature gradient dT/dx=12 deg/cm, solid curve: experimental, dotted curve: theoretical

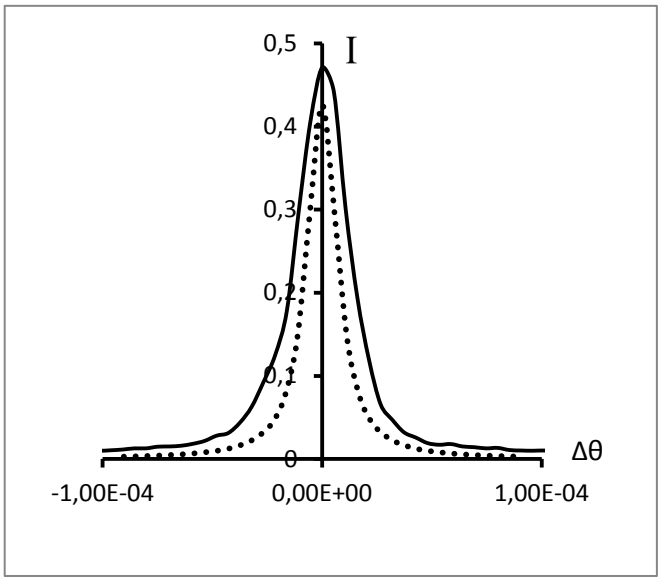

Fig. 3.31 The rocking curves of reflectivity from (002) of ADP crystal in presence temperature gradient dT/dx=18deg/cm, solid curve: experimental, dotted curve: theoretical

As can be seen, the values of theoretical reflectivity at exact Bragg angel approximately correspond to practical results. On the other hand, width of theoretical rocking curves not considerably changes with the increase of temperature gradient while in practical case width of rocking curves have slightly increase.

3.3 The X-ray diffraction on single crystal of ADP under the influence of temperature gradient applied parallel to reflecting atomic planes

In this part of the work, we continue our investigation about dependence of the intensity of the diffracted X-rays from single crystal of ammoniumdihydrogen phosphate(ADP) and quartz in the Laue geometry when direction of temperature gradient is parallel to reflecting atomic planes. In this case, the temperature gradient causes the shape of atomic planes of perpendicular to large surface of crystal change as fan-shape.

3.3.1 Experimental methods

The experiments were performed by the X-raydiffractometerDRON-3M. X-ray tubes BSV- 29 with anodes Ag and Mo were used as sources radiation x-ray. Focal spot sizes were 0.4mmhorizontallyand8mm vertically. The tube voltage and current were 40kV and 20 mA respectively. The intensity of diffracted beam was measured with a scintillation counter.T he temperature of surfaces of single crystals was measured with a copper-constantan thermocouple with accuracy ± 0.5℃.The thickness of ADP crystal and quartz was 1.88mm and3 mm respectively. Fig.3.13 shows scheme of experiment. As be seen, we used a handle hot-air blower for increase of temperature of front surface of crystal. Using this device had this advantage, which all front surface of crystal heated uniformly. This device was introduced in second chapter. With applying this device, the entrance surface was the hotter than the exit surface of the single crystal because the front surface is only heated by warm air.

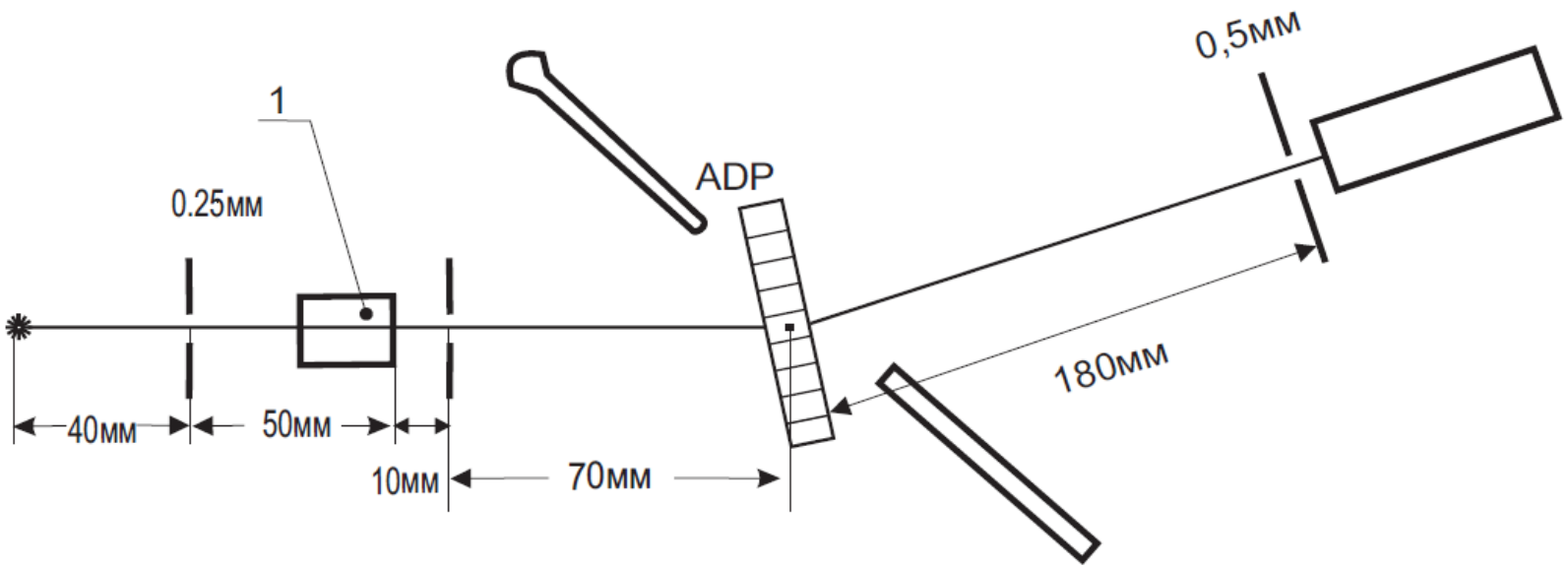

Fig.3.32 Scheme of experiment

3.3.2 Experimental results

We experimentally studied the phenomenon of pumping of the passing intensity from the transmission direction to the reflection direction for atomic plane (002) of ADP crystal with Mokα_1 and Agkα_1 lines and also for atomic planes $(10\bar{1}0)$, $(10\bar{1}1)$, $(21\bar{3}1)$ quartz with Agkα_1 line under the influence of the temperature gradient parallel to reflecting atomic planes. Thickness of single crystal of ADP and quartz selected 1.88 mm and 3 mm, respectively. The linear absorption coefficient of ADP is 2.75 cm^{-1} and 5.4 cm^{-1} for Agkα_1 and Mokα_1 lines, respectively. The linear absorption coefficient of quartz is 10.4 cm^{-1} for Mokα_1 line. The results of the experiment are shown following:

Table 3.4 The integrated intensity of reflected beam from the atomic plane (002) of ADP crystal in presence temperature gradient. t=1.88mm , K : coefficient of amplification

$\Delta T/\Delta x$ (deg/cm)	Intensity (pulses/s)	
	Mokα_1	Agkα_1
0	9857	10000
9	12857	16000
14	14714	18000
19	16714	23000
27	18571	25000
33	20571	
K	2	2.5

Table 3.32 The integrated intensity of reflected beam from different the atomic planes of quartz in presence temperature gradient. t=3mm , K : coefficient of amplification.

$\Delta T/\Delta x$ (degree/cm)	Intensity (pulses/s)		
	$(21\bar{3}1)$	$(10\bar{1}0)$	$(10\bar{1}1)$
0	1900	1698	1400
18	2200	1754	1460
23	2600	1811	1570
40	3100	1886	1660
63	4000	2452	1860
93	5000	2924	2100
106.6	5600	3773	2600
K	2.9	2.2	1.9

We obtained the amplification coefficient of the intensity of the beam reflected from atomic planes. The amplification coefficient K is defined as the ratio of the intensity of reflected beam in the presence temperature gradient, in the point where intensity of saturation begins, to the intensity without temperature gradient [109]. As be seen the value of this coefficient is various for different atomic planes and different length wave.

With usage of experimental data of Table 3.4, the graphs of the integrated intensity of the reflection versus the temperature gradient have been plotted for the atomic plane (002) single crystal of ADP.

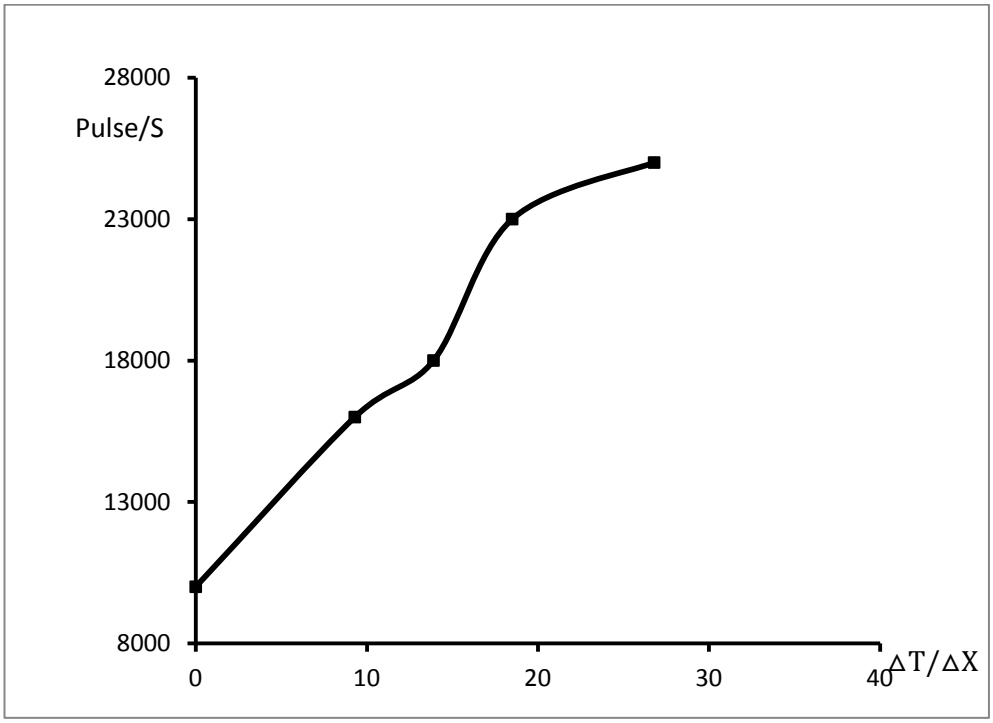

Fig. 3.33 Dependence of the integrated intensity of reflected beam on the temperature gradient for the atomic plane (002) of ADP crystal , Agkα line, t=1.88 mm.

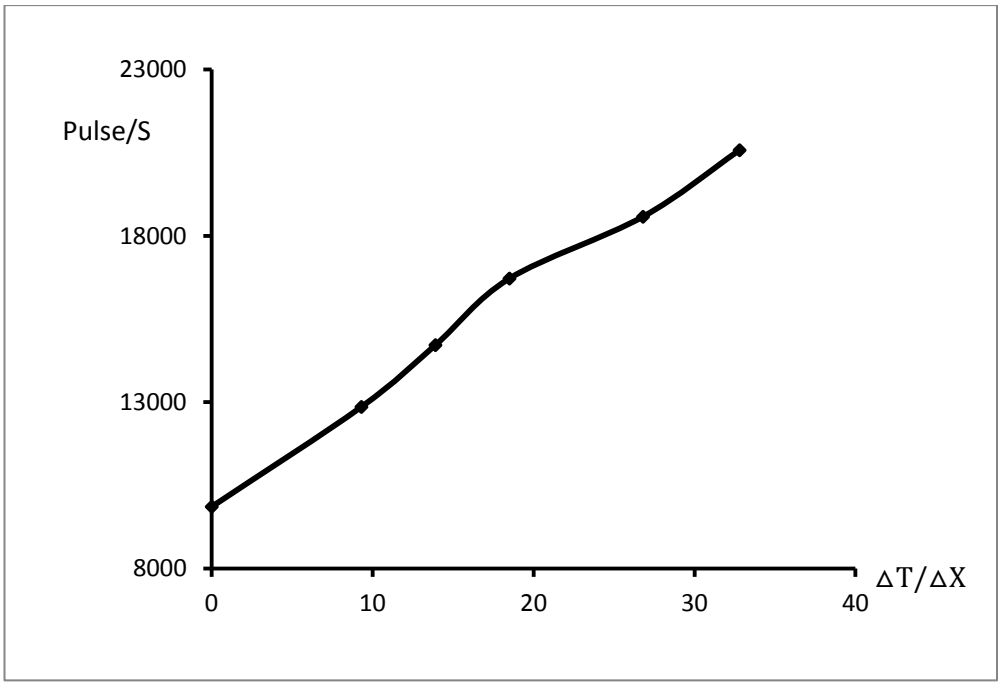

Fig. 3.34 Dependence of the integrated intensity of reflected beam on the temperature gradient for the atomic plane (002) of ADP crystal , Mokα line, t=1.88 mm.

Also with usage of experimental data of Table 3.5, the graphs of the integrated intensity of the reflection versus the temperature gradient were plotted for different atomic planes single crystal of quartz.

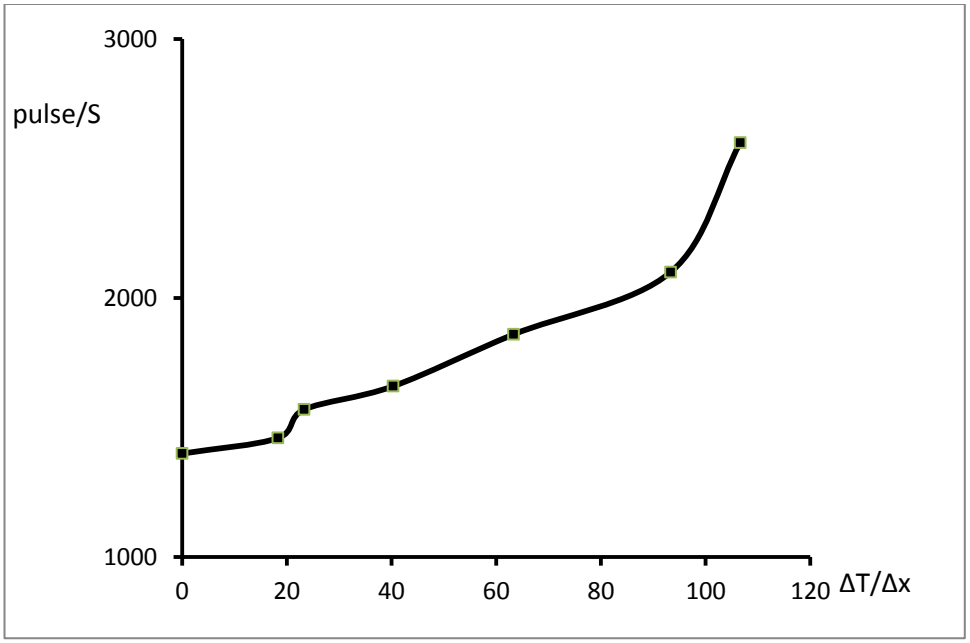

Fig. 3.35 Dependence of the integrated intensity of reflected beam on the temperature gradient for the atomic plane (10-11) of quartz crystal , Mokα line, t=3 mm

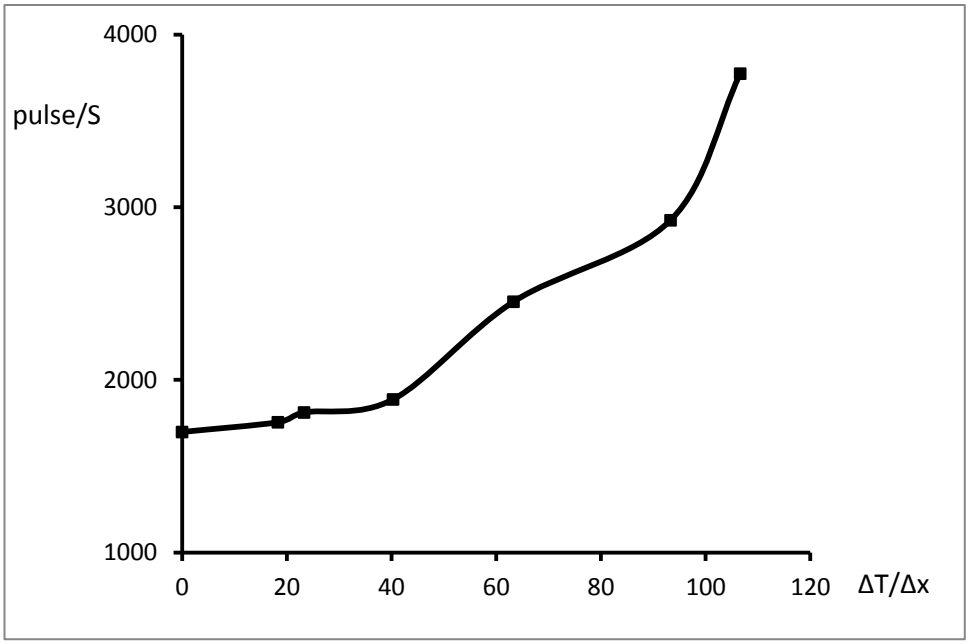

Fig. 3.36 Dependence of the integrated intensity of reflected beam on the temperature gradient for the atomic plane (10-10) of quartz crystal , Mokα line, t=3 mm

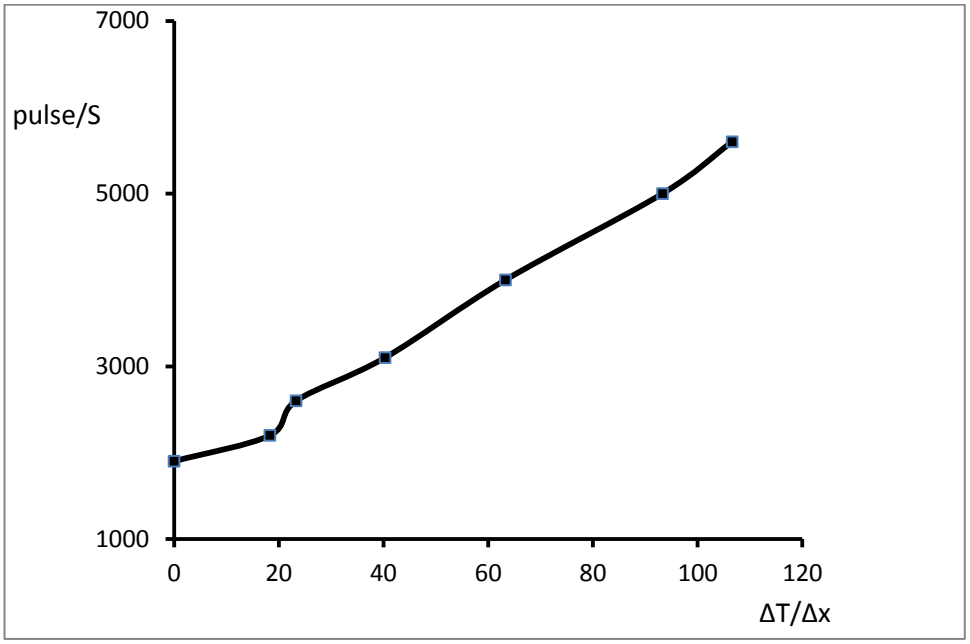

Fig. 3.37 Dependence of the integrated intensity of reflected beam on the temperature gradient for the atomic plane (21-31) of quartz crystal , Mokα line, t=3 mm

As seen in above graphs, the integrated intensity of the reflected beam increases almost linearly with increase of the temperature gradient. The integrated intensity increases more than twice for atomic plane (002) of ADP, and about three times for the atomic plane (213_1) of quartz but none of them are not saturation.

3.3.3 Theoretical analyses

The crystal under the influence of the temperature gradient applied perpendicular to the front surface of the crystal deforms as shape is shown in Fig 3.38[115]. The axis of curvature is parallel to the Y- axis and R is the radius of curvature.

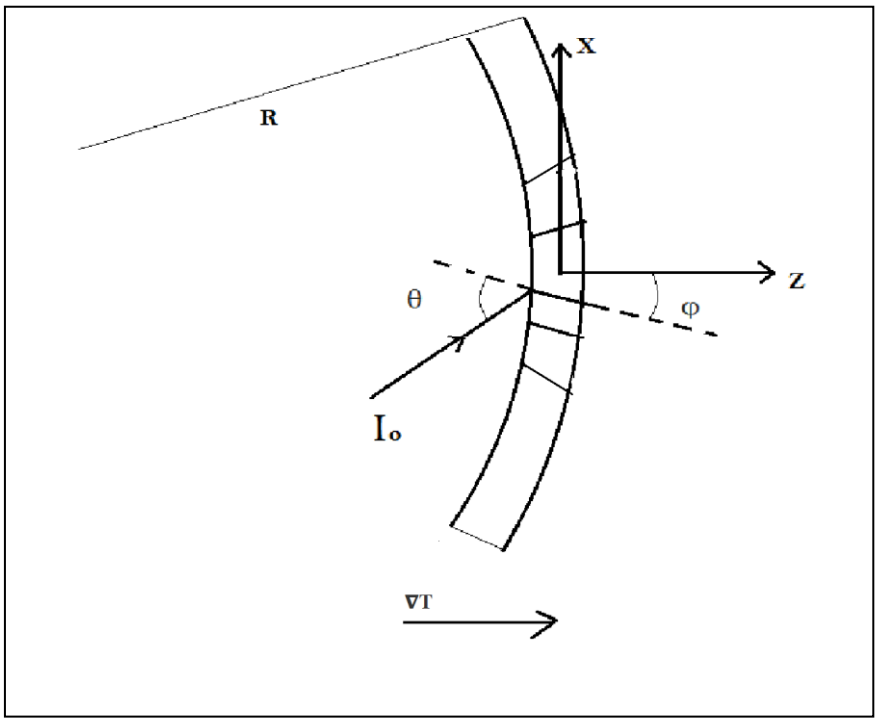

Fig.3.38 diagram of the deformed crystal under the influence of temperature gradient perpendicular to front surface

In this situation, the reflecting atomic planes reshape as fan-shape and make a small angle φ with the axis Z. In absence of the temperature gradient, the angle is equal to zero. The scalar product$\boldsymbol{h}.\boldsymbol{u}(\boldsymbol{r})$is the main parameter that determines the behavior of the wave field in the crystal. Where $\boldsymbol{h}$ is reciprocal lattice vector for the family of atomic planes (hkl), and $\boldsymbol{u}(\boldsymbol{r})$is displacement vector.

The under conditions uniform temperature gradient, the lattice planes perpendicular to ∇T are curved with a radius *R*, where according to (1.79) is equal to

$$1/_R = \pm|\nabla(aT)|, \tag{3.33}$$

Here *a* is coefficient of linear thermal expansion of the crystal. The atomic planes parallel to ∇T remain flat but become taper with respect to each other. The displacement vector is given by:

$$\boldsymbol{u}(\boldsymbol{r}) = \boldsymbol{r}[\boldsymbol{r}.\boldsymbol{\nabla}(aT)] - \frac{1}{2}(\boldsymbol{r}.\boldsymbol{r})\boldsymbol{\nabla}(aT), \tag{3.34}$$

Where $\boldsymbol{r}$is the position vector of the considered point. The vector of temperature gradient is obtained from(3.33):

$$\boldsymbol{\nabla}(aT)=\frac{1}{R}\vec{k} \tag{,3.35}$$

Also have

$$\boldsymbol{r} = x\vec{\imath}+z\vec{k}\ , \tag{3.36}$$

Under the conditions of constancy of the applied temperature gradient, components of the displacement vector obtain following [15]

$$\boldsymbol{u}(\boldsymbol{r}) = (\ x\vec{\imath} + z\vec{k})\ (\frac{z}{R}) - \frac{1}{2}\ (x^{\mathbf{2}} + z^2)(\frac{1}{R}\vec{k})\ , \tag{3.37}$$

$$u_x = \frac{xz}{R}\ , \tag{3.38}$$

$$u_z = \frac{z^2-x^2}{R}\ , \tag{3.39}$$

Now, we obtain the scalar product between the reciprocal lattice vector ***h*** and the displacement vector deformation field ***u(r)*** that this product determines the behavior of the wave field in the lattice.

$$\boldsymbol{h.u(r)} = \frac{hxz}{R} - h\frac{(\gamma-1)}{2R}(z^2 - x^2), \tag{3.40}$$

Where $\gamma=\frac{\gamma_h}{\gamma_0}$ is factor asymmetrical as γ_0 andγ_h are direction cosines for the incident and reflected directions, respectively. In case φ=0 (=1), considering to (3.40), the second term vanishes and the wave field propagates in the crystal without feeling the strain. However, even small shifts of symmetric diffraction geometry, are considerable. Even if φ ≈ 0.5 degrees, it is significant from the point of view of the formation of the diffraction of the wave field in the lattice.

We in subsection 3.1.2 represent formula of integrated intensity of reflection (3.11) that under the influences of temperature gradient and condition weak deformation becomes to (3.12).

Now we calculate α for new conditions this experiment, according to definition have

$$\alpha = \frac{\partial^2(\boldsymbol{h.u})}{\partial S_0 \partial S_h}, \tag{3.41}$$

Where

$$X= (S_0 - S_h)sin\theta_B \ , \quad z= (S_0 + S_h)cos\theta_B, \tag{3.42}$$

With usage of (3.42), expression (3.41) becomes

$$\boldsymbol{h.u(r)} = \frac{h(S_0-S_h)sin\theta_B \times (S_0+S_h)cos\theta_B}{R} - h\frac{(\gamma-1)}{2R}(((S_0 + S_h)cos\theta_B)^2 - ((S_0 - S_h)sin\theta_B)^2), \tag{3.43}$$

After doing calculation and usage of (3.41) have

$$\alpha = \frac{(1-\gamma)h}{2R} = \pm\frac{(1-\gamma)ha}{2}\frac{dT}{dx}, \tag{3.44}$$

With substituting (3.44) in expression (3.12), formula of the integrated intensity is obtained following

$$\mathrm{I_h} = \mathrm{I_i}\frac{\pi|\chi_{hr}|}{2\sin 2\theta_B} e^{-\frac{\mu t}{\cos\theta_B}} \mathrm{I_0}\left(\frac{t}{\cos\theta_B}\left(2\pi k|\chi_{hi}| \mp \frac{(1-\gamma)ha}{4\pi k|\chi_{hr}|}\frac{dT}{dx}\right)\right), \tag{3.45}$$

According to (3.45), the integrated intensity is as a temperature gradient (orα) which in case $\frac{dT}{dx} > 0$, in the certain temperature gradient has a minimum

$$\frac{dT}{dx} = \frac{8\pi^2 k^2}{(1-\gamma)ha} |\chi_{hi}||\chi_{hr}| , \quad (3.45)$$

Note that due to the smallness of the parameter α, minimum the integrated intensity is very close to the value α = 0, and this minimum is observed relatively clear in fig3.35 and fig 3.37

. The rest of the formula (3.45) fairly well describes the experimental dependence of $I_h$to$\frac{dT}{dx}$.

Conclusion

1. We investigated the dependence of the integrated intensity of diffracted beams of X-ray from a single crystal of ammonium dihydrogen phosphate (ADP) in the Laue geometry under influence temperature gradient. It is found that the integrated intensity of reflected beam almost linearly depends on magnitude of the temperature gradient applied perpendicular to the reflecting atomic planes up to saturation but when direction of diffraction vector is opposite direction of the temperature gradient for small values of the temperature gradient,with increase of the temperature gradient, the integrated intensity initially reduced by about 10% and then monotonically increases. Finally, the observed phenomenon was describable by theoretical analysis based on the asymptotic solution of dynamical diffraction of X-ray.
2. In a certain temperature gradient applied perpendicular to the reflecting atomic planes,it was observed that the integrated intensity of reflected beam of X-ray from single crystal of ammonium dihydrogen phosphate (ADP) in the Laue geometry has a minimum value. We succeed in extracting values ofχ_{hi} andχ_{hr} the imaginary and real parts of coefficient of Fourier expansion of polarizability for ADP crystal by using the formula of integrated intensity of reflection in crystals with weak deformation.

3. We measured rocking curves of the reflectivity for ADP crystal under the influence of temperature gradient in Laue-case geometry and observed that an increase in the temperature gradient lead to an increase of reflectivity and also a slight increase in width of

rocking curves. We used the asymptotic solution of dynamical diffraction of X-ray wave in crystals with weak deformation and our theoretical results were consistent with experimental results.

4. The reflecting atomic planes deform to fan-shaped when the temperature gradient vector is applied parallel to the reflecting atomic planes and perpendicular to the front surface of crystal. We investigated the effect of the fan-shaped deformation on the integrated intensity of the reflected beam from single crystals of ammonium dihydrogen phosphate (ADP) and quartz (SiO_2) in the Laue geometry. Experimental results show that with the increase ofthe temperature gradient, the integrated intensity of the reflected beam increases more than 100% for different atomic planes .A theoretical analysis has been given to explain the experimental results.

Main results of dissertation are stated in the following publications

1. V.Gh.Mirzoyan, K.G.Trouni, M.Ghannad Dezfouli. The intensity of the diffracted X-rays from single ADP crystal in the presence of temperature gradient. XTOP 2012, Biennial Conference on High Resolution X-ray Diffraction Imaging. Book of abstracts p.261, Saint- Petersburg, Russian Federation (2012)
2. K. G. Trouni, V. Gh. Mirzoyan, M. Ghannad Dezfouli and P. A. Grigoryan. integral reflection coefficients for the dynamic scattering of X-ray in weakly deformed crystals. III International Conference Electron, Positron, Neutron and X-ray scattering under external influences. Meghri, P. 95(2013)
3. K. G. Trouni,M. Ghannad Dezfouli,integratedintensity for the dynamic diffraction of thermal Neutrons in weakly deformed crystals.III International Conference Electron, Positron, Neutron and X-ray scattering under external influences. Meghri, P. 84(2013)
4. V. Gh. Mirzoyan, K. G. Trouni, P. A. Grigoryan,K. M. Gevorgyan, M. Ghannad Dezfouli.Dynamical diffraction of X-ray on ADP single crystal under the influence of thermal gradient.III International Conference Electron, Positron, Neutron and X-ray scattering under external influences. Meghri, P. 91(2013)
5. V. Gh. Mirzoyan, K. G. Trouni, P. A. Grigoryan, K. M. Gevorgyan, and M. Ghannad Dezfouli. Dynamical diffraction of X-rays in ADP single crystal under influence of

temperature gradient. Journal of contemporary physics (Armenian Academy of Sciences), Vol. 49, No. 2, pp. 74–79(2014)

6. M. Ghannad Dezfouli,K. G. Trouni, V. Gh. Mirzoyan.experimental determination of real and imaginary parts of fourier-coefficients of polarizability of ADP and KDP crystals by dynamical diffraction of x-ray.Armenian Journal of Physics, vol. 7, issue 4, p. 213(2014,)
7. M. Ghannad Dezfouli,K. G. Trouni,V.R. Kocharyan. Investigation of rocking curve of reflection on single crystals of ADP under influence of temperature gradient. Armenian Journal of Physics, vol. 7, issue 4, p. 218(2014)
8. K.G. Trouni, V.Gh. Mirzoyan, M. Ghannad Dezfouli, P.A. Grigoryan. Dynamic Diffraction of X-Ray in Quartz Single Crystalwith Fan-Shaped Deformation. Armenian Journal of Physics, vol. 9, issue 4, p. 275(2016)
9. M.Ghannad Dezfouli. Dynamical diffraction of X-ray in single crystal ADP with a fan-shaped deformation. Journal of Engineering and Applied Sciences 13(9),p.2518 (2018)

References

1. D. James. Optical principles of x-ray diffraction. LONDON G.BELL AND SONS LTD,(1962)
2. Andre Authier. Dynamical Theory of X-Ray Diffraction. Oxford,(2001)
3. R. Guinebretière. X-ray Diffraction by Polycrystalline Materials. ISTE Ltd,(2007)
4. B.W. Batterman, M. Cole. Dynamical diffraction of X-rays by perfect crystals. Rev. Mod. Phys, vol. 36, N 3, p.681-717(1964)
5. R.W. James. The Dynamical Theory of X-Ray Diffraction. Solid state physics , vol.15,p. 53-220(1963)
6. M.Z. Goldberger, F. Seitz . Theory of the reflection and the diffraction of neutrons by crystals. Phys. Rev, vol.71, p. 294-310(1947)
7. W.H. Zachariasen. Theory of X-rays Diffraction in Crystals. New York: Wiley, et Sons incur, (1945)
8. N. Kato. Recent development of dynamical theory of diffraction of waves in crystals. J. Phys. soc. Japan. 17 supplement B2,p.53-60(1962)
9. N. Kato, A.R. Lang. A study of pendellosung fringes inX-Ray diffraction. Acta Crystallogr, vol. 12, p.787-792(1959)
10. N. Kato. A theoretical study of pendellosung fringes. I. general considerations. Acta Crystallogr, vol. 14, p. 526-532(1961)
11. A.Freund. Advanced X-ray-UV Radiation Sources and Applications. SpIE proc.vol. ,1345, p.234-44(1990)
12. . G.W. Fox, P.H. Carr. The effect of piezoelectric oscillation on the intensity of X-ray Reflections from quartz. Phys. Rev, vol. 37, N 12, p.1622-1625(1931)

13. S.Nishikava, I. Sakisaka, I. Sumoto. Note on The effeck of piezoelectric oscillaton on the intensity of X-ray reflections from quartz. Phys. Rev, vol. 38, p.1078-1079(1931)
14. Y. Kakiuchi. The increase of X-ray reflection from quartz due to a strong electric field. Phys. Rev, vol.54, N 7, p.772-778(1938)
15. P. Penning, P. Polder. Anomalous Transmission of X-Rays in Elastically Deformed Crystals. Phylips Res. Repts , vol.16, N 2, p.419-440(1961)
16. S. Takagi. Dynamical theory of diffraction applicable to crystals with any kind of small distortion. Acta Crystallogr, vol.15, N 2, p.1311-1312(1962)
17. A.E. Movsisyan. Calculation of displacement functions of crystal atoms in the presence of temperature gradient. Journal of Contemporary Physics (Armenian Academy of science), vol.45, No. 4, P.281-284(2010)
18. V.R. Kocharyan, R. Sh. Aleksanyan, K.G Trouni. Interference absorption coefficient of x-ray in crystals in the presence of temperature gradient. Journal of Contemporary Physics (Armenian Academy of science, vol.4,p.190-194(2010)
19. K. Haruta. Intensity of X-ray diffracted from an elastically vibrating single crystal plate. J. of Appl. Phys, vol. 38, p.p.3312-3316(1967)
20. B. Okkerse , P. Penning . Anomalous Transmission of X-Rays in Germanium. Part II. Effects due to elastic deformation. Phil. Res. Repts. vol.18, 1, p.82-94(1963)
21. . IREntin. The effectof resonant suppression of the anomalous transmission of x rays by ultrasound.JETP Letters,t26, c.5,p.392-395(1977)
22. K.P. Assyrian, I.R. Entin. The influence of ultrasonic vibrations on a dynamic X-ray diffraction in the Bragg geometry. Solid State. t 24, c. 7, p. 2122-2129(1982)
23. G.W. Fox, J.M.Cork .The regular reflection of X-rays from quartz crystals oscillating piezoelectrically. Phys. Rev, v0l. 38, p.1420-1423(1931)
24. M.J. Colby, S. Harris. An X-ray study of a long X-cut quartz crystal vibrating under the transverse piezoelectric effect. Phys. Rev, 46,p.445-450(1934)

25. M.J.Colby and S. Harris. Effect of etching on the relative intensities of the components of double laue spots obtained from a quartz crystal. Phys. Rev. 43, p.562-563(1933)
26. M.J. Colby and S. Harris. X-ray reflections from a quartz piezoelectric oscillator in a Bragg spectrograph. Phys. Rev. 42, p.733-734(1932)
27. Carl V. Bertsch. X-ray studies of crystals vibrating piezoelectrically. Phys. Rev, vol. 49, p.128-132(1936)
28. G.W. Fox and W.A. Fraser. X-ray extinction in piezoelectrically oscillating crystals. Phys. Rev, vol. 47, p.899-902(1935)
29. A.V. Kolpakov, U.P. Xapachev. Dynamical Theory of X-ray diffraction in crystals with modulated electron density. Crystallography, vol. 18, no. 3, p. 474-479(1973)
30. P.A. Bezirganyan, V.I. Avundzhyan. The impact of vibrations on the piezoelectric scattering intensity of X-rays in the second approximation. Math. Akad. SSR, physics, I, p. 227-236(1966)
31. P.A. Bezirganyan, V.I. Avundzhyan. Effect of piezoelectric crystal lattice vibrations on the intensity of the transmitted X-ray beam. Math. Akad. SSR, physics, I, p. 147-156(1966)
32. V.I. Avundzhyan, P.A. Bezirganyan .Determining the direction of oscillation piezoelectric by X-ray diffraction pattern. Akad. SSR, 42. P. 284-287(1966)
33. V.I. Avundzhyan, P.A. Bezirganyan. Experimental study of the influence of piezoelectric vibrations on the intensity of X-ray scattering. Math. Akad. SSR, physics,vol. 2, p. 99-104(1967)
34. V.I. Avundzhyan, P.A. Bezirganyan. X-ray scattering crystal lattice under piezoelectric vibrations . Math. Akad. SSR, physics, (1967), v. 2, p. 244-251.
35. W.J.Spenser and G.T. Pearman. X-ray diffraction from vibrating quartz plates. Advans X-ray Analycis , vol. 13, p. 507-525(1970)

36. A.R.Mkrtchyan, M.A. Navasardian, V.K.Mirzoyan.Full transfer of X-ray single crystal diffraction from the direction of the passage in the direction of the reflection under the influence of gradient temperature. Technical Physics Letters. t 8 in. 11, p. 677-680(1982)
37. A.R. Mkrtchyan, M.A. Navasardian, R.G. Gabriyelyan, L.A.Kocharian, K.G.Galojan, A.A. Aslanyan. Full mirror reflection radiation of angstroms wavelengths in an ultrasonic superlattice in the case of the Laue geometry. Technical Physics Letters. 9 that, in the. 19, p. 1181-1184(1983)
38. A.G. Klein, P. Prager, H. Wagenfeld, P.J. Ellis, T.M. Sabine. Diffraction of neutrons and X-rays by a vibrating quartz crystal. Appl. Phys. Letters, vol.10, N 10, p. 293-295(1967)
39. B. Chalupa, R. Michalec, D. Galociova. Neutron diffraction of quartz crystals as a function of vibrating frequencies. Nucl. Instrum and Methods, 67, N2, p. 357-358(1969)
40. R. Michalec, B. Chalupa, D. Galociova, P. Mikula. Time modulation of a neutron beam diffracted on a single crystal excited vibrations by hight frequency pulses. Phys. Letters, A 28, N 8, p. 546-547(1969)
41. V. Petrzilka. Neutron diffraction of piezoelectric vibrating resonators. Crechosl. J. Phys. B 18, N 9, p. 1111-1116(1968)
42. B. Chalupa, R. Michalec, V. Petrzilka, J. Tichy and J. Zelenka. Diffraction of neutrons on a vibrating quartz crystal. Phys. stat. sol. 29, P. k 51 - k 54(1968)
43. R. Michalec, L. Sedlakova, B. Chalupa, D. Galociova, V. Petrzilka. Neutron diffraction effects due to the lattice displacement of a vibrating quartz single crystal. Nuclear Instruments and Methods. 53, p. 299-304(1976)
44. M.W. Moyer and T.F. Parkinson. Hight frequency modulation of monoergetic neutrons with a quartz piezoelectric crystal. Acta Crystallogr. A. 27, p. 410-415(1971)
45. T.F. Parkinson, E. Gurman, S.K. Loyalka and L.D. Mahlesten. Neutron diffraction by vibrating ADP crystals. Journal of Applicd Physics. vol 45, N 5, p. 2021-2026(1974)

46. A.R. Mkrtchyan, L.A. Kocharian, M.A. Navasardian , O.A. Hunanyan, R.G.Gabriyelyan, R.P. Vardapetyan , V.K. Mirzoyan. The neutron diffraction on single crystals of quartz in the presence of a temperature gradient. Math. Akad. SSR, Physics. vol 21, V. 5, p. 287-289(1986)
47. M.A. Navasardian, P.A. Bezirganyan. The influence of the temperature gradient on the intensity of the reflections Laue patterns. Crystallography. t 17, c. 3, p. 473-476(1972)
48. M.A. Navasardian, P.K. Karaxanyan, P.A. Bezirganyan. The influence of the temperature gradient on the intensity x-ray reflexes. Crystallography. vol. 15, c. 2, p. 235-239(1970)
49. F. Balibar, Y. Epelboin and S. Malgrange. Stady of the new wave fields appearing in crystals deformed by large thermal gradient. Acta Crystallogr. A. 31, p. 836-840(1975)
50. . Y.Sakisaka, I. Sumoto. Note on the Effect of Piezoelectric Oscillation on the Intensity of X-Ray Reflections from Quartz. Phys. Rev. 38, p. 1078-1079(1931)
51. P.A. Bezirganyan, M.A. Navasardian. The dependence of the structure and the intensity of X-ray reflections on the value and direction of the temperature gradient.Akad. SSR. N 5, p. 232-237(1968)
52. . C. Malgrange. Experimental study of the X-ray propagation in perfect crystals deformed under the action of a thermal gradient. Acta Crystallographica, vol.25, N 2, p. 356-363(1969)
53. S.Takagi. X-ray dynamical diffraction process inside a distored crystal. Z. Naturfosch. A 37, N 5,p. 460-464(1982)
54. E.G. Lapin, V.M. Samsonov, T.P. Solodov, O.I. Sumbaev, A.V. Tyunis. The effect of piezoelectric quasi mosaic at X-ray diffraction. Zh. t 73 at. 3 (9), p. 1016-1024(1977)
55. K.Yasuda, N. Kato. Enhancement of the Bragg reflection from quartz crystals due to X-ray irradiation under hight electric field. J. Appl. Crystallogr. 11, N 6, p. 705-706(1978)

56. Eiichi Asada, Tashimichi Takiguchi "Correlation between crystal perfection and reflection intensity of analyzer crystal for X-ray spectra. Japan J. Appl. Phys. 17, N 4, p. 687-693(1978)
57. K.Kando, A. Sawaoka , S. Saito. Observation of atomic behavour in crystal during shock-compression by flash X-ray diffraction. Hight velocity deformation of solids, p. 176-180(1979)
58. A. Guinier. X-ray crystallography. Ed. nat. mat. Lit. Moscow (1961)
59. R.W.G. Wyckoff, Crystal Structures, 2nd Edition, Interscience, NewYork, p. 160(1960)
60. D. Eimerl, Ferroelectrics 72. 95–130(1987)
61. Amnon Yariv, Pochi Yeh. Optical Waves in Crystals. Wiley, Inc.(1984)
62. M.A. Bloxin, I.G. Schweizer. X-ray spectral Handbook. Moscow, Nauka, p. 376(1982)
63. L.I. Mirkin. X-ray structural analysis. Moscow, Nauka, p. 326(1976)
64. M.P. Shaskol'skaya. Acoustic Crystals, Moscow, Nauka, p. 632(1982)
65. Z.G. Pinsker. The X-ray crystal optics. Moscow, Nauka, P.348(1982)
66. V.K. Mirzoyan, T.G. Dovlatyan, A. A. Eghiazaryan. The diffraction of X-rays from a single crystal Al2O3 under the influence of a temperature gradient. Surface, X-ray, synchrotron and neutron research, vol. 11, p. 41-43(2007)
67. A.R. Mkrtchyan, V.K. Mirzoyan, A. Melkonian, S.N. Noreyan , L.A. Kocharian, E.G. Bagdasarian ,T.G. Dovlatyan Uwe van Burke, B. Wagner, W. Matz, N. Scheele. Research diffraction focus X-rays in single crystals in the presence of a temperature gradient. Conversion Potential of Armenia and ISTC program's. International Workshop, 2-7 October, P. 158-161(2000)
68. A.E. Movsisyan, A.R. Mkrtchyan, V.R. Kocharyan. Study of complete transfer phenomenon for media with various heat-transfer coefficients. Charged and Neutral Particles Channeling Phenomena: Channeling -Proceeding of the 51 St Workshop of the Int'l Eloisatron Project(2008).

69. A.E. Blagov, M.V. Kovalchuk, V.G. Kohn, Yu. V. Pisarevsky. Dynamic variation in the lattice parameter of a crystal under ultrasonic treatment in X-ray diffraction experiments. Crystallography Reports, Vol. 51,N. 5, P. 729-733(2006)
70. A.E. Blagov, M.V. Kovalchuk, V.G. Kohn, V.V.Lider, Yu. V. Pisarevsky. Possibilities of controlling an X-ray beam with a crystal subjected to long- wave ultrasonic vibrations. Journal of experimental and theoretical physics, vol. 101, No. 5, p.770-778(2005)
71. H. H. Schmidt, P. Deimel and H. Daniel.Dynamical Diffraction of Thermal Neutrons by Absorbing Magnetic Crystals. J. Appl. Cryst. 8, 128(1975)
72. S.A.Takagi. Dynamical Theory of Diffraction for a Distorted Crystal. Acta Crystallogr. vol. 15, p. 1239–1253(1963).
73. G. R. Grigoryan. diffraction image of primary narrow x-ray beam in weakly deformed crystal.proceedings of the yerevan state university;PhysicalandMathematical Sciences , № 3, p. 52–55(2012)
74. P.V.Petrashen, F.N. Chukhovskii. Dynamical Scattering of X-rays in a Crystal with Constant Deformation Gradient. Sov. Phys. JETP, vol. 2, p. 243–248(1975)
75. E. Jahnke, F. Emde,F. Losch. Tables of Higher Functions, New York: McGraw-Hill (1960)
76. L.V. Azaroff, R. Kaplow, N. Kato, R.J. Weiss, A.J.C. Wilson, R.A. Young. X-Ray Diffraction, New York: McGraw-Hill,196
77. V.GH. Mirzoyan, A.R. Mkrtchyan, S.N. Noreyan. Surface. X-ray, synchrotronand neutron studies, vol. 6, p. 95(2008)
78. M.V. Kovalchuk, A.V. Targonskii, A.E. Blagov, I.S. Zanaveskina, Yu. V. Pisarevskii. New method for measuring rocking curves in X-ray diffractometry by ultrasonic modulation of the lattice parameter. Crystallography reports, vol. 56, No.5,P. 828-831(2011)
79. L.A. Haroutunyan, K.G. Trouni. Opt. Comm*u*n., vol. 90, p. 173(1992)
80. Haroutunyan, L.A. and Trouni, K.G., J. Contemp. Phys. (Armenian Ac. Sci.), vol. 34, no. 5, p. 14(1999)

81. K.G. Trouni, V.R.Kocharyan,G.R.Grigoryan.On the interference absorption of X-rays in crystals with weak deformations. J. Contemp. Phys. (Armenian Ac. Sci.), 47 pp 87-92 (2012).
82. Գ. Ռ. Գրիգորյան. Ռենտգենյան ճառագայթների և ջերմային նեյտրոնների դինամիկ դիֆրակցիան թույլ դեֆորմացված բյուրեղներում: Թեկնածուական ատենախոսություն: 107p., Երևան (2015).
83. R.Sherm and B.Fak. Neutrons. NATO Science Series; B: v.357, pp.113-118 (1996).
84. V.K. Mirzoyan, S.N. Noreyan .The dependence of the half-width of the rocking curve of quartz on the value of the temperature gradient. Math. Akad. SSR, physics, vol 26, no. 3, p. 151-154(1991)
85. A.R. Mkrtchyan, M.A. Navasardian, R.G. Gabriyelyan. Focusing x-ray radiation in the presence of the diffracting crystal temperature gradient. Technical Physics Letters, vol. 11, p. 1354-1359(1985)
86. A.R. Mkrtchyan, M.A. Navasardyan, R.G. Gabrielyan. X-ray diffraction focusing by the temperature gradient in the temperature gradient in the Laue geometry. Phys. Lett. A, vol. 116,p. 444-446(1986).
87. A.R. Mkrtchyan , V.K. Mirzoyan , A.G. Mkrtchyan , S.N. Noreyan, L.A. Kocharian, R.A. Sargsyan, V.U. Tonoyan , T.G. Dovlatyan , I.N. Wagner,the G.Prado, W. Matz, N. Schell.Changes linear absorption coefficient of synchrotron radiation in the quartz crystal in the presence of external influences. The International ISTC Workshop, Armenia, Yerevan , Part 1, p. 150-153(2000)
88. P.V. Petrashen, F.N. Chuhovsky. Dynamic X-ray scattering in crystals with a constant strain gradient. Technical Physics Letters , vol. 6, no. 2/8, p. 427-437(1975)

89. Y. Ando, N. Kato.X-ray diffraction phenomena in clastically distorted crystals. J. Appl. Crystallogr., (1970), vol. 3, p.p. 74-89(1970)
90. E.A. Tikhonov. Dynamic scattering in crystals with weak rapidly and slowly varying sinusoidal distortions. Metalofiziki, vol. 5, no. 2, p. 8-14(1983)
91. M.A. Navasardian, Y.R. Nazarian, V.K. Mirzoyan. Modulation of the diffracted X-ray radiation in the low frequency range to transmit signals. Math. Akad. SSR, physics. t.14, no. 6, p. 425-428(1979)
92. M.A. Navasardian. Controllable variation of the intensity of diffracted X-ray beams and double modulation of such beams for transmission and reception of audio information. Journal Applied Crystallography.34.P.763-766(2001)
93. Z. Janck, I. Kubena. Integrated intensity of the Laue diffraction from an elastically bent crystal. Phys. Stat. Sol. (a). 50, P.285-291(1978)
94. E.N. Kislovskii, P.V. Petrashon. Intensity of Laue diffracted beams in the general case of diffraction in an elastically bent crystal. Phys. State Sol. (a). 51, N2, p. 527-531(1979)
95. P.V. Petrashen , E.N. Kislovskii . Experimental study of X-ray diffraction in a bent crystal with a large strain gradient. Phys. State Sol. (a) (1979). 56, N2, p. 663-667(1979)
96. M.A. Navasardian, V.K, Mirzoyan, K.T. Hayrapetyan, A.R. Agumyan, J.S. Gortsakalyan. The course of the wave energy flux of X-ray radiation in the crystal with a complete transfer. Math. Akad. SSR, Physics, vol. 23, no. 4, p. 217-221(1988)
97. R.G. Gabriyelyan, A.A. Aslanyan. The theory for full transfer of a spherical X-ray wave. Math. Akad. SSR, Physics , vol. 21, no. 6, p. 337-339(1986)
98. R.G. Gabrielyan, A.R. Mkrtchyan, H.A. Aslanyan, Kh.V. Kotanjyan. The theory of X-ray diffraction in oscillating piezocrystals. Phys. State solid, (a). 92, p. 361-368(1985)
99. M. Kuriyama, T. Miyakava. Theory of X-ray diffraction by a vibrating crystal. J. Appl. Phys. 40, N 1,p.1697-1702(1996)

100. K. G. Trouni,M. Ghannad Dezfouli. Integrated intensity for the dynamic diffraction of thermal Neutrons in weakly deformed crystals.III International Conference Electron, Positron, Neutron and X-ray scattering under external influences. Meghri, P. 84(2013)
101. F.N. Chuhovsky. Dynamic scattering x-ray in curved crystal in a plane wave front. Crystallography, vol.19 in. 3, p. 482-488(1974)
102. L.V. Tykhonov, G.V. Kharkov. Symmetric Laue case-diffraction in transmission x-ray topography. Crystallography, t. 30, no. 5. A, P. 867-873(1985)
103. A.R. Mkrtchyan, R.G. Gabrielyan, A.A. Aslanian, A.G. Mkrtchyan, H.W. Kotanjyan. Focus and defocus X-rays under the action of temperature gradient and ultrasonic vibrations. Math. Akad. SSR, Physics, vol. 21, Issue 6, p. 297-305(1986)
104. V.K. Mirzoyan, A.A. Eghiazaryan, V.N. Aghabekian, P.V. Mirzoyan. Diffraction of X-ray beam in the single crystal quartz AT cut in the excitation of acoustic oscillations at the fundamental frequency. Math. National Academy of Sciences, Physics, vol. 43, no. 2, p. 104-110(2008)
105. V.K. Mirzoyan, A.R. Mkrtchyan, S.N. Noreyan. The influence of the temperature gradient in the x-ray diffraction focusing in single crystals of quartz. Surface, X-ray, synchrotron and neutron research. N 6, p. 95-97(2008)
106. V.K. Mirzoyan. A.A. Eghiazaryan, E.G.Bogdasaryan, P.V. Mirzoyan. The spatial modulation of the diffracted X-ray beam by acoustic waves. Math. National Academy of Sciences, Physics, vol. 42, N 6, p. 355-362(2007)
107. M.A. Navasardian, P.A. Bezirganyan. The dynamics of changes in the intensity of Laue - reflected beam with a continuous change in value of the temperature gradient. Math. Akad. SSR, physics, 8, N 2, p. 108-117(1973)
108. V.R. Kocharyan, R. Sh. Aleksanyan, K.G Trouni. Interference absorption coefficient of x-ray in crystals in the presence of temperature gradient. Journal of Contemporary Physics (Armenian Academy of science), vol.4,p.190-194(2010)

109. K.T. Hayrapetyan, S.N. Noreyan, V.V. Margaryan. Study of angular width of an X-ray beam fully pumped from quartz single crystal in the presence of temperature gradient. Journal of Contemporary Physics (Armenian Academy of science), vol.45, p.140-144(2010)

110. V. Gh. Mirzoyan, K. G. Trouni, P. A. Grigoryan, K. M. Gevorgyan, and M. Ghannad Dezfouli. Dynamical diffraction of X-rays in ADP single crystal under influence of temperature gradient journal of contemporary physics (Armenian Academy of Sciences), Vol. 49, No. 2, pp. 74–79(2014)

111. V.GH. Mirzoyan, S.N. Noreyan. J. Contemp. Phys.(Armenian Ac. Sci.), vol. 26, no. 2, p. 13(1991)

112. K.G. Trouni, V.R. Kocharian, G.R. Grigoryan. On the interference absorption of X-rays in crystals with weak deformations. Journal of Contemporary Physics (Armenian Academy of Sciences), 47, P. 87-92(2012).

113. V. Gh. Mirzoyan, K. G. Trouni, P. A. Grigoryan,K. M. Gevorgyan, M. Ghannad Dezfouli.Dynamical diffraction of X-ray on ADP single crystal under the influence of thermal gradient.III International Conference Electron, Positron, Neutron and X-ray scattering under external influences. Meghri, P. 91(2013)

114. V.T. Deshpande, A.A. Khan. X-ray determination of the thermal expansion of ammonium dihydrogen phosphate. Acta Cryst.16, p.936(1963)

115. M. Ghannad Dezfouli,K. G. Trouni, V. Gh. Mirzoyan.Experimental determination of real and imaginary parts of fourier-coefficients of polarizability of ADP and KDP crystals by dynamical diffraction of x-ray.Armenian Journal of Physics, vol. 7, issue 4, p. 213-217(2014,)

116. M. Ghannad Dezfouli,K. G. Trouni,V.R. Kocharyan. Investigation of rocking curve of reflection on single crystals of ADP under influence of temperature gradient. Armenian Journal of Physics, vol. 7, issue 4, p. 218-223(2014)

117. K.G. Trouni, V.Gh. Mirzoyan, M. Ghannad Dezfouli, P.A. Grigoryan. Dynamic Diffraction of X-Ray in Quartz Single Crystal with Fan-Shaped Deformation. Armenian Journal of Physics, vol. 9, issue 4, pp. 275-278 (2016)

118. M.Ghannad Dezfouli. Dynamical diffraction of X-ray in single crystal ADP with a fan-shaped deformation. Journal of Engineering and Applied Sciences,vol.13,pp.2518-2520 (2018)